8-2018

Effects of dissolved CO_2 on cleaning of RO membranes

Victoria Guerrero
Clemson University, vguerre@g.clemson.edu

EFFECTS OF DISSOLVED CO_2 ON CLEANING OF RO MEMBRANES

A Thesis
Presented to
the Graduate School of
Clemson University

In Partial Fulfillment
of the Requirements for the Degree
Master of Science
Environmental Engineering and Earth Sciences

---

by
Victoria Guerrero
August 20018

Accepted by:
Dr. David A. Ladner, Committee Chair
Dr. David L. Freedman
Dr. Tanju Karanfil

ABSTRACT

Membrane fouling is a major operational issue in reverse osmosis (RO) desalination plants. In the last 25 years, over 3,000 papers were published to address this issue. Current control strategies mostly consider the use of chemicals (e.g. acids and antiscalants) in feed water, pre-treatment techniques, and clean-in-place (CIP). Due to chemical consumption, by-product formation is observed in concentrate streams, which is an environmental and human health concern. Recently, dissolved carbon dioxide has been proposed as an alternative cleaning method. Only a few studies are available on the use of CO_2, but the initial results are promising. These studies have demonstrated the effective scale inhibition and reinstatement of membrane performance, which could also extend the life-cycle of RO membranes.

The primary goal of the present research was to determine the cleaning efficiency of dissolved CO_2 using a carbon dioxide saturation tank to inject CO_2 in water. Flux recovery was determined on different RO membranes scaled with inorganic salts, organic substances, and combined fouling.

The hypothesis of the work is that the presence of CO_2 bubbles formed due to depressurization upon entrance of the membrane cell and the low pH owing to the formation of carbonic acid, help shear the foulants away. The present research showed that a 15-minutes CO_2 cleaning effectively cleaned scaled membranes, with an average flux recovery of 92.5 ± 33.7% for membranes scaled with $CaSO_4$, 95.0 ± 29.4% for $CaCO_3$, 103.1 ± 25.6% for humic acid, 94.6 ± 24.0% for $CaSiO_3$ and 107.9 ± 8.5% for combined fouling. Controls were performed with an acidic solution and air to isolate effects from pH and scouring present during CO_2 cleaning. Furthermore, some of the experiments resulted

in relatively weak foulant layers that could be removed with deionized (DI) water flushing alone.

Based on the present research, carbon dioxide has proven so far to be more eco-friendly and effective at least with some inorganic and organic scaling solutions. Furthermore, it might be even cheaper than common chemical agents.

ACKNOWLEDGMENTS

I would like to acknowledge my advisor Dr. David A. Ladner, who always gave me encouraging words and advice, as well as the other members of my research group, who listened and provided feedback throughout our group meetings. I would also like to say thanks to Jessica Hart and Darryl Fendley from BlueInGreen for supplying their carbon dioxide dissolution system and all the staff in the Environmental Engineering and Earth Sciences department at Clemson. Lastly, I would like to thank my family and friends for their unconditional love and support; without them I would not have become the professional I am today.

TABLE OF CONTENTS

Page

Table of Contents (Continued)

Page

LIST OF TABLES

LIST OF FIGURES

Figure Page

List of Figures (Continued)

Figure Page

List of Figures (Continued)

Figure Page

List of Figures (Continued)

Figure Page

List of Figures (Continued)

Figure Page

ABBREVIATIONS & ACRONYMS

CPA	Composite polyamide
DI	Deionized
HA	Humic acid
MF	Microfiltration
RO	Reverse osmosis
SEM	Scanning electron microscopy
UF	Ultrafiltration

1. INTRODUCTION

1.1. Reverse osmosis

Problems with water are growing worse each day, with water scarcity and pollution occurring globally. Reverse osmosis (RO) is a membrane treatment process used to separate dissolved solutes from water. This technique has become increasingly popular due to the variety of objectives it may accomplish. These include: desalination of seawater or brackish water, advanced treatment for water reuse, softening, natural organic matter removal to minimize disinfection by-products (DBP) formation, and specific contaminants removal (e.g. metal ions and aqueous monovalent salts, including sodium, chloride, copper, chromium, and lead).

One of the major operational issues in RO desalination plants is membrane fouling, which results in the loss of performance of the membrane (i.e. higher operating pressure, lower permeation flux, and lower salt rejection, which represents the percentage of salt removed from the feedwater stream) and thus, higher operating costs. The deposition of inorganic compounds and dissolved organic substances creates the development of a concentration gradient across the boundary layer near the membrane surface due to a difference in mass transport between bulk solution and membrane (i.e. concentration polarization layer) (Wibisono et al. 2014). Properties and identification methods of common scaling solutions are presented in Table A.1 (Appendix A).

The nature of fouling strongly depends on the feed water source. Seawater sources are characterized by high total dissolved solids (TDS) typically ranging from 18,000 to 45,000 mg/L, particulates, organic carbon, and colloidal contaminants. Brackish waters have TDS

usually ranging from 1000 to 10,000 mg/L, organic carbon, and colloidal contaminants (Antony et al. 2011) which is why they operate under lower applied pressure than seawater (Crittenden et al. 2005).

Plants treating brackish surface water or groundwater can typically encounter troublesome inorganic scales, such as carbonates, sulfates, and silicates, which cling to membranes and are difficult to remove. On the other hand, organics (e.g. emulsified organics) can adsorb to the membrane surface resulting in flux loss (i.e. membrane productivity) which can be permanent in some cases (i.e. irreversible fouling). Organic fouling exacerbates microbial fouling, as many organics are nutrients for microbes; thus, it is recommended that the total organic carbon (TOC) be less than 3 ppm to minimize fouling potential (Kucera 2015). Humic substances in aquatic environments are the major fraction of natural organic matter (NOM); not only does humic acid cause flux reduction, but it also colors the membrane surface, thus facilitating the visual inspection of the fouled membrane.

There are two likely scale formation mechanisms, surface and bulk crystallization/precipitation, which occur when the solution gets supersaturated (i.e. the concentration of ions in solution exceeds their saturation limit). Surface crystallization occurs as a result to the lateral growth of mineral deposits on the surface of the membrane whereas bulk crystallization is caused by the precipitation of crystal particles formed in the bulk phase leading to the formation of cake layer (Antony et al. 2011).

There are two possible strategies to minimize fouling problems: fouling can either be prevented (i.e. pretreatment, use of antiscalants, operating below saturation levels) or

cleaned (Van Der Bruggen et al. 2003). Cleaners for inorganic scales typically consist of acidic and/or basic chemical solutions (Greenlee et al. 2009), with most inorganics being more amenable to acids. Calcium silicate is generally associated with aluminum (Darton & Fazel 2001) and can typically be prevented by either pre-treatment or acidification (Partlan 2013). Cleaners for organic scales can also be acids or bases, with bases usually being most effective. Chelators and surfactants can be effective for organics as well. Table A.2 summarizes the different categories of chemical cleaning agents, applications, and action mechanisms. Due to chemical consumption, antiscalants or cleaning products can react with different components present in water, thus forming by-products which will remain in the concentrated stream; by-products formation is an environmental and human health concern (Greenlee et al. 2010; Shahid et al. 2017).The use of chemical agents can also damage the membrane and reduce its life span.

Other drawbacks related to chemical consumption might include inefficient removal of the fouling and an inadequate recovery performance with an insufficient dosage of chemicals, or harmful effects on the selective membrane layer, including a pH range not compatible with the recommendations of the manufacturers, as well as significant additional costs when overdosing (Ang, Tiraferri, et al. 2011; Coutinho de Paula & Amaral 2017).

1.2. Membrane cleaning/flux enhancement

1.2.1. Gas sparging: two-phase flow in membrane processes

A (gas/liquid) two-phase flow has been extensively used worldwide in membrane processes such as microfiltration (MF), ultrafiltration (UF), nanofiltration (NF), RO,

membrane distillation, electrodialysis, and membrane bioreactors (MBRs) (Wibisono et al. 2014). This technique can be used either for flux enhancement (primarily in MF and UF membranes) by reducing the concentration polarization layer, or for membrane cleaning.

Mechanical scouring is an innovative engineering technique; the aim of this method is to create hydrodynamic instabilities which disturb the concentration polarization layer, sweep away formed cake layers and remove biofouling from membrane surfaces or net-spacers (Cui at al. 2003; Moreno et al. 2017; Wibisono et al. 2014). It is interesting to mention that one study showed that air-liquid two-phase flow enhanced RO membrane flux by a factor of 1.66, which meant that permeate flux increased by 166% and the level of rejection also increased, up to 91%, due to the high and transient wall shear stress induced by the sparging (Alsalhy et al. 2013).

1.2.2. Carbon dioxide as a sparging agent

Air/water cleaning has represented a widespread alternative for gas sparging. However, it is noteworthy to mention air has a much lower solubility in water than that of CO_2 (0.023 g/L and 1.27 g/L respectively, at 1 atm at 25°C, calculated using Henry's law (Burton et al., 2013)). This relatively low solubility does not only limit the effectiveness of two-phase flow cleaning, it also increases the formation of undesired stagnant bubbles (Moreno et al. 2017; Willems et al. 2009).

The use of carbon dioxide has a few advantages. To begin with, once the CO_2 saturated water leaves the membrane cell, the gas will no longer be dissolved in water and will be released into the atmosphere (Moreno et al. 2017). A low pH is another positive aspect

which is observed throughout the cleaning due to the formation of carbonic acid, this can facilitate the removal of inorganic scaling.

The use of CO_2 might also have some negative potential effects, mostly associated to its manufacturing process. There are 3 primary sources, one of them involves extracting CO_2 from an underground supply. CO_2 can also be produced by a wide variety of industrial operations, namely the combustion of fuels high in carbon content, steam methane reforming, and fermentation of sugar to alcohol. Impurities can be filtered out, moisture removed in driers and purified CO_2 compressed for liquefaction. A third option includes the by-products of the operation of a primary process, such as H_2 and NH_3 production.

The combustion of fossil fuels is a main contributor to the greenhouse effect (with an approximate contribution of 30% [Douglas & Costas 2005)]) and increasing the greenhouse gases concentrations in the atmosphere would go against the objectives stated in the Kyoto protocol. It is noteworthy to mention the increasing demand of CO_2 which is also used in tertiary or enhanced oil recovery operations and well stimulation, and in food processing and beverage bottling. It is thus important to find "greener" processes to obtain the CO_2.

1.2.3. Dissolved carbon dioxide: an alternative to chemical cleaning

A novel approach to membrane cleaning is the idea of forming gas bubbles at the membrane itself, thus providing shear stress at the point of foulant contact. When using gaseous carbon dioxide, a study initially termed this cleaning method "CO_2 bubble nucleation" and was successfully used to remove biofilms and fouling deposits from a low-

pressure RO membrane and completely restore the original flux (Ngene et al. 2010). This nucleation would occur due to local pressure differences within the module and the presence of nucleation sites on the surface of the membrane foulants; bubbles were then traced with an image processing tool, ImageJ (see Figure 1).

Results showed approximate fouling removal (in terms of reduction in the hydraulic resistance after the membrane's cleaning) values of 43 ± 5%, 85 ± 3% and 100 ± 3% for water rinsing, water/N_2 sparging, and water/dissolved CO_2 solution, respectively. From the pictures, stagnant bubbles are observed in the second test cell (N_2 sparging); these reduced the mechanical scouring effect, whereas continuous bubble formation and detachment occur within the flow channel in the third test cell (dissolved CO_2). A higher bubble coverage area increased the shear stress and helped clean the membrane's biofouling (Willems et al. 2009; Ngene et al. 2010); upon formation, bubbles will coalesce with other larger bubbles, thus getting swept along with the flow. It was also suggested that the presence of imperfections due to the fouling deposits and surface roughness enhanced the bubble formation and its subsequent growth (Coffey 2008; Ngene et al. 2010).

Lowering the pH of a pulp mill plant from 8.5 to 7.5 successfully eliminated lime scale formation when using CO_2 in heat exchangers (Hart et al. 2011). This demonstrated that pH adjustment is a benefit of CO_2 addition, along with bubble nucleation. CO_2 was also added for scale prevention in a RO membrane, posterior to a membrane bioreactor (MBR) combined with a submerged UF membrane treatment (Joss et al. 2011).

Supercritical CO_2 (10,000 kPa at 35°C) also resulted efficient in removing biofouling induced on a RO membrane using *pseudomonas aeruginosa* (PA01 GFP) as a model bacterial strain (Mun et al. 2012). Biofilm cells were reduced by >8 log after a 30- minutes cleaning, without any significant damage to the membrane.

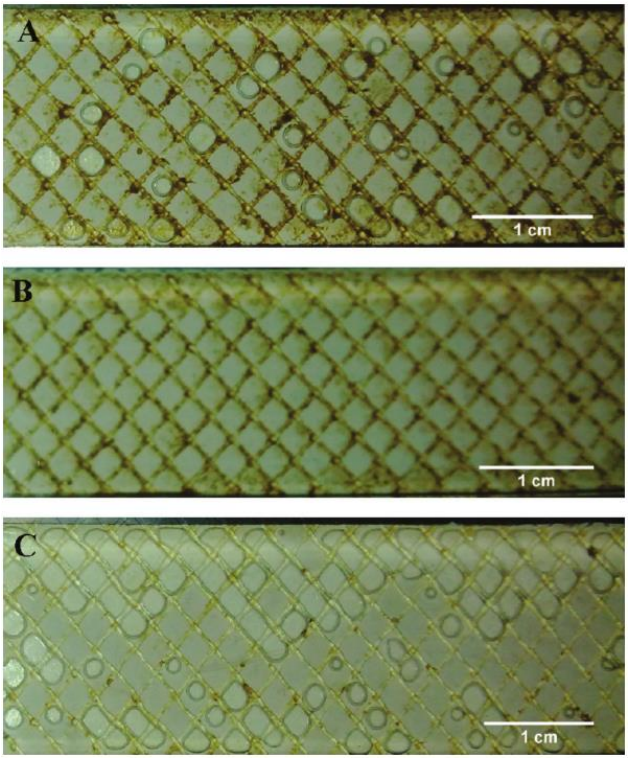

Figure 1. *Images of flow cells after cleaning protocol: (A) water rinsing, (B) water/N_2 sparging, and (C) water/CO_2 nucleation (Ngene et al. 2010).*

Dissolved CO_2 was also tested to remove inorganic fouling, and it was injected by bubbling CO_2 gas into water held in a pressurized vessel (Partlan 2013). After controls were performed with other cleaning methods, it was concluded the CO_2 approach was effective to clean membranes scaled with calcium carbonate (achieving an average 80% flux recovery), whereas it proved to be ineffective for silica-based scales.

Two more studies investigated CO_2 for fouling removal. One of them employed sodium alginate as a model of polysaccharides foulants in presence of different

concentrations of sodium chloride and calcium ions with the aim to enhance membrane fouling (Alnajjar 2017). CO_2 cleaning was performed under different operating conditions and tested against other cleaning methods. Results showed approximate average flux recovery values of 20%, 25% and 80% for MilliQ water, a cleaning solution at pH 4, and a CO_2 solution, respectively.

The second study used CO_2 to control inorganic scale formation on the surface of RO membranes in wastewater reclamation; the gas cleaning caused an increase in solubility of inorganic salts in water and inhibited scale formation on the membrane surface (Shahid, et al 2017[a]; Shahid et al 2017[b]; Shahid & Choi 2018). Additionally, CO_2 resulted in fewer environmental impacts when compared to antiscalants, given that no by-products were generated in the concentrate stream.

In the last 25 years, over 3,000 papers were published to address the issue of RO membrane fouling, indicating researchers' great interest in this area (Jiang et al. 2017). Fouling control strategies mostly consider use of chemicals (e.g. acids and antiscalants) in feed water, pre-treatment techniques, and clean-in-place (CIP) (Shahid, Pyo & Y. G. Choi 2017). It is noteworthy that to the author’s knowledge there are only four studies available on the use of CO_2 as an alternative cleaning method for RO membranes focused on single-foulant solutions (Ngene et al. 2010; Mun et al. 2012; Partlan 2013; Alnajjar 2017). Furthermore, dissolved CO_2 has not yet been used for combined fouling removal or control.

The objective of this research was to evaluate CO_2 injection into a RO membrane cell using a novel carbon dioxide apparatus. Membranes were first scaled with various agents, then cleaning was performed. The work was divided into the following objectives.

Objective 1. To develop a method for bench-scale testing of dissolved CO_2 using a saturation tank to clean RO membranes scaled with calcium carbonate, calcium sulfate, calcium silicate, and humic acid. Determine cleaning efficiency and compare against other cleaning methods and experimental controls (low pH solution; air gas; DI water).

Objective 2. To perform a multi-component study based on combined fouling (inorganic and organic). Determine flux recovery after cleaning scaled membranes with dissolved CO_2. Compare with flux recoveries achieved through experimental control (air gas).

The hypothesis of the work is that the presence of CO_2 bubbles formed due to depressurization upon entrance of the membrane cell and the low pH owing to the formation of carbonic acid, help shear the foulants away.

2. MATERIALS AND METHODS

2.1. Bench-scale setup

A bench-scale test setup (Figure 3) was adapted from a system used previously by David Ladner (Ladner et al. 2010) and Erin Partlan (Partlan 2013). Appendix B explains the differences between Partlan's work and the current research. A plunger pump (model 231, Cat Pumps) cycled water through a membrane cell (GE Osmonics SEPA II; now Sterlitech), which held the RO membrane coupon (7.60 inches long, 5.60 inches wide [see Figure 2]). The concentrate flow from the membrane cell was diverted to the feed tank for recycle, whereas the permeate flow was dispensed to a beaker on top of a balance for continuous conductivity and mass readings.

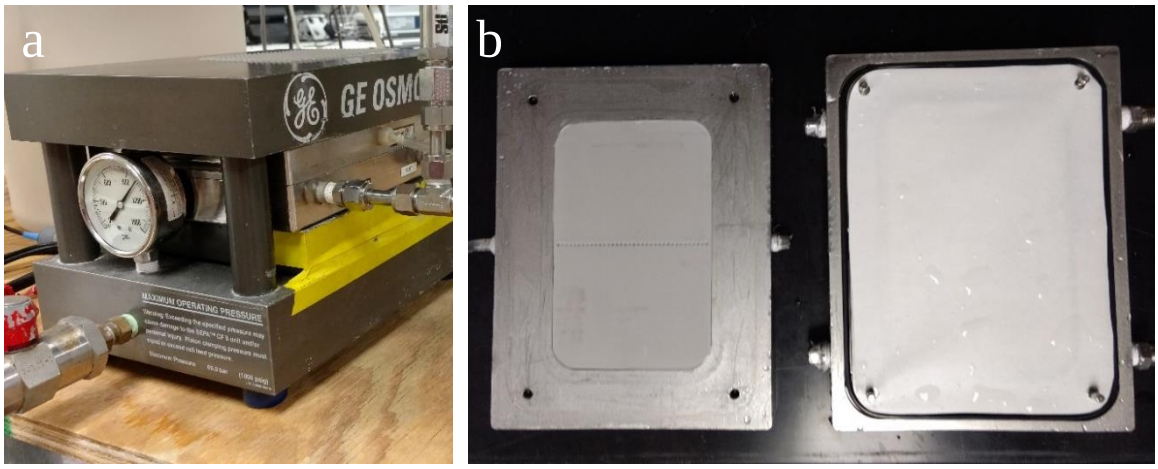

Figure 2. *(a) Exterior and (b) interior of the membrane cell. The permeate and RO membrane can be seen on the right picture.*

A saturation tank was used for the CO_2/air cleaning. Both water and gas flows converged into this pressurized tank; it was first filled with the gas, whereas the water entered as a spray to ensure efficient mass transfer. A more thorough description is included in Appendix B.

Due to the corrosivity of brackish water, the membrane test cell, the saturation tank, tubing, and wetted parts of the pump were made of 316 stainless steel. A LabView (National Instruments) program was used to record data on a continuous basis (i.e. every thirteen seconds) and convert mass readings from the balance into flux readings. A data acquisition unit (SCB-68, National Instruments) was used to input data into LabView from the balance, concentrate pressure gauge, pH meter, and two conductivity probes (Eutech instruments).

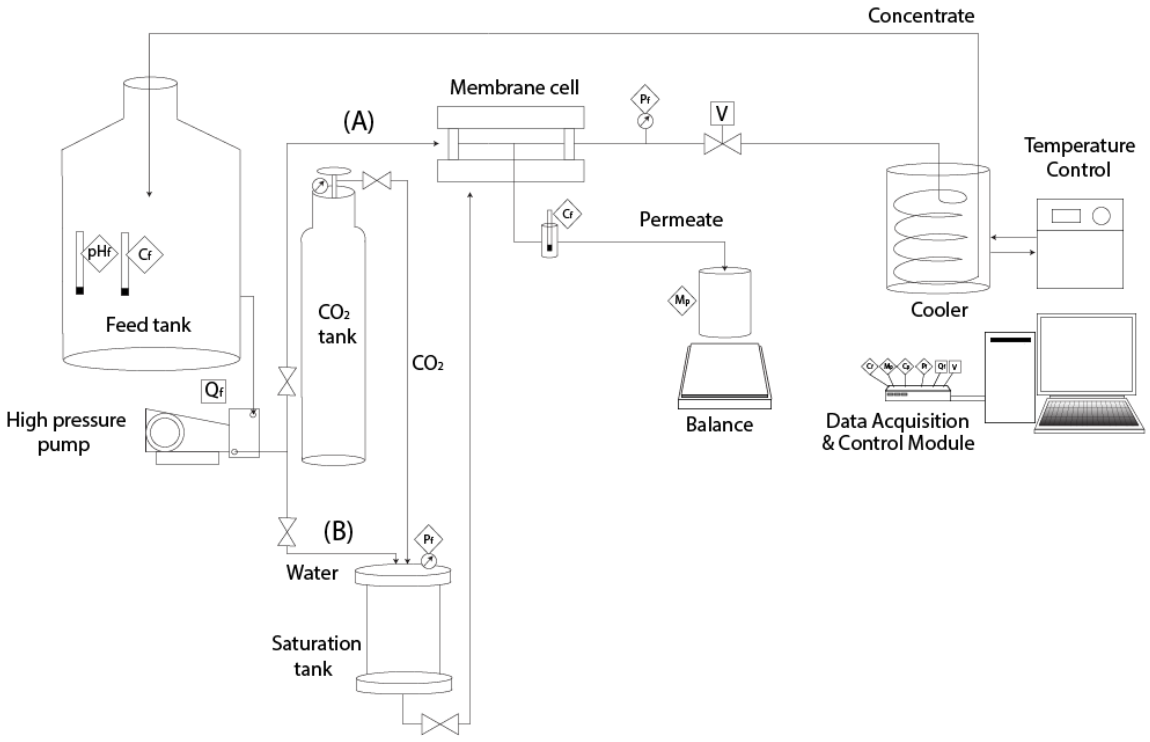

Figure 3. *Bench-scale RO membrane test setup for (A) scaling/chemical cleaning; (B) CO_2/air cleaning. Square symbols denote controls (V for needle valve actuator voltage and Q_f for the feed flow rate control). Diamond symbols stand for the data acquisition (pH_f for feed pH, C_f and C_p for feed and permeate conductivity respectively, M_p for permeate mass, and P_f for pressure gauge).*

The LabView program also provided an interface for both manual and automated control of the pump speed and valve actuator. The pump speed was controlled by a phase

inverter (S-11, Toshiba) and the concentrate needle valve position (which regulated the pressure in the membrane cell) was controlled by a valve actuator (MCJ-000AB-3-SS-2MG4, Hanbay Laboratory Automation).

2.2. RO Membrane

A composite polyamide CPA2 (Hydranautics) brackish water membrane was used in all experiments. The CPA2 membrane has a polyamide active layer with a pH range of 2-10, a maximum temperature of 45°C, and a maximum pressure of 4,137 kPa (600 psi). Detailed membrane specifications are presented in Appendix C. Membrane coupons were cut from a spiral wound element (4 inches diameter and 40 inches length) and maintained in an aqueous solution of 0.02% sodium azide to avoid mold and bacterial contamination.

2.3. Monitoring Data

Appendix D shows the Labview interface as well as every MATLAB plot monitored during a typical run. The main parameter of concern was the permeate flux, which was recorded every thirteen seconds. pH was measured using a pH probe submerged in the feed tank (in conjunction with the pH/ORP 350 transmitter, Cole-Parmer). For chemical cleaning (not including the gas sparging), small adjustments were made if necessary to reach the corresponding target pH, by either adding hydrochloric acid or water.

Rejection (R) was also recorded and monitored to ensure proper membrane function, which was calculated by the ratio between the feed and permeate conductivity (C_p, C_f) measured with two submerged conductivity probes, as described by Equation 1. During the scaling step, rejection ranged from 90.00% to 99.99%, with an average of 95%.

$$R = \left(1 - \frac{C_p}{C_f}\right) \times 100\% \quad (1)$$

2.4. Scaling solutions

2.4.1. Single-foulant solutions (inorganic and organic)

The feed water was designed to mimic brackish groundwater as this source of drinking water commonly encounters scaling issues. Experiments were conducted with typical scales formed in groundwater treatment, namely calcium carbonate, calcium silicate, and calcium sulfate. Calcium sulfate and calcium carbonate were the most studied inorganic scalants in the past ten years, indicating their importance in RO inorganic fouling (Jiang et al. 2017). Humic acid was also tested; this organic foulant allowed a comparison to the inorganic scales. Ten g/L NaCl was used as a background electrolyte in all experiments, allowing measurement of membrane integrity via salt rejection. As previously mentioned, there are few studies on the use of CO_2, the cleaning mechanism, and the effects on the foulants are still uncertain, thus synthetic water was preferred over real water to know the exact concentration of the fouling species and conduct a more precise analysis.

Partlan's recipes were used and adapted for the first two inorganic scaling types, calcium carbonate and calcium silicate (Partlan 2013), whereas the third inorganic scaling type, calcium sulfate, was based on a recipe from the literature (Shaffer et al. 2017). The humic acid solution was created and adapted from Xie's recipe (Xie et al. 2016). Said recipes are represented by each row in Table 1.

Lab reagents included NaCl (Macco Organiques, s.r.o.); Na_2CO_3 (VWR), $CaCl_2 \cdot 2H_2O$ (EMD Chemicals); Na_2SO_4 (Fisher Chemical); $Na_2SiO_3 \cdot 9H_2O$ (J. T. Baker); HCl (Fisher Chemical); and humic acid (MP Biomedicals; catalog number 198763; lot number 7078J).

Table 1. *Summary of recipes for the feed solutions. Blank spaces mean the component was not included in the solution. Two different concentrations were tested for $CaCO_3$ and $CaSO_4$ for fouling and cleaning efficiency comparison.*

Purpose		**Feed Solution**						
		NaCl	**Na_2CO_3**	**$CaCl_2$**	**Na_2SO_4**	**Na_2SiO_3**	**HCl**	**Humic acid**
$CaSO_4$	Recipe 1	171 mM		30 mM	30 mM			
	Recipe 2	128 mM		48 mM	48 mM			
$CaCO_3$	Recipe 3	171 mM	3 mM	3 mM				
	Recipe 4	128 mM	4.5 mM	4.5 mM				
Humic acid	Recipe 4	171 mM						37.5 mg/L (*)
$CaSiO_3$	Recipe 5	171 mM		3.5 mM		5 mM	10 mM	
Combined fouling	Recipe 6	171 mM	1.2 mM	16 mM	15 mM			37.5 mg/L (*)

(*) The humic acid was dissolved in water and filtered before running the TOC analyzer, obtaining a DOC concentration of 8.90 mg/L.

2.4.2. Multiple-foulant solutions

Given that multiple fouling ions are usually present in raw waters, a multi-component system study (i.e. organic and inorganic fouling) was conducted to analyze the CO_2 cleaning efficiency. Calcium carbonate and calcium sulfate scales were chosen to represent common inorganic fouling species, whereas the organic foulant was represented by HA. The combined fouling recipe comprised 16 mM $CaCl_2$, 1.2 mM Na_2CO_3, 15 mM Na_2SO_4, and 37.5 mg/L HA (see Table 1). The original recipes for calcium carbonate and calcium

sulfate were divided in half and then these solutions were mixed with humic acid, so that the ionic strength of the final mixture would be similar to the single-foulant solutions.

2.5. Scaling procedure

During scaling the crossflow velocity was kept constant and the pressure was controlled by the actuator-driven needle valve for all flux experiments (approximately 900 mL/min and 3,447 kPa [500 psi] respectively). A new membrane coupon was used for each run. Before each membrane installation, the new coupon and membrane cell components were rinsed in deionized water. With the membrane cell connected, the system was flushed to remove all stagnant water and replaced with fresh DI water. Then, the system was pressurized, and DI circulated for one hour to compact the membrane.

To scale the membranes, the feed was switched to a prepared fouling solution (with components as described in the previous sections). Measurements of pH and conductivity on the scaling solution were taken before each scaling step. To expedite scaling, the permeate was wasted to allow concentration of the feed and increase the propensity of scale formation. Scaling solutions were recirculated until reaching a 50 or 60% flux decline. Fresh DI water circulated for ten minutes after the scaling step to compare before and after flux values, and check whether the membrane was fouled before proceeding to the cleaning step (either chemical or gas cleaning approach).

2.6. Cleaning procedure

2.6.1. Gas sparging cleaning

Gas sparging cleaning involved the use of a saturation tank. Both water and gas flows converged into this pressurized container until the tank level reached 75% capacity

(approximately 5.66 L of water were necessary to accomplish this). The pump was then shut down and the saturation tank's bottom valve was opened to let the water flow through the membrane (i.e. batch mode), which was driven by headspace pressure (approximately 758-862 kPa [110-125 psi] for CO_2, and 793-1,172 kPa [115-170 psi] for air). High purity (99.5%) carbon dioxide and ultra-zero grade compressed air (Airgas) were used. The system was then flushed with fresh DI water to obtain a clean water flux measurement and determine the flux recovery.

A side experiment was conducted to measure the resulting carbon dioxide concentration. Two approaches were used; in both cases samples were taken directly out of the saturation tank after emptying it to 50% capacity and a dilution was necessary to estimate the dissolved carbon dioxide concentration. One of the methods involved measuring the samples pH whereas the other one made use of a test kit (LaMotte). Further details are presented in Appendix E.

2.6.2. Chemical Cleaning

Trials without dissolved gas did not utilize the saturation tank. HCl was the chemical agent used as an acidic solution with a pH of 4 to have a similar value to the pH during CO_2 cleaning. The procedure for chemical cleaning was based on industry convention for membrane cleaning, which circulates a cleaning solution through the RO system without added pressure (Fritzmann et al. 2007). A circulation time of 30 minutes was used, as done previously (Partlan 2013).

pH was regularly monitored to ensure a consistent pH throughout the cleaning cycle. Due to dissolution of membrane scale, the cleaning solution pH was expected to increase rapidly in the case of calcium carbonate scaling (alkaline) and frequent addition of HCl was required to maintain the target pH. For other scaling solutions, if the pH slightly decreased, DI was used instead. After cleaning, the system was flushed with DI water and a clean water flux measurement was taken to evaluate the flux recovery.

2.7. Membranes visual inspection

SEM analysis was conducted to make a qualitative assessment of the different types of scalants deposited on the membrane, before and after conducting the membrane cleaning. Small samples (0.40 x 0.20 inches approximately) were first cut from the mid-section of the membrane and were then mounted on a stage and sputter-coated with platinum for five minutes. The surface analysis of the samples was then performed using an analytical variable pressure scanning electron microscope (Hitachi, Schottky Emission VP FE-SEM SU6600).

3. RESULTS AND DISCUSSION

3.1. Flux recovery

Flux values were compared at different stages, taking an average of the last ten readings (within a time span of 1.85-2.00 min) at several points:

(1) after membrane compaction, called the initial DI flux (J_i),

(2) at the end of the scaling run, called the final scaling flux (J_s), after reaching a 50 or 60% flux decline from the beginning of the scaling step,

(3) after scaling using DI water to verify membrane's fouling (J_{as}),

(4) at the end of the cleaning run (J_c),

(5) after cleaning, called the final DI flux (J_f), to evaluate flux regained by cleaning.

Flux readings were taken at a pressure of 3,447 kPa (500 psi), except for during the gas sparging when the pressure was less than 690 kPa (100 psi). It is noteworthy that even using the same membrane material (i.e. CPA2), variability in the initial flux is expected between coupons either due to the membrane itself or because of slight differences in membrane preparation and installation (Partlan 2013); in this research the initial DI water flux ranged from approximately 80-100 liters per square meter per hour (LMH) after one hour of membrane compaction, with an average of 93 LMH. It is noteworthy to mention that during DI water controls, step 4 from Figure 4 was replaced by DI flushing for 30 minutes.

$$R = \frac{J_f}{J_i} \tag{2}$$

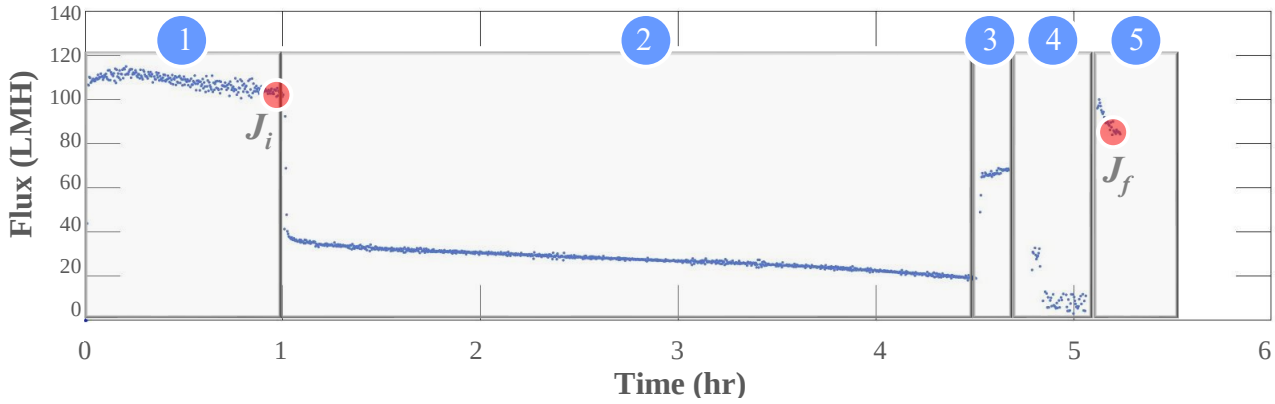

Figure 4. *Flux vs time plot during a typical run consisting of five stages: 1) membrane compaction (0 to 1 hr), 2) scaling step (1 to 4.5 hr), 3) DI water after scaling (4.5 to 4.65 hr), 4) cleaning (4.65 to 4.95 hr), and 5) DI water after cleaning (4.90 to 5.10 hr). Circled points show flux values used to calculate R.*

To compare the percent flux recovery (R), the final DI flux (J_f) was divided by the initial DI flux (J_i) (see Equation 2 and Figure 4).

3.1.1. CO_2 cleaning

Throughout the gas cleaning, the carbonated water in the concentrate line from the membrane cell exited rapidly with an average crossflow velocity of 392 mL/min; the amount of time necessary for the saturation tank to empty itself was on average about 15 minutes, with an initial and final headspace pressure of 827 and 345 kPa (120 psi and 50 psi) respectively. Additionally, bubbles were observed in the permeate line within a minute, confirming that once the CO_2 saturated water leaves the membrane cell, the gas is no longer dissolved in water (Moreno et al. 2017).

The percent flux recovery for each fouling solution is shown in Figure 5. The reason some of the values are over 100% may be related to the variability in the measurements, as well as a possible decompaction of the membrane. Except for humic acid, CO_2 cleaning showed a higher flux recovery (typically above 95%) than the control experiments with DI

water; however, some of the experiments resulted in relatively weak foulant layers that could be removed with DI flushing alone.

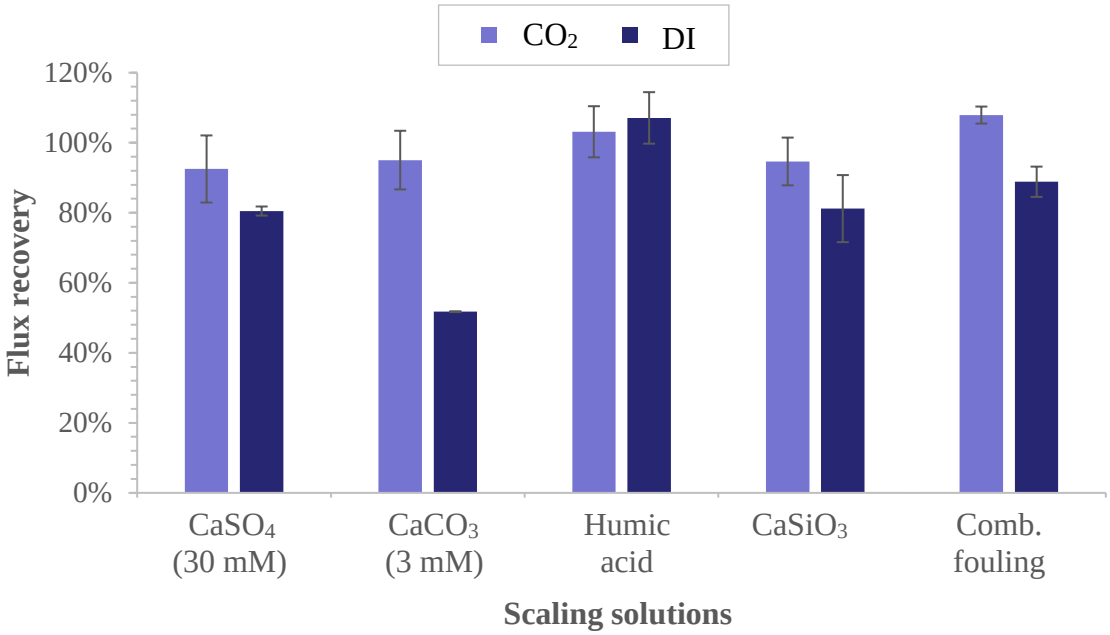

Figure 5. *Percentage of flux recovery for each scaling solution after CO_2 cleaning and DI water control. Each column represents the average value of the duplicates performed, whereas the error bars show the individual results.*

In the combined scaling solution, it is also possible that the presence of HA lowered the $CaCO_3$ and $CaSO_4$ saturation indexes by aqueous complexation, thus reducing $CaCO_3$ and $CaSO_4$ scaling on the membrane (Ray et al. 2017). This could have facilitated the cleaning of the membrane scaled with combined fouling and increased the flux recovery. Furthermore, another study showed that pure $CaCO_3$ crystals were more tenacious and compact than mixed solutions (Chong & Sheikholeslami 2001). This could also explain the higher flux recovery of the combined fouling membrane in contrast to the $CaCO_3$ scaled membrane. The complete set of data is presented in Appendix F.

3.1.2. Carbon dioxide concentration

The theoretical maximum concentration of dissolved CO_2 (dCO_2) had an average value of 11.9 g/L (see Appendix E, Table E.1). Considering a 95% transfer efficiency (estimated percent saturation at flow rate provided by the saturation tank's supplier), the actual dCO_2 was on average 11.3 g/L. According to LaMotte CO_2 test kit, the concentration of carbon dioxide dissolved in water was approximately 1,027 ppm (1.027 g/kg of solution), whereas a slightly higher concentration was predicted based on the pH measurement (1,460 ppm or 1.460 g/kg of solution). This theoretical prediction could result higher because ideal conditions are assumed (which do not occur in real life). Both measurements represent an efficiency of 10%, however, it is noteworthy to mention that a lot of the CO_2 might have escaped while taking the samples, measuring the pH, and conducting the titration, thus explaining the lower values obtained. Further details are presented in Appendix E.

Partlan reported in 2013 approximate values of 12, 20, and 8 volumes of CO_2 at 500, 400, and 300 psi respectively representing concentrations of 23.8, 39.3, and 15.7 g CO_2/L of solution. In spite of the current lower CO2 measurements and lower operating pressure, flux recovery values using the saturation tank obtained higher results than those of Partlan's. This might suggest the fouling solutions used in 2013 were probably more tenacious, thus, they were harder to clean.

One study showed that saturation levels ranging from 2 to 15 g/L of dissolved CO_2 can be reached when combining different temperature and pressure settings, including a wide variety of carbonated beverages from tonic water to sparkling wines; for instance, champagne contains an average value of 12 g/L (Descoins et al. 2006). A can of Coca-

Cola®, which is said to be the most carbonated soda, contains approximately 6.20 g/L or 3.10 volumes of CO_2.

3.1.3. Carbon dioxide cleaning mechanism

Control experiments with hydrochloric acid and air were performed to help elucidate the CO_2 cleaning mechanism. Furthermore, given that some of the previous DI controls had shown reversible fouling, the concentration of the fouling solutions was increased to aim for irreversible fouling. At the same time, the concentration of sodium chloride was reduced to 7.5 g/L to decrease the osmotic pressure and allow for higher flux and greater fouling.

The air solution obtained the highest flux recovery (95%) for $CaSO_4$ whereas dissolved CO_2 was the most effective for $CaCO_3$ (102%) (Figure 6). It seems the $CaSO_4$ scaling solution did not cause irreversible fouling on the membrane; nevertheless, in the case of calcium carbonate which is a more tenacious kind of scaling, the acidic solution and air were not effective enough in comparison to carbon dioxide, obtaining flux recovery values of 46 and 63% respectively. This would suggest that mechanical action by CO_2 bubbles was important in the cleaning mechanism.

It is an interesting feature, on the other hand, that a low pH cleaning regime was not effective according to our data; it did not perform better than DI water. Upon further look at the literature, HCl is presented as a useful chemical agent which should dissolve the precipitates (Zondervan & Roffel 2007). This would imply that the low pH of the CO_2 solution is a minor mechanism in scale removal as previously reported (Partlan 2013).

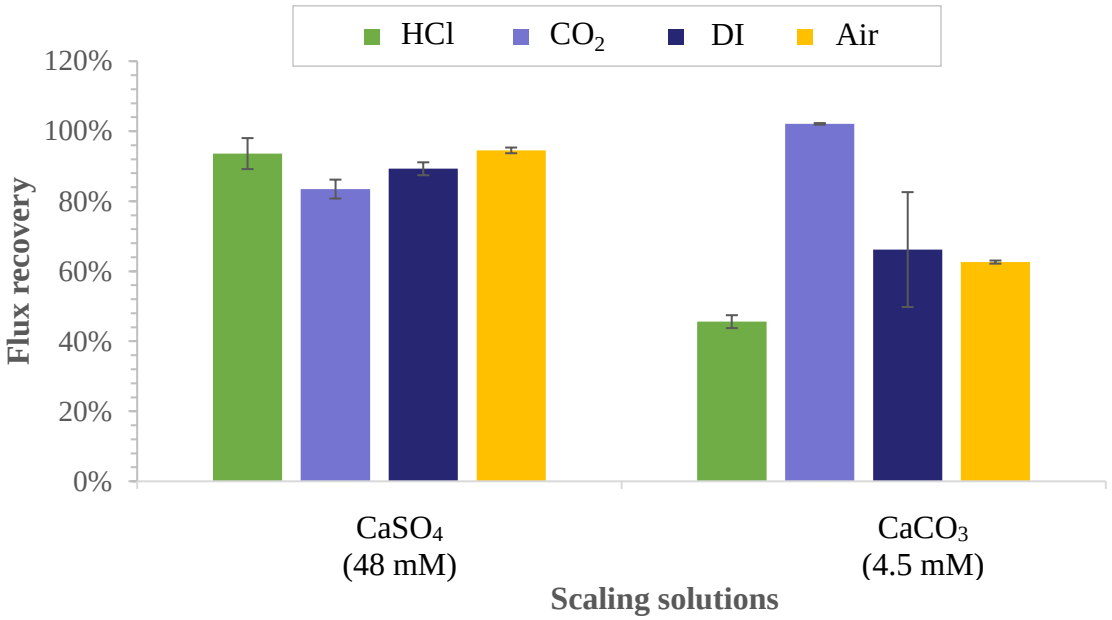

Figure 6. *Percentage of flux recovery for $CaSO_4$ and $CaCO_3$ using different cleaning methods and a control experiment. Each column represents the average value of the duplicates performed, whereas the error bars show the individual results.*

3.1.4. Changes in pH

Changes in pH can alter the surface charge of the membrane, thus affecting the level of rejection achieved (Childress & Elimelech 1996). For CPA membranes, a pH higher than 8.50 or close to 4-5 can cause a decrease in rejection (Cadotte et al. 1980). An experiment was therefore conducted to verify the membrane's rejection was not affected due to the combination of low pH and mechanical scouring during gas cleaning (i.e. our main objective was to rule out abrasion as an undesirable effect of exposure to the CO_2). A second scaling run was performed after the CO_2 cleaning and DI after cleaning, and the membrane's rejection levels were compared during both scaling runs. No significant difference (approximately between 1 and 2%) was observed between both rejection levels, thus supporting the idea that the membrane was not damaged by CO_2 cleaning.

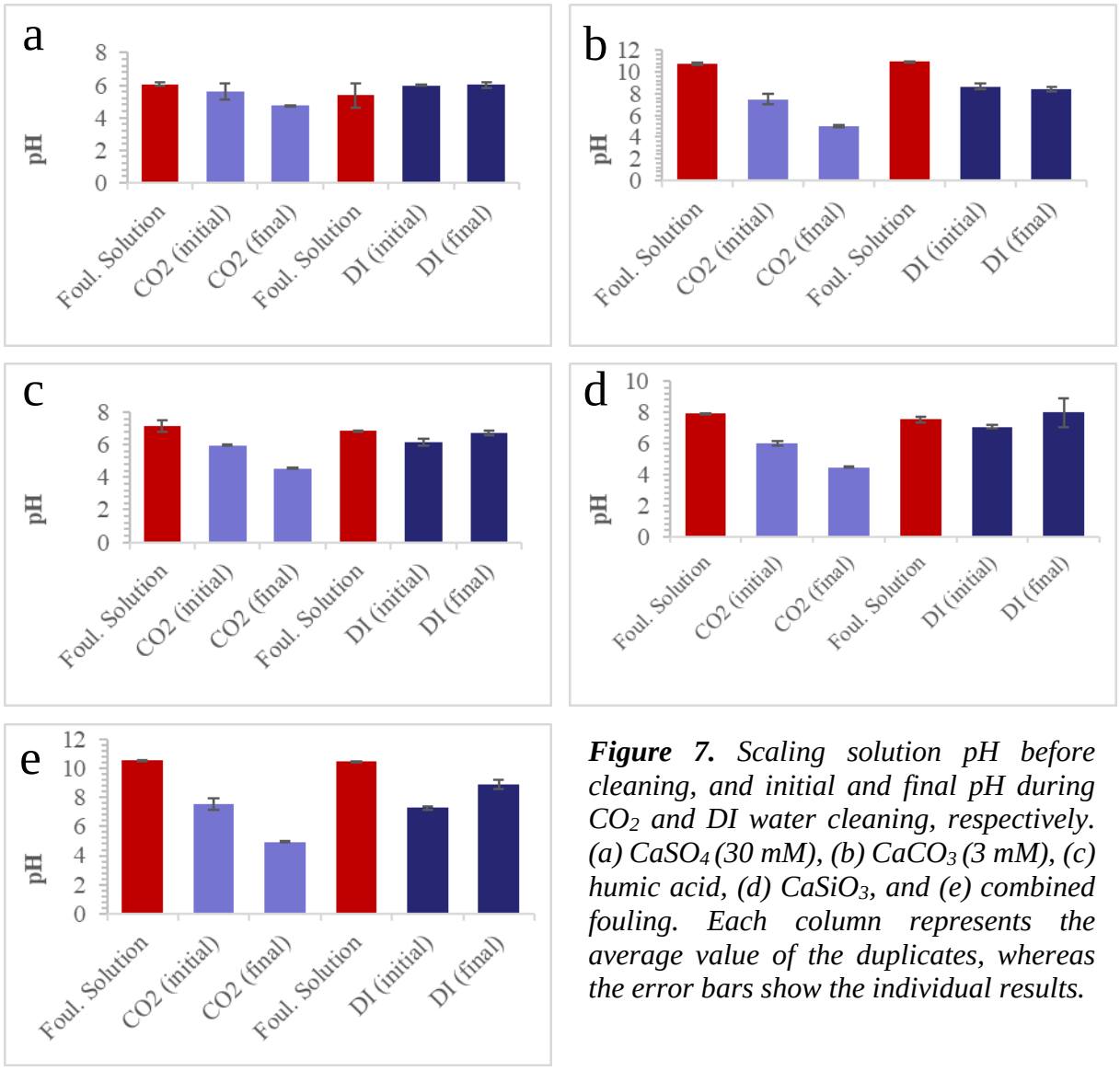

Figure 7. *Scaling solution pH before cleaning, and initial and final pH during CO_2 and DI water cleaning, respectively. (a) $CaSO_4$ (30 mM), (b) $CaCO_3$ (3 mM), (c) humic acid, (d) $CaSiO_3$, and (e) combined fouling. Each column represents the average value of the duplicates, whereas the error bars show the individual results.*

Figure 7 shows the average values of the different scaling solutions' pH, as well as the changes in pH after cleaning the membrane with CO_2 and DI water. There was a consistent drop during the gas sparging, going as low as 4.44 in one of the runs with $CaSiO_3$. Throughout the DI run, however, the pH would remain nearly constant (in the case of $CaSO_4$ for example, whose pH is close to DI water's pH) or increase (for instance, the combined fouling had a basic pH, so it is only logical the pH during the cleaning would

increase as some of the salts got swept by the water), with a minimum value of 5.80 when experimenting with $CaSO_4$.

3.2. Visual inspection - membrane autopsy

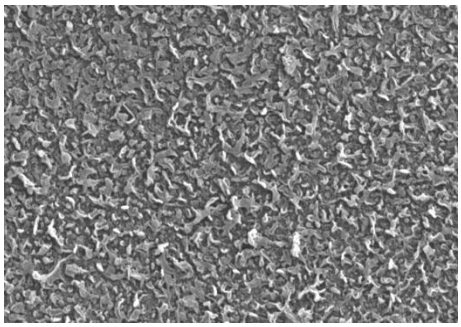

Figure 8. *SEM image of a clean RO membrane at 10,000x magnification.*

Figure 10 presents different SEM images showing scaled membranes and scaled membranes after cleaning at 10,000x magnification; for comparison, Figure 8 shows a clean membrane. All SEM images at 1,000x magnification can be found in Appendix F. The first picture (Figure 10a) shows one of the most common non-alkaline scales, calcium sulphate, which unlike alkaline and silica-based scales, is not dependent on the solution's pH and has relatively high solubility. $CaSO_4$ can mostly precipitate in three crystallographic forms: gypsum or calcium sulphate dihydrate form, plaster of Paris or calcium sulphate hemihydrates and calcium sulphate anhydrite (Lee & Lee 2000). At ambient temperatures of 20°C (which was the average temperature during the scaling step), gypsum is the predominant form with platelets and needles as its primary morphologies (Gilron & Hasson 1987; Uchymiak et al. 2008; Lee & Lee 2000). Based on SEM imaging, gypsum occurred as needles-like morphology (Figure 10a). From Figures 10b and c, we can see the membrane looks clean, thus suggesting a relatively weak foulant layer.

Figure 10d shows a membrane scaled with $CaCO_3$. One of the most common scales in RO membranes, it produced two crystal morphologies as revealed by SEM imaging at 10,000x magnification. The rhombohedral crystal appears to be calcite, while the semi spherical structure appears to be a vaterite crystal. The average calcite particle size is usually about 10 µm, whereas the diameter of vaterite particles ranges from 0.05 to 5 µm (Antony et al. 2011). These crystals were expected; in precipitation experiments, vaterite and calcite were formed at temperatures below 30°C (Partlan 2013), which is within the range of temperatures of the present scaling runs (approximately 18 to 21.5ºC). Calcite is the most thermodynamically stable crystal under ambient conditions; vaterite, on the contrary, is the least stable form but may be stabilized under certain temperature conditions or in the presence of other ions or inhibitors (Tzotzi et al. 2007; Antony et al. 2011).

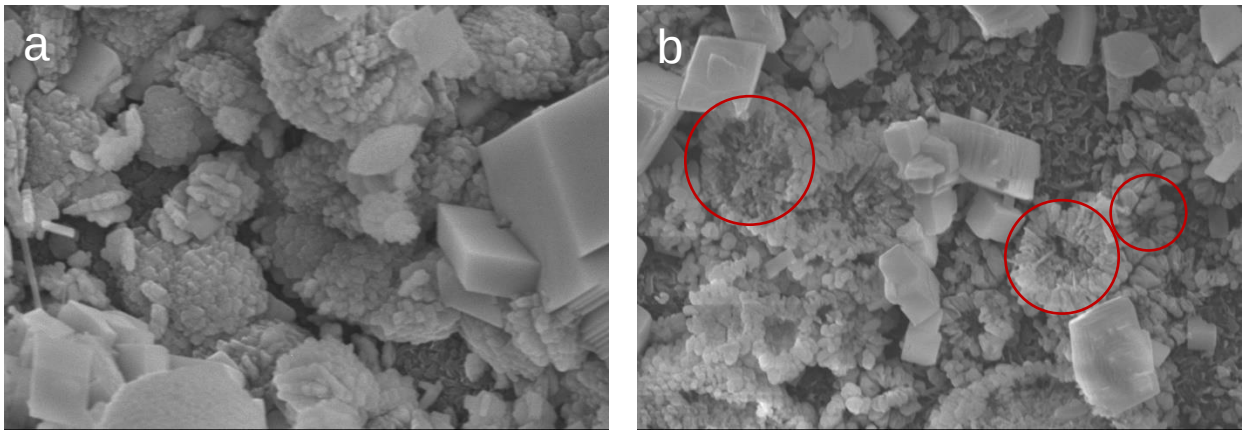

Figure 9. *SEM images at 10,000x magnification. (a) RO membrane scaled with $CaCO_3$, (b) RO membrane scaled with $CaCO_3$ cleaned with dissolved CO_2. Some of the morphological changes are highlighted with red circles.*

From Figure 10e, the scaling appears to have suffer a morphological change since it looks partially dissolved (see Figure 9). This can lead us to believe the CO_2 might have created a path within the deposits for the water to flow, thus obtaining a high flux recovery

value, as showed in Figures 5 and 6. We can see from Figure 10f that the membrane is covered by crystals which are intact, as opposed to Figure 10e where the CO_2 had partially dissolved them. This confirmed CaCO3 tenaciousness and adherence to the membrane.

Figure 10g shows a common silicate-based scale, $CaSiO_3$, which is dependent on the solution's pH. In this case, $CaSiO_3$ appears to be in a crystalline round shape as well as in a more amorphous form; silicate scaling on the membrane surface occurs when supersaturated silicic acid (H_2SiO_3) polymerizes to form insoluble colloidal or gel-like silica (Antony et al. 2011). As with Figure 10e, we believe once again the CO_2 might have created a path within the deposits for the water to flow (Figure 10h), whereas Figure 10i might suggest a relatively weak foulant layer.

Figure 10j shows combined fouling (i.e. the combination of $CaCO_3$, $CaSO_4$ and humic acid), which produced conglomerates of mostly semi spherical particles, covering the whole surface of the membrane. Figure 10k shows the same pattern as Figures 10e and h; it is noteworthy to mention that the CO_2 cleaning achieved in this case a flux recovery value of 105%. Even though scaling is observed on the membrane surface on Figure 10l, a flux recovery of 90% was achieved when flushing DI alone.

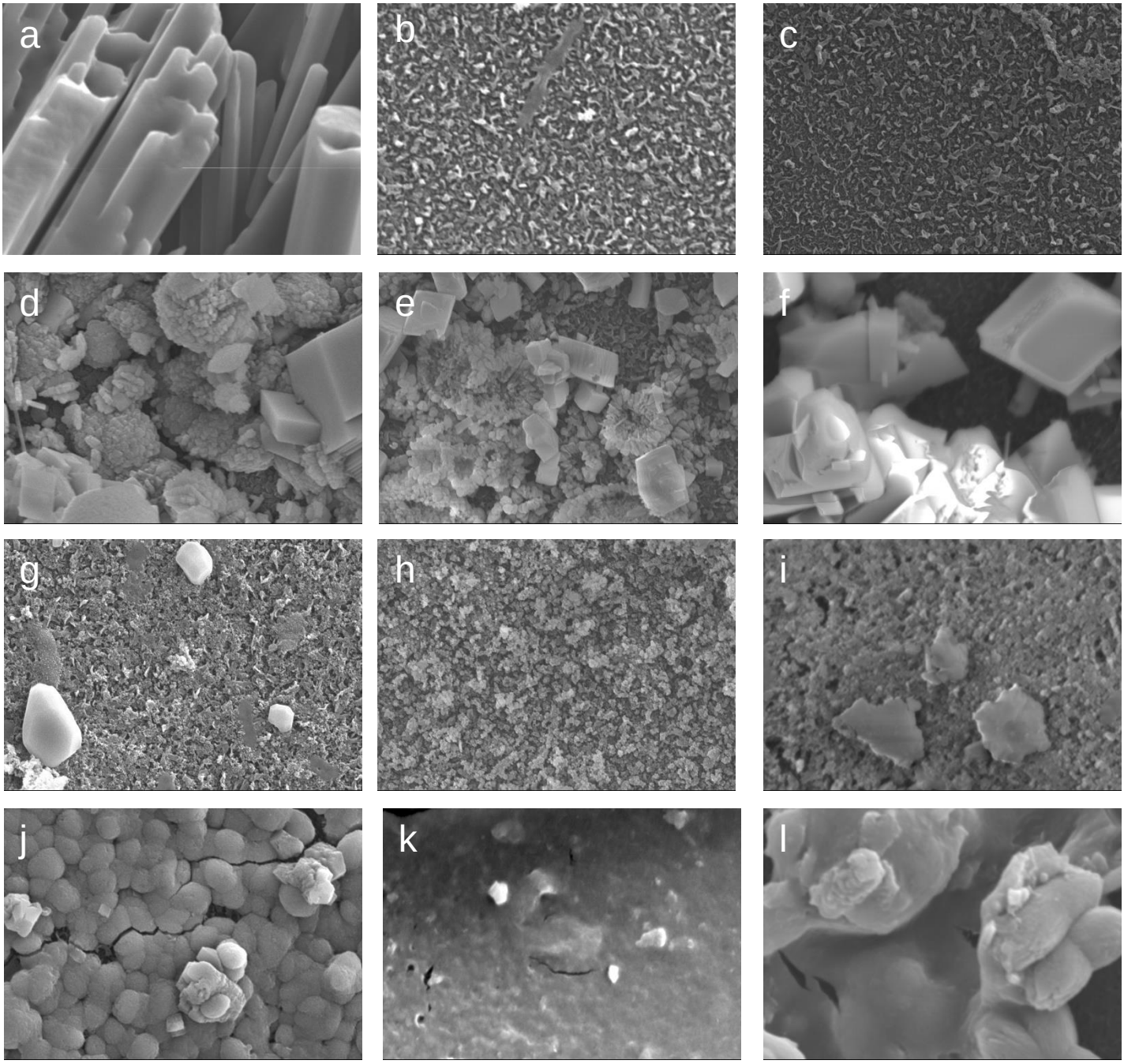

Figure 10. *SEM images of RO membranes at 10,000x magnification. (a) $CaSO_4$ scaled membrane, (b) $CaSO_4$ scaled membrane cleaned with dissolved CO_2, (c) $CaSO_4$ scaled membrane cleaned with DI, (d) $CaCO_3$ scaled membrane, (e) $CaCO_3$ scaled membrane cleaned with dissolved CO_2, (f) $CaCO_3$ scaled membrane cleaned with DI, (g) $CaSiO_3$ scaled membrane, (h) $CaSiO_3$ scaled membrane cleaned with dissolved CO_2, (i) $CaSiO_3$ scaled membrane cleaned with DI, (j) combined fouling ($CaCO_3$, $CaSO_4$ and humic acid) scaled membrane, (k) combined fouling scaled membrane cleaned with dissolved CO_2, and (l) combined fouling scaled membrane cleaned with DI.*

4. CONCLUSION

First and foremost, both objectives were accomplished. Single foulant scaling and a multi-component study were conducted, determining the flux recovery efficiency of the different cleaning methods. The present research showed that dissolved CO_2 effectively cleaned scaled membranes, with an average flux recovery of 92.5 ± 33.7% for membranes scaled with $CaSO_4$, 95.0 ± 29.4% for $CaCO_3$, 103.1 ± 25.6% for humic acid, 94.6 ± 24.0% for $CaSiO_3$ and 107.9 ± 8.5% for combined fouling. DI, on the other hand, achieved flux recovery values of 80.5 ± 4.6%, 51.8 ± 0.4%, 107.1 ± 25.9%, 81.2 ± 33.6%, and 88.9 ± 15.2%, respectively. A caveat in this work is that some of the experiments resulted in relatively weak foulant layers that could be removed with DI flushing alone, suggesting that some of the scaling recipes should be modified and re-tested, as described in the following section.

It is also noteworthy to highlight the performance of the saturation tank, even though measurements showed a 10% efficiency (delivering 1.027 g CO_2/kg of solution); the pressure allowed the gas to pass through the membrane, thus helping shear the foulants away. The scaling solution that was most tenacious was $CaCO_3$. Neither an acidic solution (pH 4) nor air sparging were able to clean the membrane as thoroughly as CO_2; this supports the hypothesis that mechanical action by CO_2 bubbles was important in the cleaning mechanism.

5. FUTURE WORK

Considering the potential benefits of CO_2, it is necessary to continue exploring the potential of this cleaning method to assess its efficiency. It is important to determine whether the CO_2 cleaning can be enhanced using additives; considering some foulants might be difficult to remove (e.g. silica-based scales), modification of the feed water characteristics (i.e. pretreatment, chemical consumption) might produce scales more amenable to CO_2 cleaning and achieve better results. One study showed that an insignificant addition of "greener" solvents such as ethyl alcohol or isopropyl alcohol combined with CO_2 gave satisfactory results in removing oils from MF membranes allowing to increase the process rate and cleaning efficiency, as well as reduce energy consumption (Michałek et al. 2015). Adding surfactants to water could be another alternative; these reduce the water's superficial tension, thus enhancing bubble formation and subsequent growth (Coffey 2008).

CO_2 could also be used as part of backwash in MF/UF membranes. It is also useful to find a way to add the gas to the feed during pumping through the membrane; not only could dissolved CO_2 be used for membrane cleaning but for scale prevention. The current bench-scale system would only allow us to conduct this if the pressure was kept below 1,172 kPa (170 psi); the use of a pump that could withstand a higher pressure would make continuous operation feasible (Partlan 2013).

Additionally, testing of water samples from full-scale plants should be performed; multi-component systems will allow us to study if there are any synergistic effects on crystallization and deposition mechanisms of inorganic fouling on membranes. Pilot plant

testing would let us compare advantages and disadvantages (e.g. capital and operation costs, system complexity, sustainability, energy use) of dissolved CO_2 against cleaning methods in place. Other gases with solubility similar to that of CO2 could be tested as well (i.e. ammonium). Moreover, optimization of operating conditions is required for better control in a cost-effective way (e.g. operating pressure, cleaning time). A study suggested that the membrane cleaning with CO_2 occurred within the first minutes, even though the cleaning was performed for 15 minutes (Ngene et al. 2010). The crossflow velocity is another important factor since it influences the scale formation; as it increases, the concentration polarization ratio decreases (thus leading to a decreased rate of surface crystallization) but high crossflow velocity requires high energy consumption (Oh et al. 2009). Performing mass balances would also let us quantify the amount of scaling, allowing us to optimize the operational parameters.

Membrane modification may be another promising strategy to reduce foulants and membrane interaction and thus improve the fouling reversibility that eases the membrane cleaning (She et al. 2016).

APPENDICES

APPENDIX A: Additional background information

Table A.1. Properties and identification methods of selected foulants (Source: *She et al. 2016*).

Types of Fouling	Foulants	Examples	Size and shape	Charge	Characterization method
Colloidal and organic fouling	Polysaccharides	Alginate	200-2000 kDa, extended random coil	Negatively charged, ~3 meq/g (up to 6 meq/g)	Colorimetric method (phenol-sulfuric acid method at UV of 485 nm)
		Xanthan and gellan	100-2500 kDa, linear	Negatively charged	(1) TOC and UV254. (2) LC-OCD and 3D FEEM (or 3D FTIR)
		Schizophyllan	400-500 kDa, rigid rod-like	Neutral	Using protein assay kit to analyze at UV562
	Humic substance	Humic acid (IHSS)	Mw of a few kDa to a few hundred kDa. Globular molecule (linear under high pH, low ionic strength, and low concentration)	Negatively charged (pH_{pzc}=3), typical total acidity: 5-10 meq/g	
	Proteins	Bovine serum albumin (BSA)	67 kDa	pH_{IEP}=4.7 (total acidity 1.5 meq/g including both carboxylic and amine groups)	
		Bovine immunoglobulin G	155 kDa	pH_{IEP}=6.6	

Types of Fouling	Foulants	Examples	Size and shape	Charge	Characterization method
Colloidal and organic fouling	Inorganic colloids	Bovine hemoglobin	68 kDa	pH_{IEP}=7.1	SEM-EDX
		Bovine pancreas ribonuclease A	13.7 kDa	pH_{IEP}=7.8	
		Lysozyme	14.4 kDa	pH_{IEP}=11.0	
		Silica	Round	Negatively charged (pH_{pzc}=3)	
		Aluminum silicate minerals	Angular	Negatively charged at pH~7	
		Ferric oxides/hydroxide	Varies depending on crystalline or amorphous	Positively charged, pH_{pzc} for goethite ~9	
	Others	Transparent exopolymer particles (TEP)	Transparent, sticky, and amorphous substances. Exists in different forms (e.g. strings, disks, sheets, fibers) and sizes (up to 100 s of mm long).	-	(1) Microscopic enumeration, and (2) Colorimetric determination. Both methods are based on staining with alcian blue.
		Latex	Mean diameter of 3 μm, nearly monodispersed spherical shape	-	-
Inorganic scaling	Inorganic scales	Calcium sulphate (or Gypsum)	Needle-like and plate-like	Non-alkaline scale that is pH independent	SEM-EDX

Note: "-" indicates not available.

Types of Fouling	Foulants	Examples	Size and shape	Charge	Characterization method
Inorganic scaling		Calcium carbonate	Varied from forms. Calcite: 10 µm, rhombohedral; aragonite clusters: outward oriented needles; vaterite: 0.05 to 5 µm, spherical.	Alkaline scale that is dependent on the bicarbonate alkaline and pH	
		Calcium phosphate	Amorphous	Alkaline scale that is dependent on the bicarbonate alkaline and pH	
		Silicate scale	Crystalline	The formation of silica scale is dependent on the pH	
Biofouling	Bacteria	Pseudomonas	Rod-shaped	-	Polymerase chain reaction (PCR) denaturing gradient gel electrophoresis (PCR-DGGE) and Fluorescence in Situ Hybridization
		E. Coli	Rod-shaped	-	
		Corynebacterium	Rod-shaped	-	
		B. subtilis	Rod-shaped	-	
	Fungi	Penicillium	Brush-like and flask-shaped	-	
		Trichoderma	Divergent and flask-shaped	-	
	Microalgae	Chlorella sorokiniana	Cell diameter ~5 µm	Negatively charged at pH 7.2	

Note: "-" indicates not available.

Table A.2. Categories of cleaning agents, applications and action mechanisms (Source: *Coutinho de Paula & Amaral 2017)*.

Categories	Application	Mechanism of action	Cleaning agent
Acids	Removal of inorganic salt deposits	Hydrolysis or dissolution or chelation (Zondervan & Roffel 2007)	Hydrochloric acid (HCl) Citric acid ($C_6H_8O_7$) Phosphoric acid (H_3PO_4)
Alkalis	Removal of inorganic colloids (silt), silica and metal silicates Removal of organic fouling and biofilms	Hydrolysis and solubilization. Electrostatic interactions between the inlay and the negatively charged membranes when the pH of the solution is high (D'Souza et al. 2005)	Sodium hydroxide (NaOH)
Chelating agents	Removal of metal oxides	Metal ion adsorption agents. Breaking the structural integrity of divalent cations, removal of the anchor layer on the fouling layer, which serves as binding agents for organic molecules (Ang et al. 2011a)	Tetra-sodium salt of ethylene-diaminetetraacetic acid (Na_4EDTA) Citric acid ($C_6H_8O_7$) Oxalic acid ($H_2C_2O_4$)
Surfactants	Removal of organic fouling and biofilms	These have both hydrophilic and hydrophobic groups and are semi-soluble in organic and aqueous solvents. Can solubilize macromolecules by the formation of micelles around them, which help clean the surface of the dirty membrane (Ang et al. 2011b)	Sodium salt of dodecyl sulphate (Na-SDS)
Inert salts	Removal of organic hydrophilic forming of gel	These promote swelling of the fouling layer in the presence of a salt solution, and reaction and ion exchange with the Na+ polysaccharide-calcium complex on the fouling layer (Lee & Elimelech 2007)	Sodium chloride (NaCl) Sodium nitrate ($NaNO_3$) Sodium sulphate (Na_2SO_4) Potassium chloride (KCl)
Biocides	Microbiological growth inhibition	Metabolic inactivation of microorganisms (Matin et al. 2011)	Sodium bisulphite ($NaHSO_3$) Sodium metabisulphite ($Na_2S_2O_5$) Hydrogen peroxide (H_2O_2)

APPENDIX B: Saturation tank vs pressure vessel

This appendix will describe all the differences between Partlan's work in 2013 and the present research. The first difference is related to the bench scale set up. Figure B.1 shows the bench scale apparatus used by Partlan; the vertically installed cylindrical pressure vessel was replaced by the saturation tank. The previous method of entrainment involved bubbling CO_2 into the pressurized vessel pre-filled with 7.5 liters of water (this volume was selected to avoid rapid pressurization). Bubbling was then achieved by slowly leaking CO_2 into the pressure vessel until the headspace reached a target pressure of 500 psi.

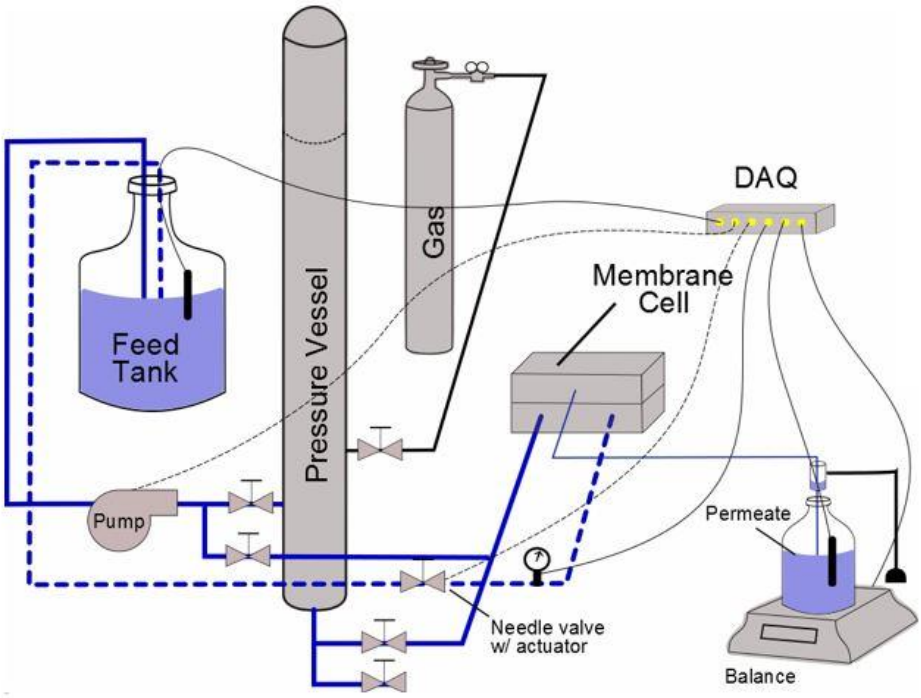

Figure B.1. *Partlan's bench-scale apparatus. A series of valves allowed for flow either through the pressure vessel or directly to the membrane. From the membrane, flows splitted into permeate (thin blue line) and concentrate (dotted blue line). The concentrate was returned to the feed tank for continuous operation. In total recycle mode, the permeate was manually returned to the feed tank to maintain feed concentration. Dashed lines from DAQ represent computer control of pump speed and needle valve opening; solid lines represent data input to DAQ from conductivity probes and balance.*

After reaching 500 psi, the valve between the pressure vessel and the line to the gas cylinder was closed to ensure no leakage of gas into or out of the pressure vessel. The total run time from 500 psi to a final pressure of 180 psi in the pressure vessel was 7.5 minutes. In the present research, on the other hand, the saturation tank was filled with 5.66 L of water and the amount of time necessary to empty itself was on average about 15 minutes, with an initial and final headspace pressure of 827 and 345 kPa (120 psi and 50 psi) respectively. This shows our cleaning was conducted under a lower pressure and with a lower amount of water, but lasted twice the time.

A carbon dioxide dissolution system (CDOX®, BlueInGreen) was used, which comprises a gas and water panel, and a 7.54 L saturation tank (see Figures B.2 and B.3). The top set of pipes in the panel is connected to the pump which pushes the water from the feed tank into the saturation tank. Water is atomized and falls through the CO_2 headspace (see Figure b.1). The bottom set of pipes is connected to the carbon dioxide tank; the yellow coil air hose has a maximum pressure of 1,379 kPa (200 psi). Water and gas tubing maximum pressure is 1,207 kPa (175 psi). The saturation tank also includes a mechanical pop-off (cryogenic safety pressure relief valve) which is also set at 1,207 kPa (175 psi).

Another difference to Partlan's work involves the scaling solutions tested. Whereas Partlan used alkaline and silica-based scaling solutions (i.e. $CaCO_3$ and $CaSiO_3$), we decided to also test $CaSO_4$ (suggested by Partlan on her thesis), humic acid, and combined fouling using $CaSO_4$, $CaCO_3$ and humic acid.

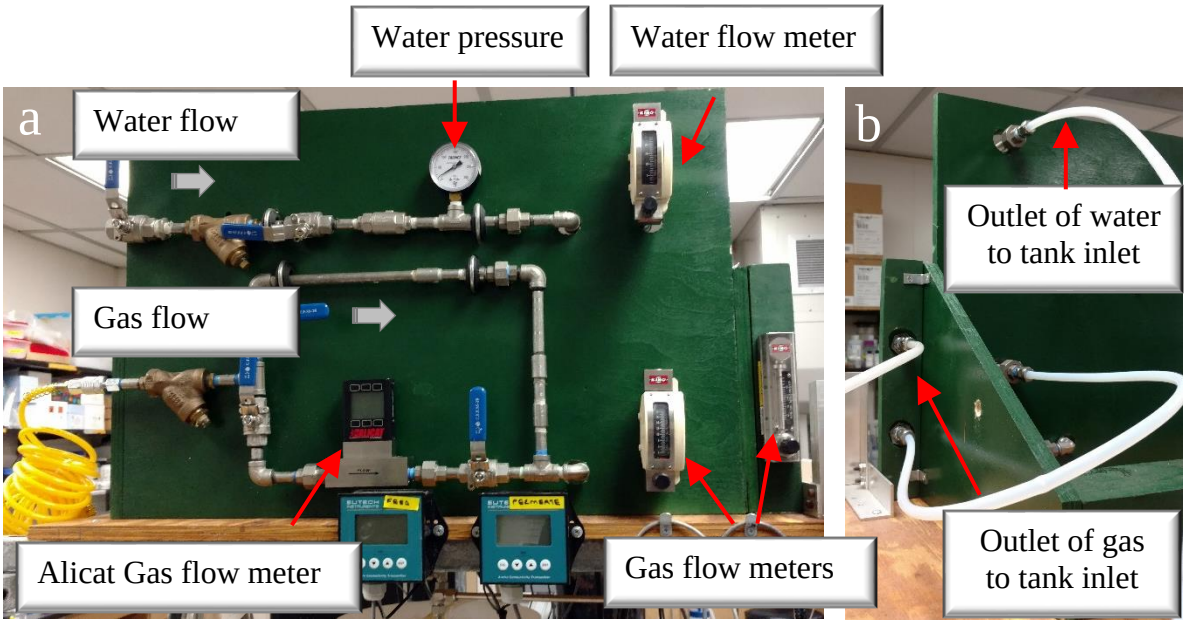

Figure B.2. *(a) Front and (b) back of gas and water panel.*

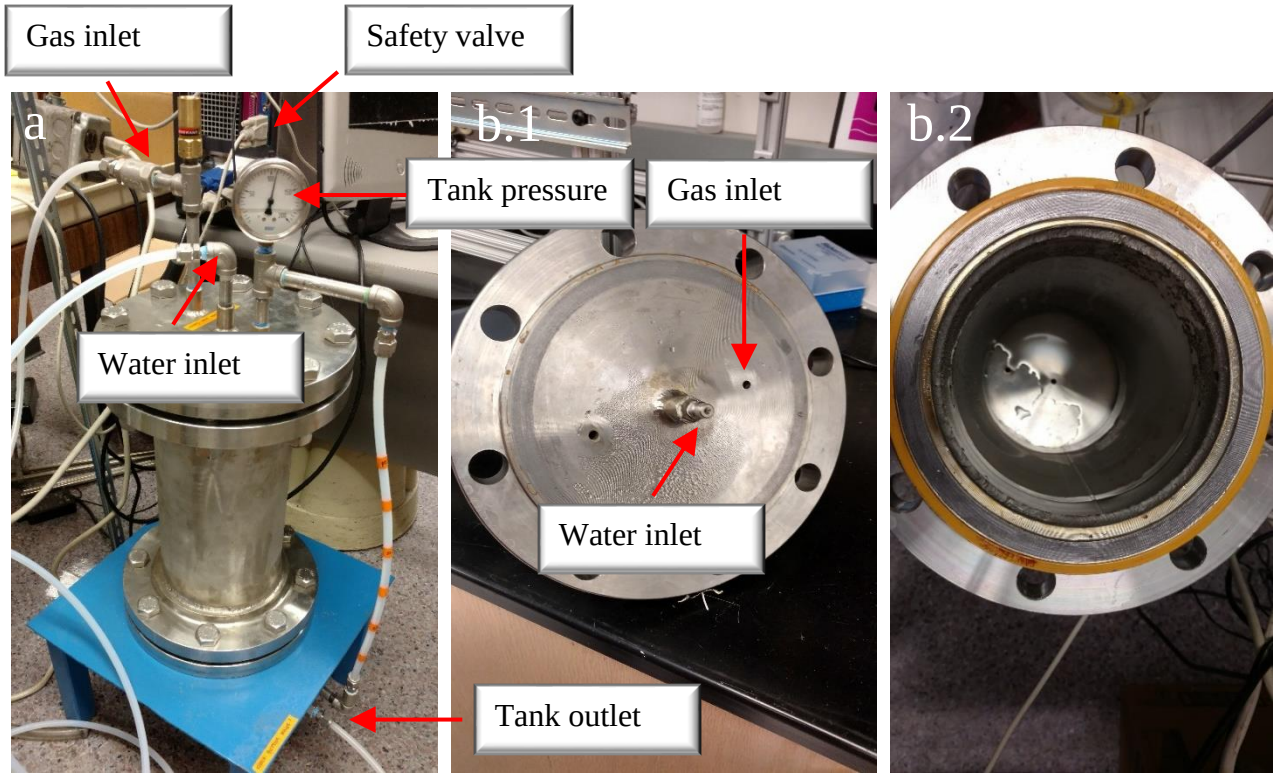

Figure B.3. *(a) Exterior and (b) interior of the saturation tank, including (b.1) top and (b.2) bottom of the saturation tank.*

The flux recovery values were also calculated using different equations. Instead of using Equation 1, Partlan basically calculated the flux recovery as the flux regained by cleaning relative to the flux lost due to scale (see Equation 2 and Figure B.4).

$$R = \frac{J_f}{J_i} \quad (1)$$

$$R = \frac{J_f - J_{as}}{J_i - J_{as}} \quad (2)$$

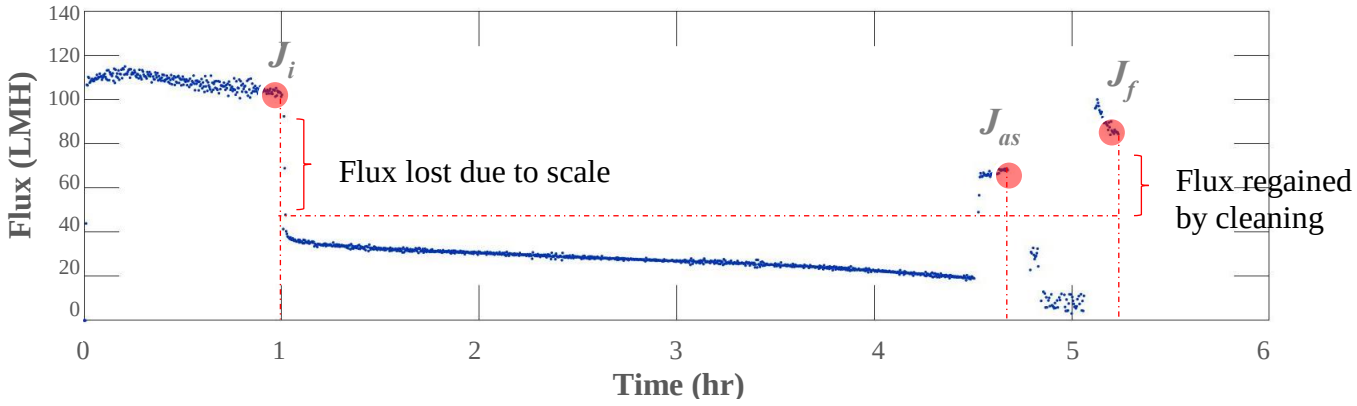

Figure B.4. *Example of a permeate flux plot showing the values used to calculate flux recovery according to Partlan's equation.*

From Figures B.5 and B.6, we observe the same trends with either equation, however, flux recovery values using Partlan's equation were generally lower than using the current equation. Overall, the same trends were also observed when comparing both sets of data (see Figure B.7). Nevertheless, flux recovery values using the saturation tank were higher than when using the pressure vessel. As previously stated, this might suggest the fouling solution used in 2013 was probably more tenacious, thus, harder to clean. The complete data set for $CaSiO_3$ was not available, which I why a direct comparison was not possible.

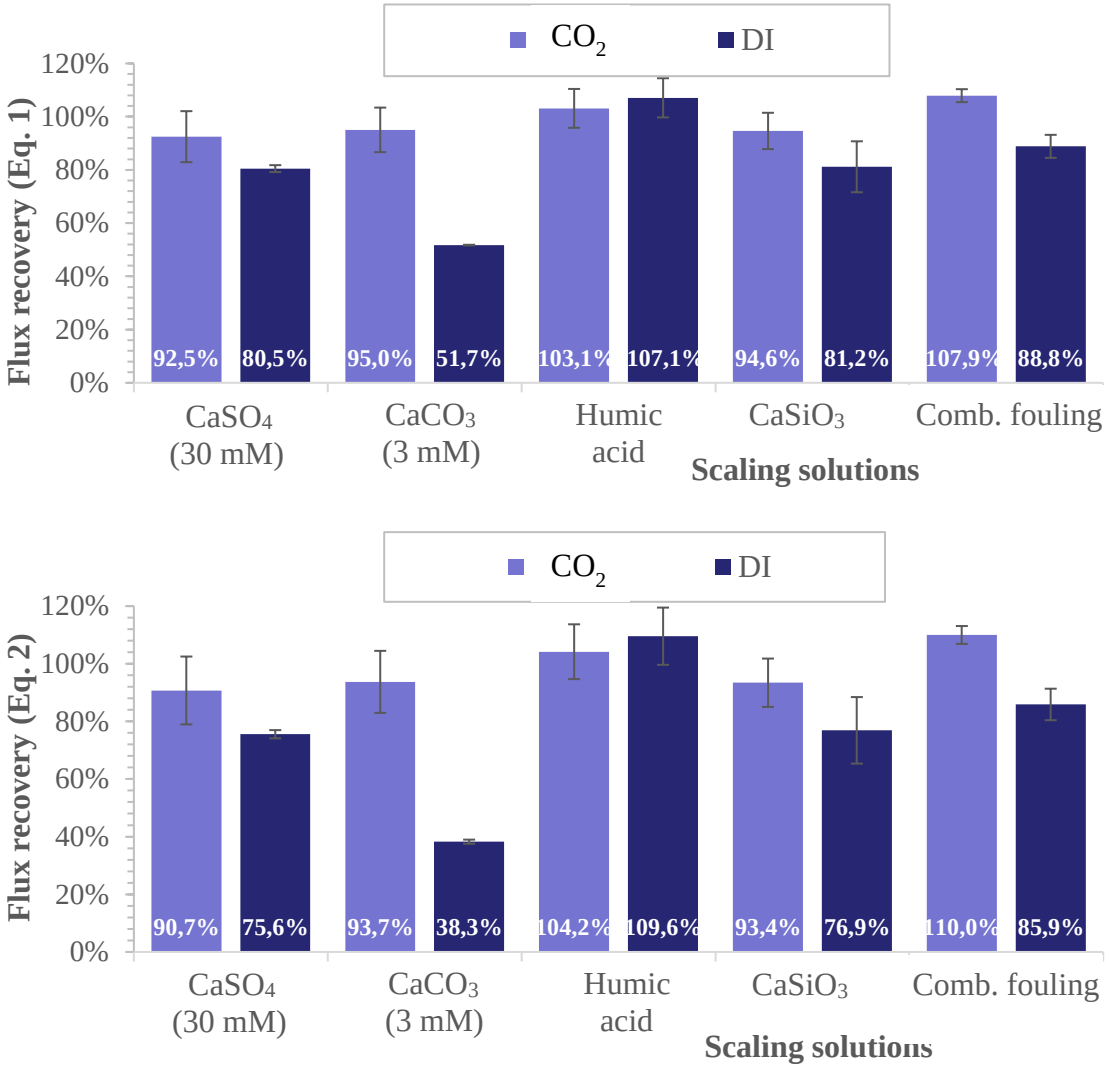

Figure B.5. *Percentage of flux recovery for each scaling solution after CO_2 cleaning and DI water control using (a) Equation 1 and (b) Equation 2 (Partlan, 2013). Each column represents the average value of the duplicates performed, whereas the error bars show the individual results.*

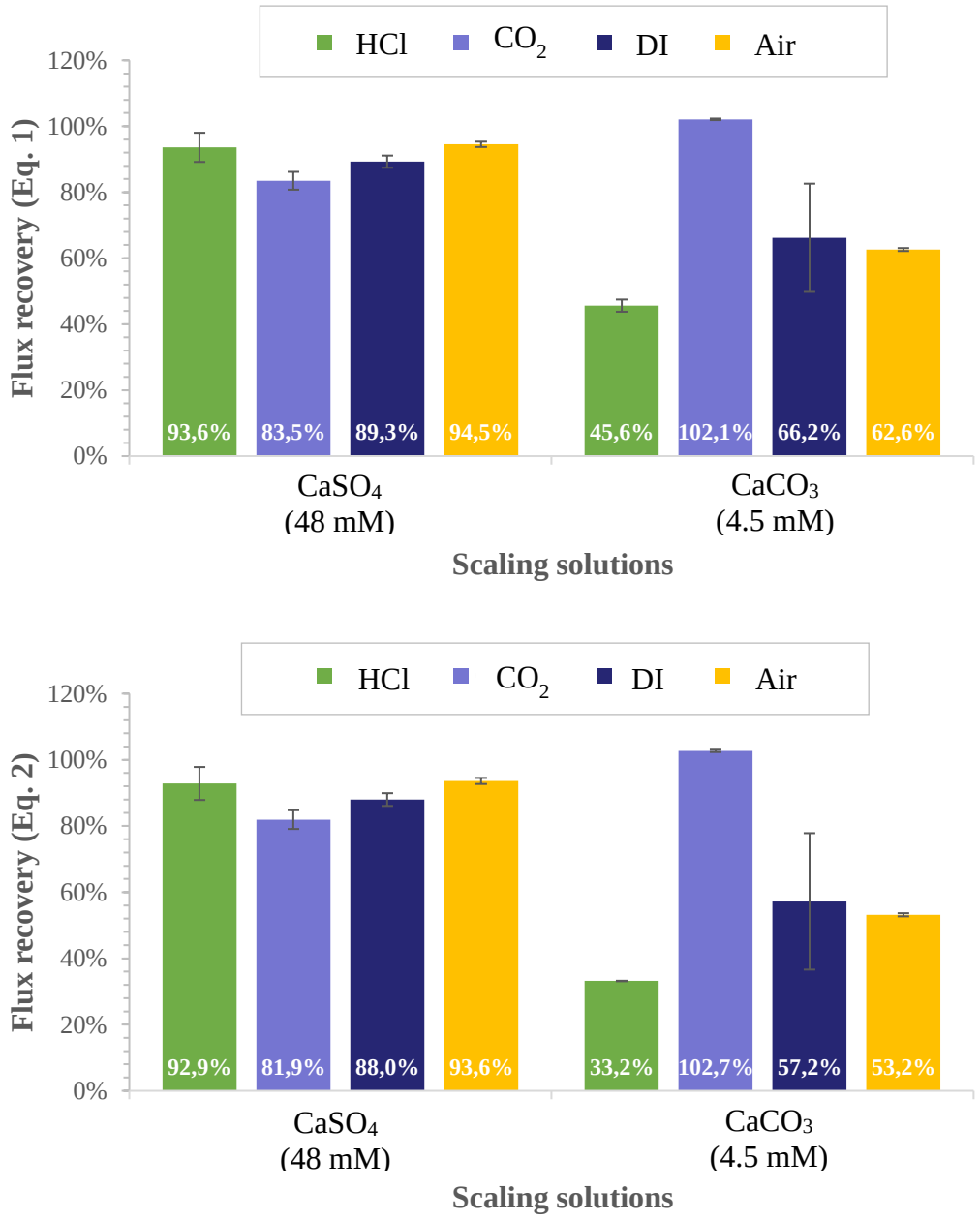

Figure B.6. *Percentage of flux recovery for $CaSO_4$ and $CaCO_3$ using (a) Equation 1 and (b) Equation 2 (Partlan, 2013). Each column represents the average value of the duplicates performed, whereas the error bars show the individual results.*

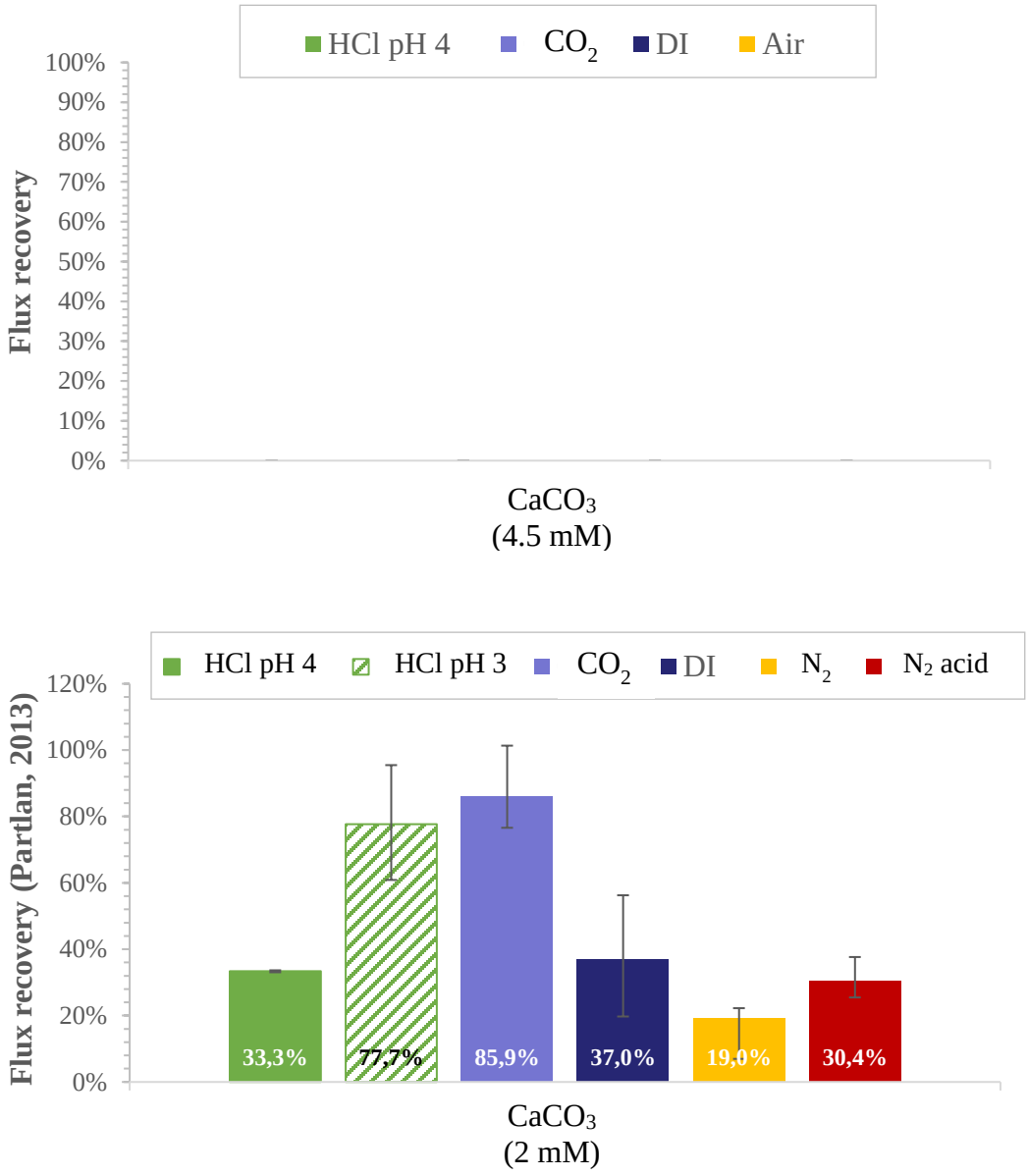

Figure B.7. *Direct comparison of flux recovery values to Partlan's data in 2013, using $CaCO_3$. Each column represents the average value of the experiments performed, whereas the error bars show the individual results.*

APPENDIX C: RO membrane

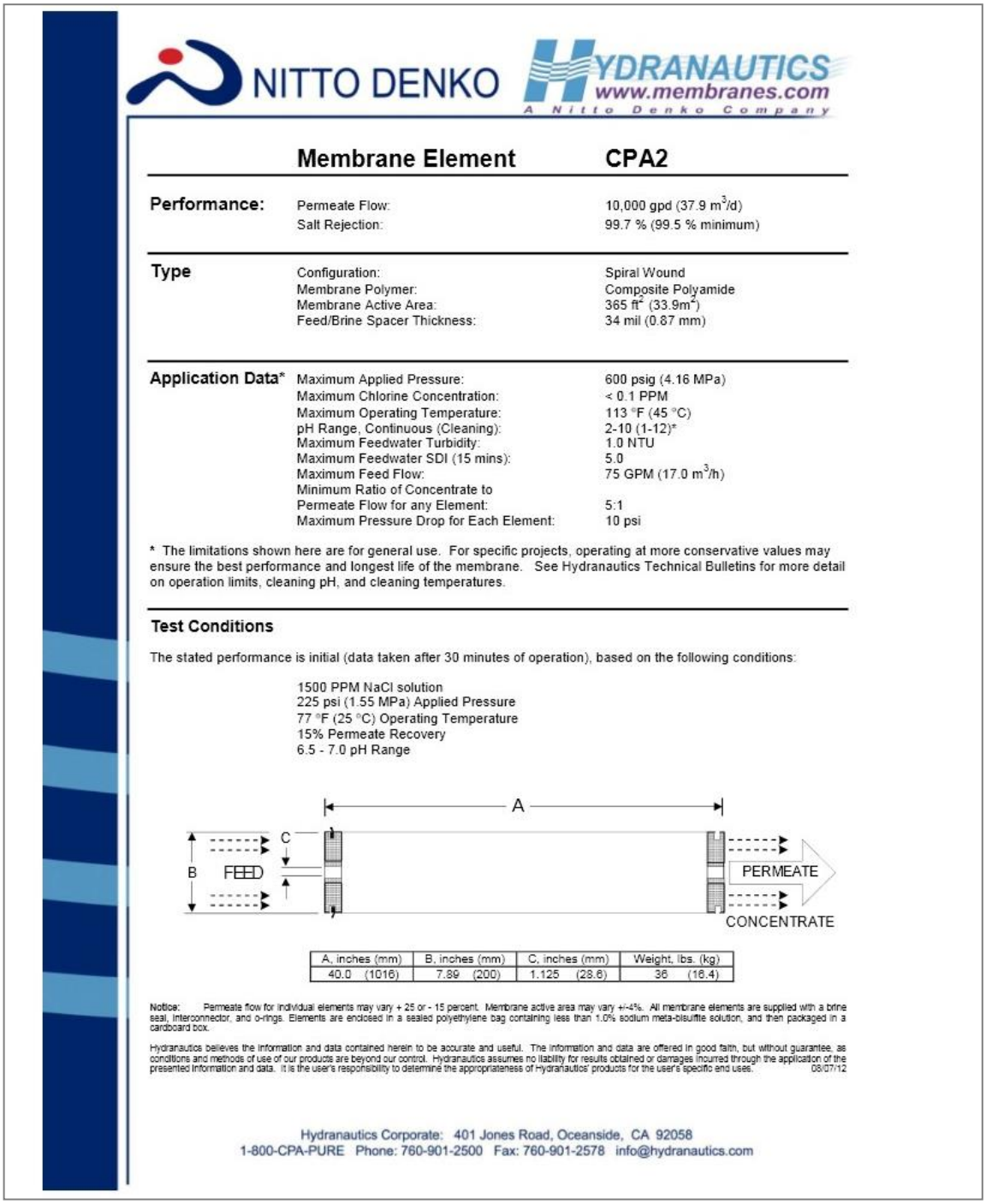

NITTO DENKO HYDRANAUTICS www.membranes.com A Nitto Denko Company

	Membrane Element	CPA2
Performance:	Permeate Flow:	10,000 gpd (37.9 m^3/d)
	Salt Rejection:	99.7 % (99.5 % minimum)
Type	Configuration:	Spiral Wound
	Membrane Polymer:	Composite Polyamide
	Membrane Active Area:	365 ft^2 (33.9m^2)
	Feed/Brine Spacer Thickness:	34 mil (0.87 mm)
Application Data*	Maximum Applied Pressure:	600 psig (4.16 MPa)
	Maximum Chlorine Concentration:	< 0.1 PPM
	Maximum Operating Temperature:	113 °F (45 °C)
	pH Range, Continuous (Cleaning):	2-10 (1-12)*
	Maximum Feedwater Turbidity:	1.0 NTU
	Maximum Feedwater SDI (15 mins):	5.0
	Maximum Feed Flow:	75 GPM (17.0 m^3/h)
	Minimum Ratio of Concentrate to Permeate Flow for any Element:	5:1
	Maximum Pressure Drop for Each Element:	10 psi

* The limitations shown here are for general use. For specific projects, operating at more conservative values may ensure the best performance and longest life of the membrane. See Hydranautics Technical Bulletins for more detail on operation limits, cleaning pH, and cleaning temperatures.

Test Conditions

The stated performance is initial (data taken after 30 minutes of operation), based on the following conditions:

1500 PPM NaCl solution
225 psi (1.55 MPa) Applied Pressure
77 °F (25 °C) Operating Temperature
15% Permeate Recovery
6.5 - 7.0 pH Range

A, inches (mm)	B, inches (mm)	C, inches (mm)	Weight, lbs. (kg)
40.0 (1016)	7.89 (200)	1.125 (28.6)	36 (16.4)

Notice: Permeate flow for individual elements may vary + 25 or - 15 percent. Membrane active area may vary +/-4%. All membrane elements are supplied with a brine seal, interconnector, and o-rings. Elements are enclosed in a sealed polyethylene bag containing less than 1.0% sodium meta-bisulfite solution, and then packaged in a cardboard box.

Hydranautics believes the information and data contained herein to be accurate and useful. The information and data are offered in good faith, but without guarantee, as conditions and methods of use of our products are beyond our control. Hydranautics assumes no liability for results obtained or damages incurred through the application of the presented information and data. It is the user's responsibility to determine the appropriateness of Hydranautics' products for the user's specific end uses. 08/07/12

Hydranautics Corporate: 401 Jones Road, Oceanside, CA 92058
1-800-CPA-PURE Phone: 760-901-2500 Fax: 760-901-2578 info@hydranautics.com

Figure C.1. *CPA2 membrane specifications.*

APPENDIX D: Monitoring data

D.1 Monitoring data from LabView

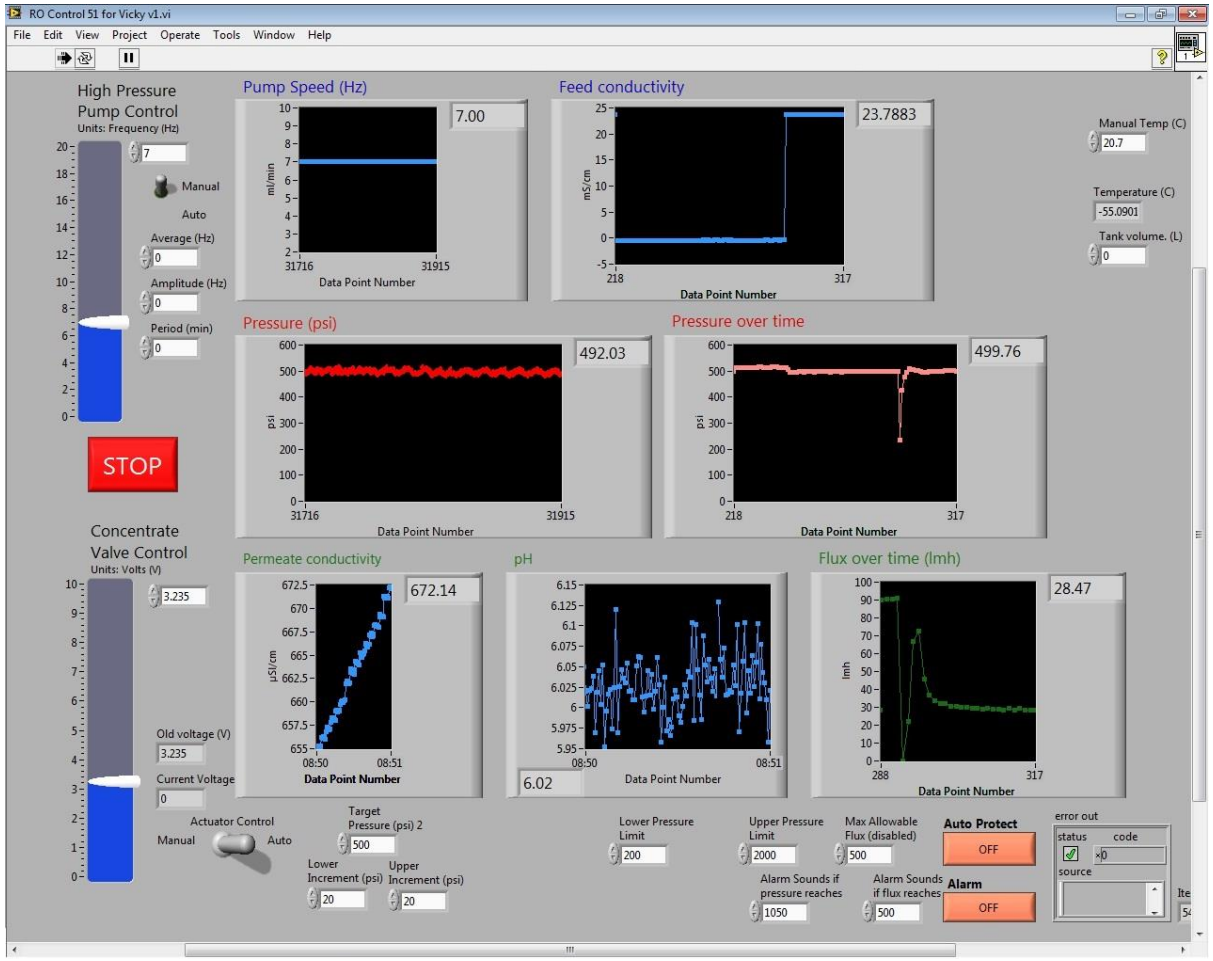

Figure D.1. *Screenshot of LabView's interface during a typical run.*

D.2 Monitoring data from MATLAB

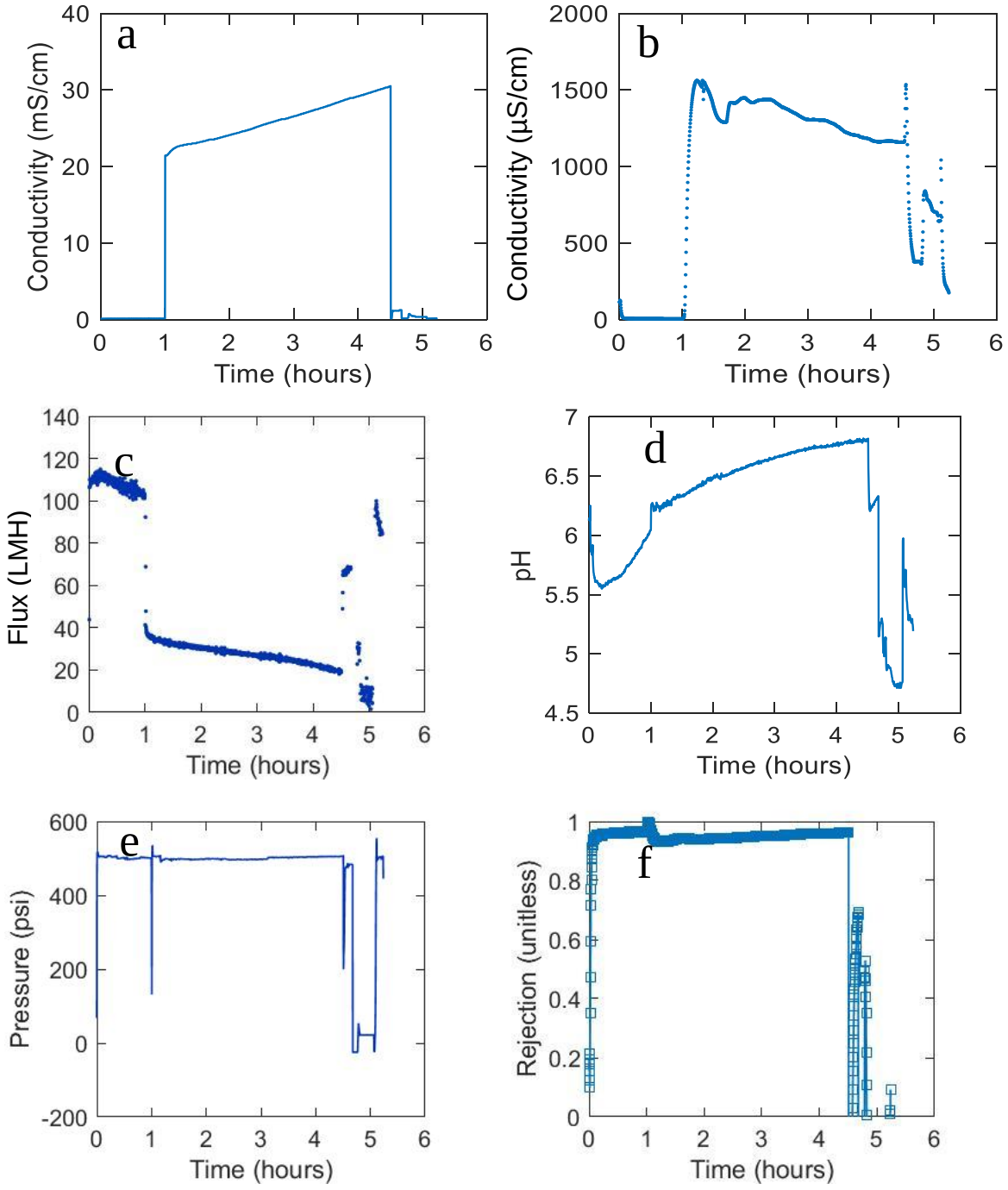

Figure D.2. *Example of plots monitored during a typical run, (a) feed and (b) permeate's conductivity; (c) permeate's flux; (d) pH; (e) system's pressure; and (f) membrane's rejection. Runs consisted of five different stages, in this case as follows: membrane compaction (0 to 1 hr), scaling run (1 to 4.5 hr), DI water after scaling (4.5 to 4.65 hr), cleaning (4.65 to 4.95 hr), and DI water after cleaning (4.90 to 5.10 hr).*

Table D.1. Operational parameters

Parameter	Units	Value	
Pressure (system)	kPa	3,447	
	psi	500	
Temperature	ºC	~ 18-21.5	
Flow	mL/min	~ 950	
		(CO_2)	(Air)
Pressure (saturation tank)	kPa	758-862	793-1,172
	psi	110-125	130-170
Cleaning	min	~ 15 (gas) 30 (chemical)	

APPENDIX E: Carbon dioxide measurements

E.1 Carbon dioxide measurements

As mentioned in section 2.6.1, two approaches were used to calculate the concentration of dissolved carbon dioxide in water. One of them used the sample's pH and the system's equilibrium constant (*K*) to calculate the amount of carbonic acid was calculated (which translated into the amount of carbon dioxide). On a pH between 4 and 6, carbonic acid is the predominant form, which is produced when CO_2 gets in contact with water, as shown in the following equations.

$$CO_2 + H_2O \leftrightarrow H_2CO_3 \quad (1)$$

$$H_2CO_3 \leftrightarrow H^+ + HCO_3^- \quad (2)$$

$$HCO_3^- \leftrightarrow H^+ + CO_3^{-2} \quad (3)$$

$$K = \frac{[H^+][HCO_3^-]}{[H_2CO_3]} = 4.47E^{-07} \quad (4)$$

The second method made use of those same water samples and a carbon dioxide test kit (LaMotte). A standard alkali was used to titrate the water samples to an indicator's endpoint. The test result was directly read from the titrator, recording it as ppm of carbon dioxide.

E.1.1 Test kit instructions

1. A test tube was filled to 20 mL line with sample water, avoiding splashing or prolonged contact with air.

2. Two drops of phenolphthalein indicator, 1% were added to the test tube. If the solution remained colorless, step 3 would follow. If the solution turned red, this meant no free carbon dioxide was present.

3. A direct reading titrator was filled with carbon dioxide reagent B. The titrator was then inserted into the center hole of the titration tube cap.

4. While gently swirling the tube, carbon dioxide reagent B was added, one drop at a time, until a faint pink color was produced and persisted for 30 seconds.

   The test result was directly read from the titrator, recording it as ppm of carbon dioxide.

Note: due to the high amount of carbon dioxide in the saturation tank, several dilutions were necessary to perform this test.

E.2 Carbon dioxide results

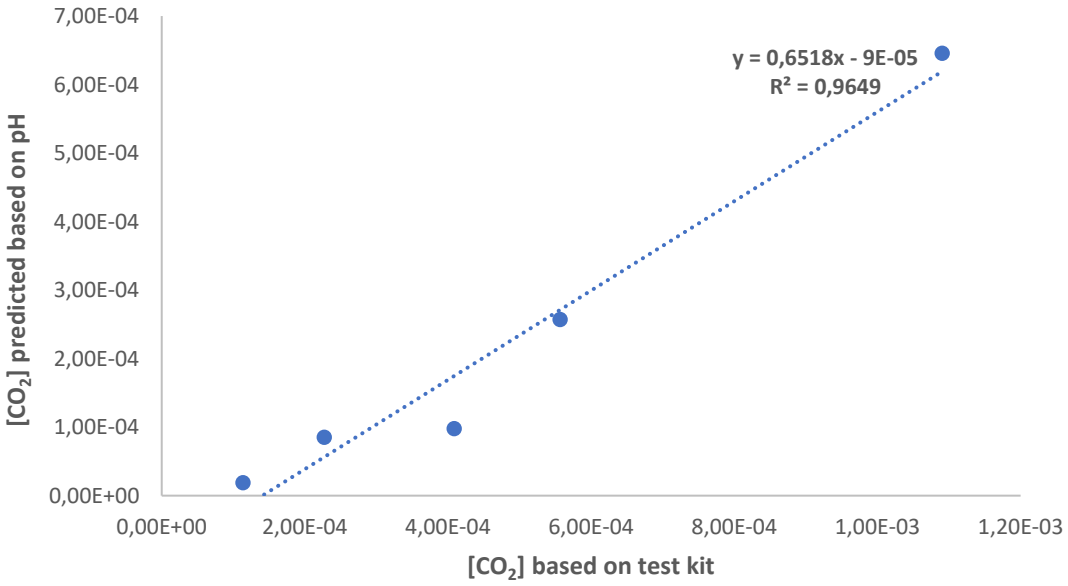

Figure E.1. *Correlation between test kit and pH's measurement results.*

Table E.1. *Actual and maximum theorical concentration of dissolved CO_2 (dCO_2).*

Sat Tank Pressure (psi)	Max theoretical dCO_2 (mg/L)	Max theoretical dCO_2 (g/L)	Actual dCO_2 (mg/L)	Actual dCO_2 (g/L)
125	15,564	16	14,786	14.8
120	15,004	15	14,254	14.3
115	14,444	14	13,722	13.7
110	13,884	14	13,190	13.2
100	12,764	13	12,126	12.1
90	11,644	12	11,062	11.1
80	10,524	11	9,998	10.0
70	9,404	9	8,934	8.9
60	8,284	8	7,870	7.9
50	7,164	7	6,806	6.8
Average	**11,868**	**11.9**	**11,274**	**11.3**

APPENDIX F: Additional results section

F.1 Quantitative data

Table F.1. Summary of experimental runs sorted by scaling solution.

		Scaling solution			(1)	(2)		Membr. Rejection			(3)		(4)		(5)	
Scaling solution	Cleaning solution	pH	Feed Cond. (i)	Feed Cond. (f)	Initial DI Flux	Scaling Flux (i)	Scaling Flux (f)	Min	Max	Ave	DI after scaling	Cleaning Flux	Cleaning pH (i)	Cleaning pH (f)	DI after cleaning	R
$CaCO_3$ (12 mM)	CO_2	11.1	13.0	34.4	99.3	40.8	17.7	94.4	99.9	95.6	88.2	7.7	9.2	5.6	101.2	101.9
$CaCO_3$ (3 mM)	CO_2	10.9	15.3	22.9	94.6	41.8	20.6	87.0	99.7	97.3	55.2	6.7	7.1	4.9	82.0	86.7
$CaCO_3$ (3 mM)	CO_2	10.7	15.3	21.6	93.5	45.8	22.2	94.7	100.0	95.2	56.5	7.1	7.9	5.2	96.6	103.4
$CaCO_3$ (3 mM)	CO_2	10.9	13.8	23.8	90.7	44.7	21.2	93.3	99.8	94.5	64.8	8.1	7.5	5.1	94.0	103.6
$CaCO_3$ (3 mM)	DI	10.9	14.7	21.5	94.6	42.1	19.6	95.3	99.8	96.1	48.6	49.5	8.4	8.2	48.8	51.6
$CaCO_3$ (3 mM)	DI	11.0	14.8	21.4	87.2	43.3	20.0	94.5	99.9	95.4	45.3	44.9	8.9	8.6	45.2	51.9
$CaCO_3$ (3 mM)	DI	10.8	15.4	21.7	95.0	44.5	20.8	96.0	100.0	96.6	48.2	48.5	7.6	9.3	50.0	52.7
$CaCO_3$ (3 mM)	N/A	10.8	14.7	20.8	89.5	45.8	22.5	92.9	97.5	93.9	-	-	-	-	-	-
$CaCO_3$ (4.5 mM)	Air	10.8	15.1	28.0	95.4	44.2	17.3	95.2	99.9	95.9	67.0	9.3	9.5	5.6	80.5	84.3
$CaCO_3$ (4.5 mM)	Air	10.7	15.8	23.6	98.2	50.9	19.9	93.4	99.8	94.4	53.8	3.2	7.7	6.9	61.9	63.1

Scaling solution	Cleaning solution	Scaling solution			(1)	(2)		Membr. Rejection			(3)		(4)		(5)	
		pH	Feed Cond. (i)	Feed Cond. (f)	Initial DI Flux	Scaling Flux (i)	Scaling Flux (f)	Min	Max	Ave	DI after scaling	Cleaning Flux	Cleaning pH (i)	Cleaning pH (f)	DI after cleaning	R
$CaCO_3$ (4.5 mM)	Air	10.7	15.0	24.4	100.0	50.0	20.0	94.1	99.9	95.5	54.7	2.8	6.9	7.7	62.2	62.2
$CaCO_3$ (4.5 mM)	Air	10.6	15.5	17.4	85.3	45.6	14.2	96.6	99.9	97.7	54.0	10.2	6.3	7.2	87.7	102.9
$CaCO_3$ (4.5 mM)	CO_2	10.9	12.2	15.7	68.6	39.5	29.3	93.6	99.9	94.5	58.8	7.6	8.0	5.1	101.0	147.2
$CaCO_3$ (4.5 mM)	CO_2	11.0	12.1	32.7	98.1	46.9	13.3	91.6	99.9	93.1	92.1	9.4	8.3	5.2	110.7	112.8
$CaCO_3$ (4.5 mM)	CO_2	10.8	12.4	13.8	96.9	57.5	22.8	84.5	99.8	85.7	39.4	8.6	7.5	5.1	99.1	102.3
$CaCO_3$ (4.5 mM)	CO_2	10.9	12.4	19.9	68.7	45.5	22.7	90.9	99.9	92.2	52.2	6.8	8.1	5.1	90.6	131.9
$CaCO_3$ (4.5 mM)	CO_2	10.9	12.2	26.0	89.4	44.8	17.8	90.6	99.7	92.1	55.6	6.9	7.3	5.1	91.1	101.9
$CaCO_3$ (4.5 mM)	DI	10.9	12.1	24.8	93.8	48.3	19.5	90.3	99.9	92.0	60.7	48.1	8.2	9.9	46.7	49.8
$CaCO_3$ (4.5 mM)	DI	10.9	12.1	28.1	90.8	43.5	19.5	96.7	99.3	97.4	72.3	73.9	8.5	9.5	75.0	82.6
$CaCO_3$ (4.5 mM)	HCl 4	5.6	21.5	22.9	95.4	40.7	10.4	94.4	99.9	96.5	27.9	76.6	4.1	4.1	85.1	89.2
$CaCO_3$ (4.5 mM)	HCl 4	10.9	12.5	16.0	99.5	53.1	21.3	90.7	99.9	91.5	41.4	42.8	4.3	4.0	47.2	47.5
$CaCO_3$ (4.5 mM)	HCl 4	10.5	12.3	22.7	82.0	50.9	25.2	91.2	99.8	92.1	69.1	73.9	4.4	4.1	75.6	92.2
$CaCO_3$ (4.5 mM)	HCl 4	10.9	12.1	23.9	97.1	43.3	15.3	85.5	99.1	88.5	40.9	39.1	4.0	4.0	42.5	43.8

Scaling solution	Cleaning solution	Scaling solution			(1)	(2)		Membr. Rejection			(3)		(4)		(5)	
		pH	Feed Cond. (i)	Feed Cond. (f)	Initial DI Flux	Scaling Flux (i)	Scaling Flux (f)	Min	Max	Ave	DI after scaling	Cleaning Flux	Cleaning pH (i)	Cleaning pH (f)	DI after cleaning	R
$CaCO_3$ (4.5 mM)	N/A	10.7	14.6	20.4	92.9	45.9	18.4	94.7	99.6	95.0	-	-	-	-	-	-
$CaCO_3$ (6 mM)	CO_2	11.0	12.6	19.4	84.9	48.8	15.2	93.9	99.9	95.2	36.3	6.6	7.3	5.1	69.0	81.2
$CaCO_3$ (6 mM)	HCl 4	10.9	12.6	24.3	91.1	44.4	22.0	92.9	99.8	94.4	70.6	74.0	4.3	4.1	79.0	86.7
$CaCO_3$ + $CaSO_4$	CO_2	10.4	17.3	25.4	98.2	39.5	19.3	92.0	100.0	92.7	81.1	7.8	7.6	5.3	97.6	99.4
$CaCO_3$ + $CaSO_4$	CO_2	10.5	18.0	31.6	97.3	38.4	18.9	94.3	100.0	94.7	83.5	8.4	7.6	5.2	99.7	102.5
$CaSiO_3$	CO_2	7.9	15.2	30.7	93.6	44.9	17.4	95.0	99.9	97.5	68.5	6.8	6.2	4.5	82.2	87.8
$CaSiO_3$	CO_2	8.0	14.6	32.2	92.5	43.8	17.5	96.3	100.0	97.6	75.9	6.6	5.9	4.4	93.8	101.5
$CaSiO_3$	CO_2	7.9	15.9	29.3	97.0	46.6	18.2	94.0	99.7	97.7	63.5	6.1	5.7	4.5	78.0	80.4
$CaSiO_3$	DI	7.4	15.7	33.1	94.7	44.8	17.1	95.6	100.0	96.9	66.8	67.3	7.2	8.9	67.8	71.6
$CaSiO_3$	DI	7.9	15.1	28.1	89.7	45.2	22.0	92.6	99.9	96.9	77.7	84.3	6.2	6.7	84.1	93.8
$CaSiO_3$	DI	7.7	14.7	31.2	93.5	45.5	18.7	95.3	99.7	97.6	80.9	82.9	6.9	7.1	84.9	90.8
$CaSiO_3$	DI	7.9	14.8	30.3	90.2	44.2	17.6	95.0	100.0	97.6	68.9	70.3	6.8	6.5	69.6	77.2
$CaSiO_3$	DI	7.8	15.5	29.2	83.7	41.6	17.0	95.0	99.7	98.0	56.7	58.2	6.2	6.6	57.8	69.0

		Scaling solution			(1)	(2)		Membr. Rejection			(3)		(4)		(5)	
Scaling solution	Cleaning solution	pH	Feed Cond. (i)	Feed Cond. (f)	Initial DI Flux	Scaling Flux (i)	Scaling Flux (f)	Min	Max	Ave	DI after scaling	Cleaning Flux	Cleaning pH (i)	Cleaning pH (f)	DI after cleaning	R
$CaSiO_3$	N/A	7.9	15.5	28.1	94.2	44.7	21.9	95.8	99.9	97.1	-	-	-	-	-	-
$CaSO_4$ (30 mM)	Air	6.6	21.3	30.9	80.8	34.9	17.5	95.1	100.0	96.5	63.1	8.4	6.5	5.6	81.9	101.3
$CaSO_4$ (30 mM)	Air	6.4	21.5	30.8	88.4	37.3	18.1	95.0	99.9	96.6	67.4	4.8	6.1	5.7	84.1	95.1
$CaSO_4$ (30 mM)	CO_2	6.2	21.5	30.5	102.8	38.8	19.3	93.1	100.0	95.0	68.1	6.2	5.1	4.8	85.2	82.9
$CaSO_4$ (30 mM)	CO_2	5.9	21.3	31.0	85.8	32.1	14.8	94.0	100.0	95.4	61.4	7.0	6.1	4.7	87.5	102.1
$CaSO_4$ (30 mM)	CO_2	6.1	21.0	31.6	82.7	30.5	14.7	93.6	100.0	95.0	54.9	7.1	6.0	4.7	87.2	105.5
$CaSO_4$ (30 mM)	CO_2	6.3	21.2	31.3	93.8	38.8	19.0	91.7	99.9	93.6	74.5	8.3	6.3	4.9	87.8	93.6
$CaSO_4$ (30 mM)	DI	4.7	21.7	30.2	86.0	38.5	17.9	90.7	100.0	92.4	62.3	69.7	6.0	5.8	70.3	81.8
$CaSO_4$ (30 mM)	DI	6.2	20.7	30.8	90.4	36.8	17.7	92.3	99.9	94.8	65.0	71.9	6.0	6.2	71.6	79.2
$CaSO_4$ (30 mM)	DI	5.8	21.0	30.4	91.9	35.3	16.6	95.0	100.0	96.2	58.9	74.6	6.1	6.1	74.7	81.3
$CaSO_4$ (30 mM)	N/A	5.8	20.4	29.6	100.8	38.7	20.0	93.3	100.0	95.1	-	-	-	-	-	-
$CaSO_4$ (30 mM)	N/A	5.7	20.1	30.6	93.2	36.4	18.5	93.8	99.9	95.3	67.7	-	-	-	-	-
$CaSO_4$ (39 mM)	CO_2	6.0	19.4	22.2	102.4	38.4	15.6	91.5	99.9	93.5	37.4	7.5	5.9	4.6	92.6	90.5

		Scaling solution			(1)	(2)		Membr. Rejection			(3)		(4)		(5)	
Scaling solution	Cleaning solution	pH	Feed Cond. (i)	Feed Cond. (f)	Initial DI Flux	Scaling Flux (i)	Scaling Flux (f)	Min	Max	Ave	DI after scaling	Cleaning Flux	Cleaning pH (i)	Cleaning pH (f)	DI after cleaning	R
$CaSO_4$ (48 mM)	Air	6.3	23.8	25.8	90.6	33.1	12.5	91.7	99.9	93.0	35.6	7.9	6.1	4.6	84.9	93.7
$CaSO_4$ (48 mM)	Air	6.3	24.8	26.2	85.0	32.4	12.6	99.5	100.0	99.6	36.4	2.6	6.2	6.5	81.0	95.3
$CaSO_4$ (48 mM)	CO_2	5.8	21.0	22.3	91.2	37.1	7.2	92.8	100.0	94.3	22.9	7.3	5.8	4.6	90.6	99.3
$CaSO_4$ (48 mM)	CO_2	5.8	18.2	19.8	100.6	41.4	2.5	92.3	99.9	93.9	16.7	6.4	5.8	4.6	91.3	90.7
$CaSO_4$ (48 mM)	CO_2	6.3	21.4	22.9	99.8	39.1	9.2	90.6	100.0	92.2	25.8	6.4	5.8	4.6	86.0	86.2
$CaSO_4$ (48 mM)	CO_2	6.6	21.5	23.4	98.5	38.2	7.8	91.4	100.0	94.0	24.6	6.2	5.9	4.5	79.6	80.8
$CaSO_4$ (48 mM)	DI	6.3	21.2	22.9	94.2	38.6	11.2	90.5	99.9	93.0	31.4	75.4	6.0	7.2	85.9	91.1
$CaSO_4$ (48 mM)	DI	6.0	20.7	22.0	90.3	37.1	8.8	92.2	100.0	94.9	26.4	73.7	6.0	6.1	78.9	87.4
$CaSO_4$ (48 mM)	HCl 4	6.1	21.3	23.2	91.5	36.0	8.0	92.8	99.9	95.1	24.7	69.4	4.1	4.1	89.7	98.0
Comb. fouling	Air	10.1	18.2	21.5	90.6	42.7	21.4	96.3	100.0	97.3	62.6	2.6	7.0	7.4	70.8	78.1
Comb. fouling	CO_2	10.4	17.7	24.9	91.4	38.9	19.0	91.9	99.9	92.9	76.9	7.3	7.9	5.0	96.4	105.5
Comb. fouling	CO_2	10.6	18.3	25.8	90.8	39.3	19.2	93.6	99.9	94.2	86.8	1.4	7.1	4.9	100.2	110.3
Comb. fouling	CO_2	10.5	18.1	25.4	90.5	41.0	19.8	92.2	100.0	93.3	79.2	7.3	7.2	5.0	101.9	112.5

Scaling solution	Cleaning solution	Scaling solution			(1)	(2)		Membr. Rejection			(3)		(4)		(5)	
		pH	Feed Cond. (i)	Feed Cond. (f)	Initial DI Flux	Scaling Flux (i)	Scaling Flux (f)	Min	Max	Ave	DI after scaling	Cleaning Flux	Cleaning pH (i)	Cleaning pH (f)	DI after cleaning	R
Comb. fouling	DI	10.5	17.4	25.6	98.4	41.6	20.7	92.2	100.0	93.1	74.9	77.8	7.4	8.6	83.2	84.5
Comb. fouling	DI	10.5	17.3	25.5	98.9	43.3	20.8	88.6	99.9	90.8	76.6	88.5	7.2	9.2	92.1	93.2
Comb. fouling	DI	10.1	18.0	24.1	96.7	39.6	19.8	94.4	99.9	95.0	78.9	81.7	7.3	9.0	86.8	89.7
Comb. fouling	N/A	10.3	17.6	19.6	94.6	47.7	7.5	90.8	98.5	92.3	-	-	-	-	-	-
Humic acid	CO_2	7.5	15.3	27.9	96.1	48.3	23.0	94.8	99.9	96.1	91.6	8.3	5.9	4.5	106.2	110.4
Humic acid	CO_2	6.8	15.0	27.5	92.2	42.8	20.0	95.1	100.0	95.5	75.7	7.1	6.0	4.6	88.4	95.8
Humic acid	DI	6.8	14.2	9.6	87.8	47.3	22.8	89.1	99.9	95.9	82.5	88.0	5.9	6.6	100.5	114.4
Humic acid	DI	6.9	14.7	26.3	96.9	49.3	24.2	94.1	99.9	94.7	87.8	98.7	6.3	6.9	96.7	99.7
NaCl	DI	6.8	13.8	25.3	85.3	43.6	21.3	91.3	99.9	93.8	85.6	89.9	6.7	6.9	87.2	102.2
NaCl	DI	6.2	15.0	30.8	100.6	42.0	20.9	93.1	99.9	93.6	88.6	88.5	6.5	7.1	89.4	88.9

Note: the numbers (1)-(5) correspond to the different steps described on section 3.1 Flux recovery.

Experiments were conducted on a step-by-step process. Initially, only the membrane's compaction and the scaling runs were operated to learn how to operate the system. The second stage involved adding the DI water after scaling to learn how much fouling was caused by the scaling runs. Then came the cleaning of the membrane and finally, the DI water after cleaning was added to study the flux recovery. These experiments are presented in Table F.1. Different scaling solutions concentrations were tested and adapted as necessary to produce more fouling. Figures F.1-F.7 show the permeate flux plots for all the scaling solutions.

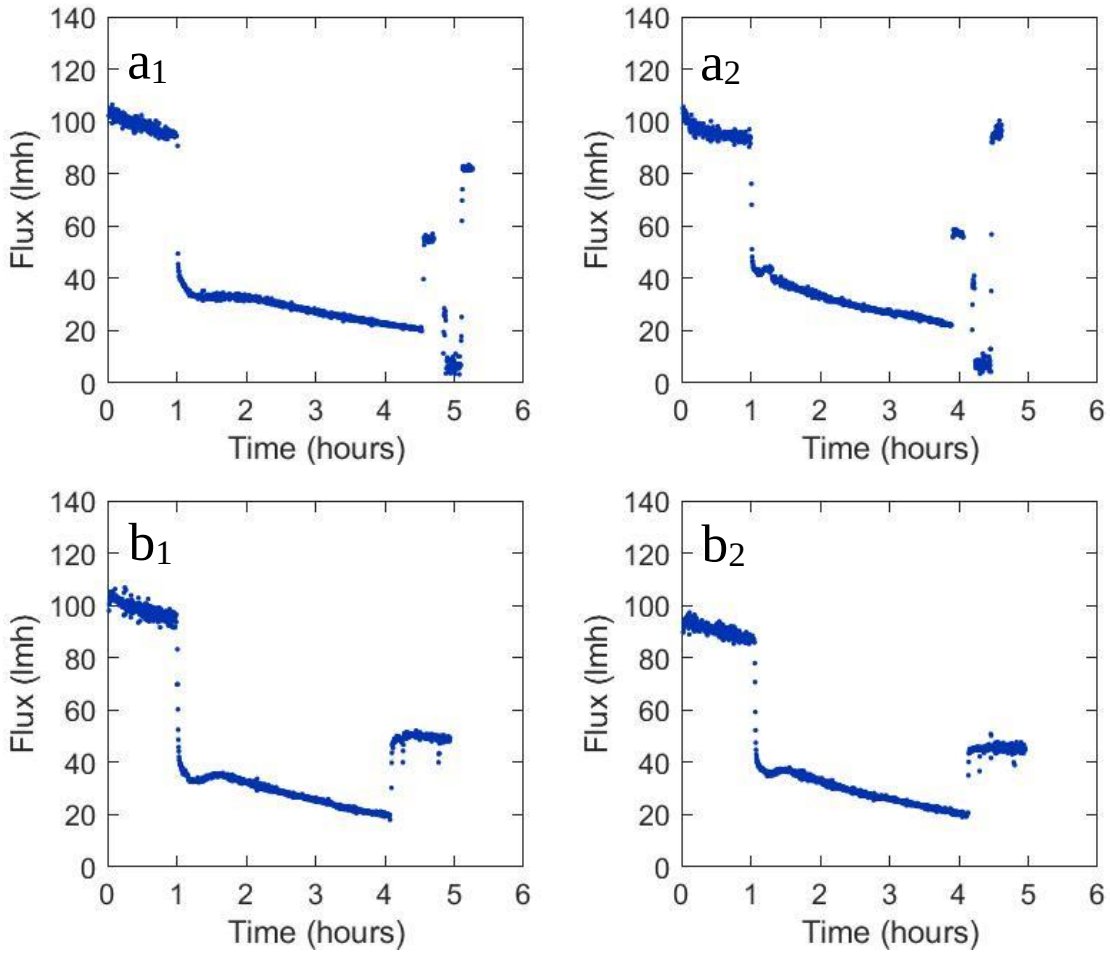

Figure F.1. *Permeate flux plots for 3 mM $CaCO_3$ using: (a) dissolved CO_2, and (b) DI water.*

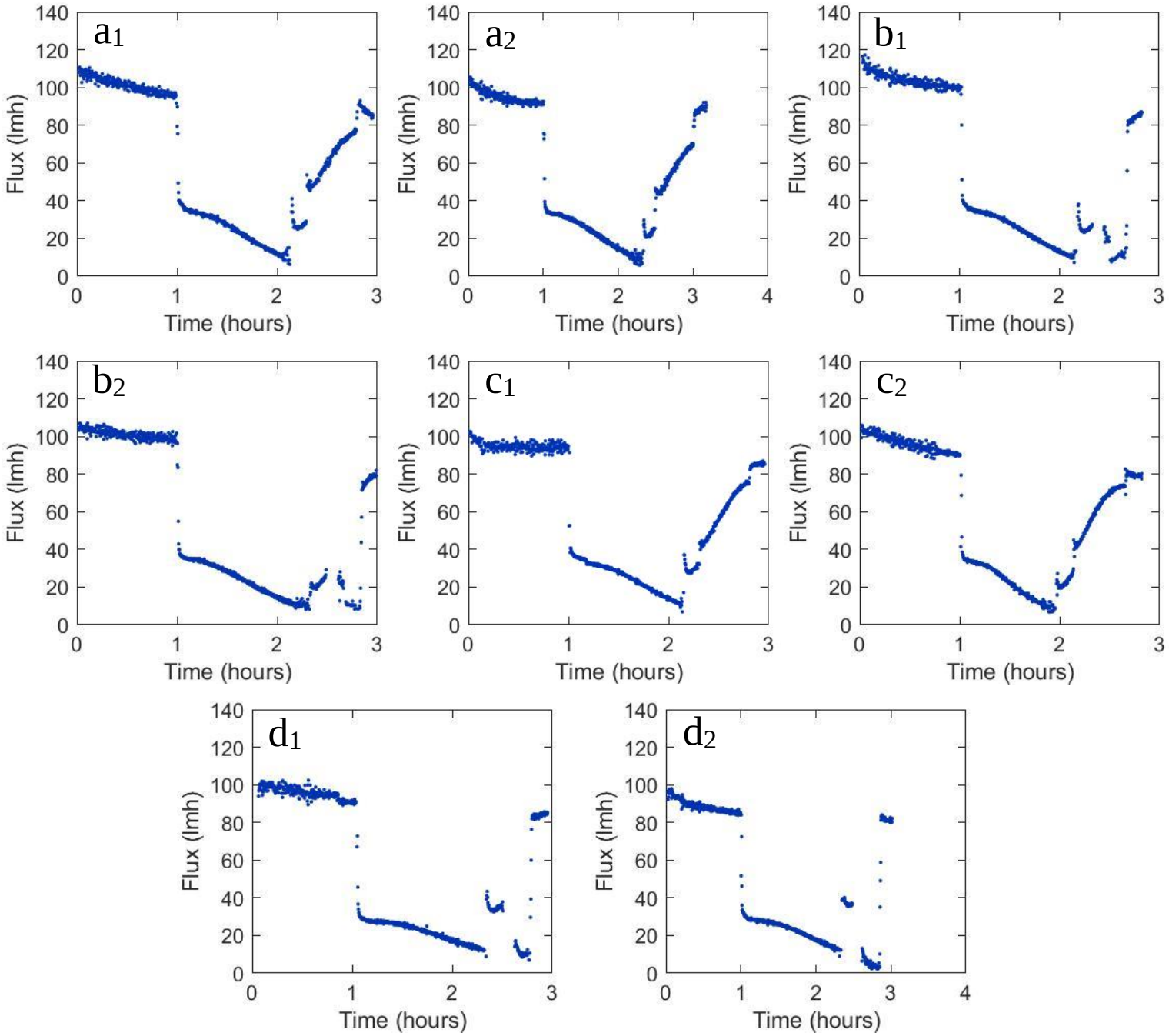

Figure F.2. *Permeate flux plots for 4.5 mM $CaCO_3$ using: (a) HCl, (b) dissolved CO_2, (c) DI water, and (d) air.*

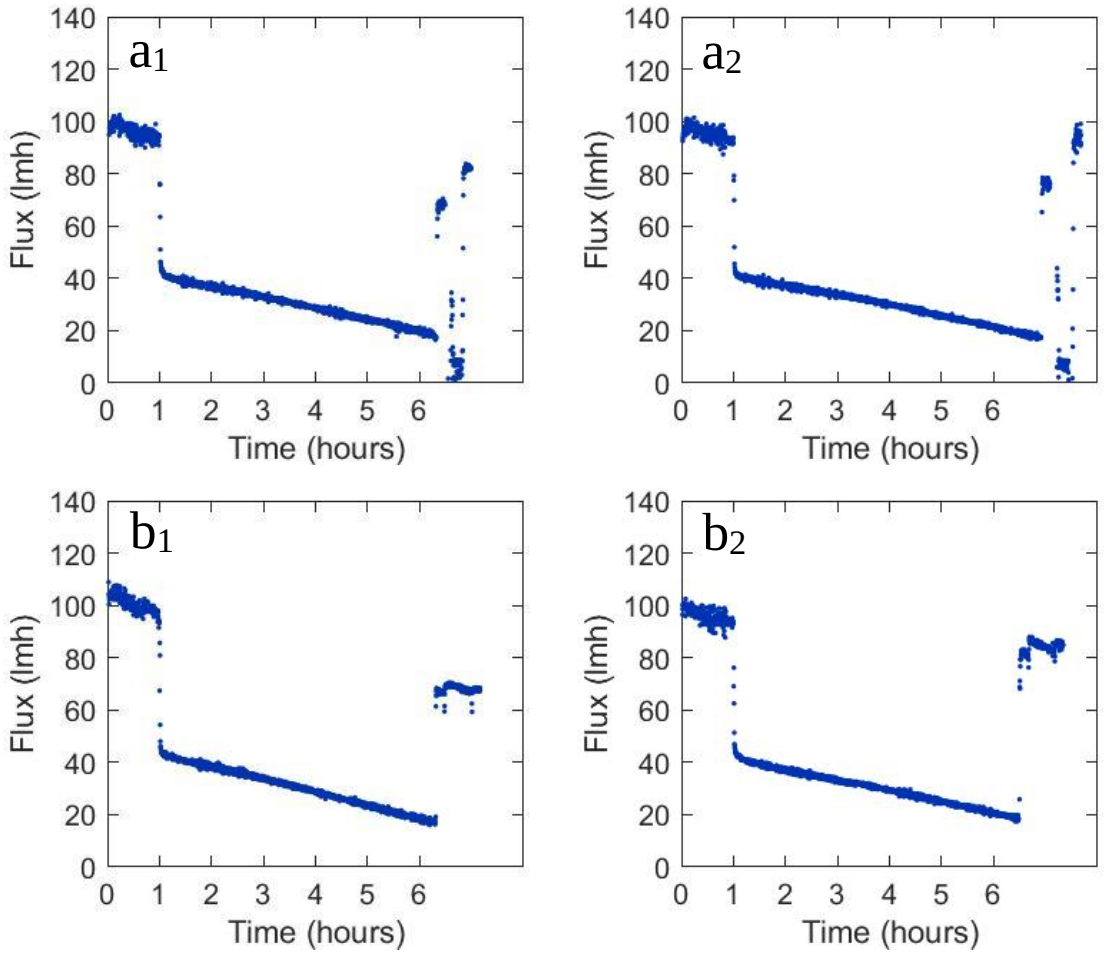

Figure F.3. *Permeate flux plots for $CaSiO_3$ only using: (a) dissolved CO_2, and (b) DI water.*

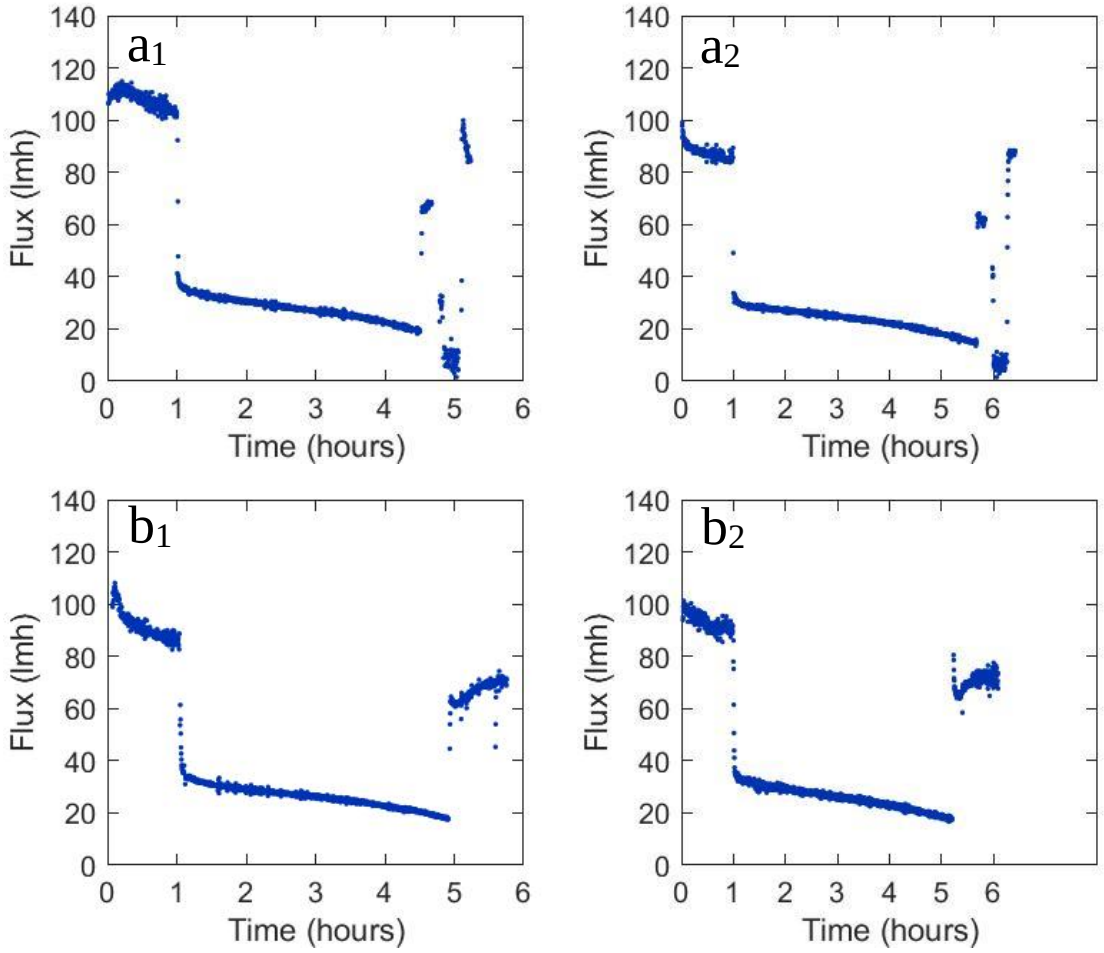

Figure F.4. *Permeate flux plots for 30 mM $CaSO_4$ using: (a) dissolved CO_2, and (b) DI water.*

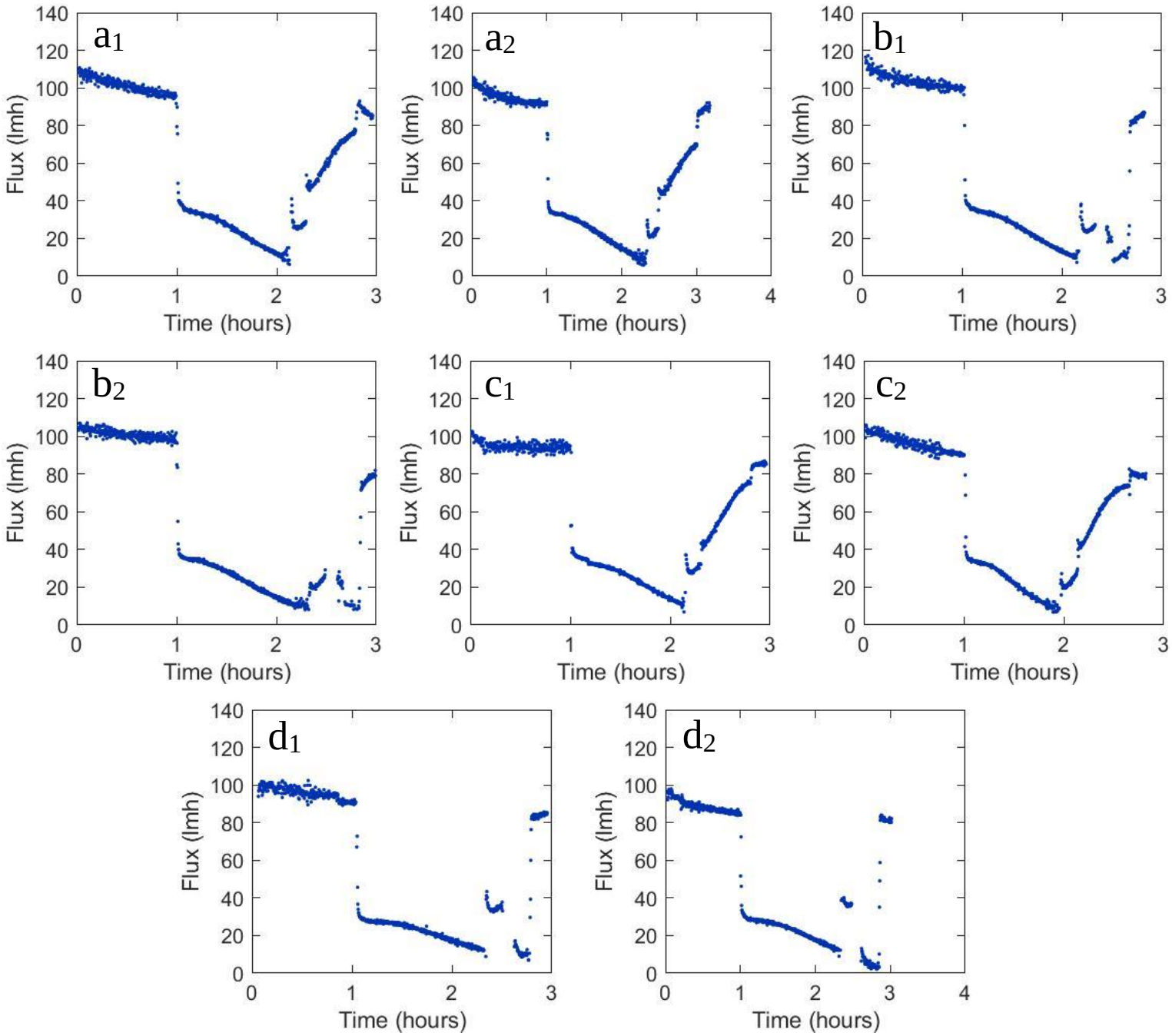

Figure F.5. *Permeate flux plots for 48 mM $CaSO_4$ using: (a) HCl, (b) dissolved CO_2, (c) DI water, and (d) air.*

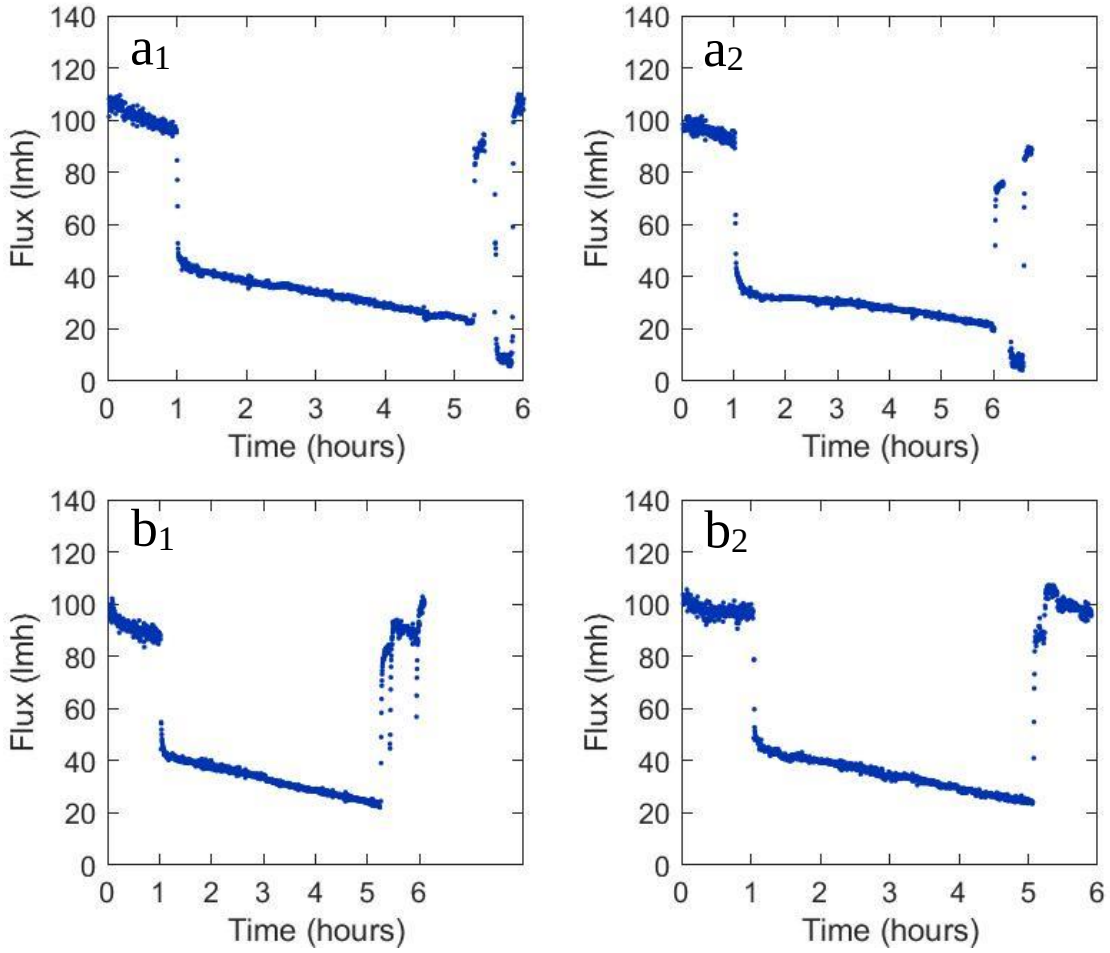

Figure F.6. *Permeate flux plots for humic acid using: (a) dissolved CO_2, and (b) DI water.*

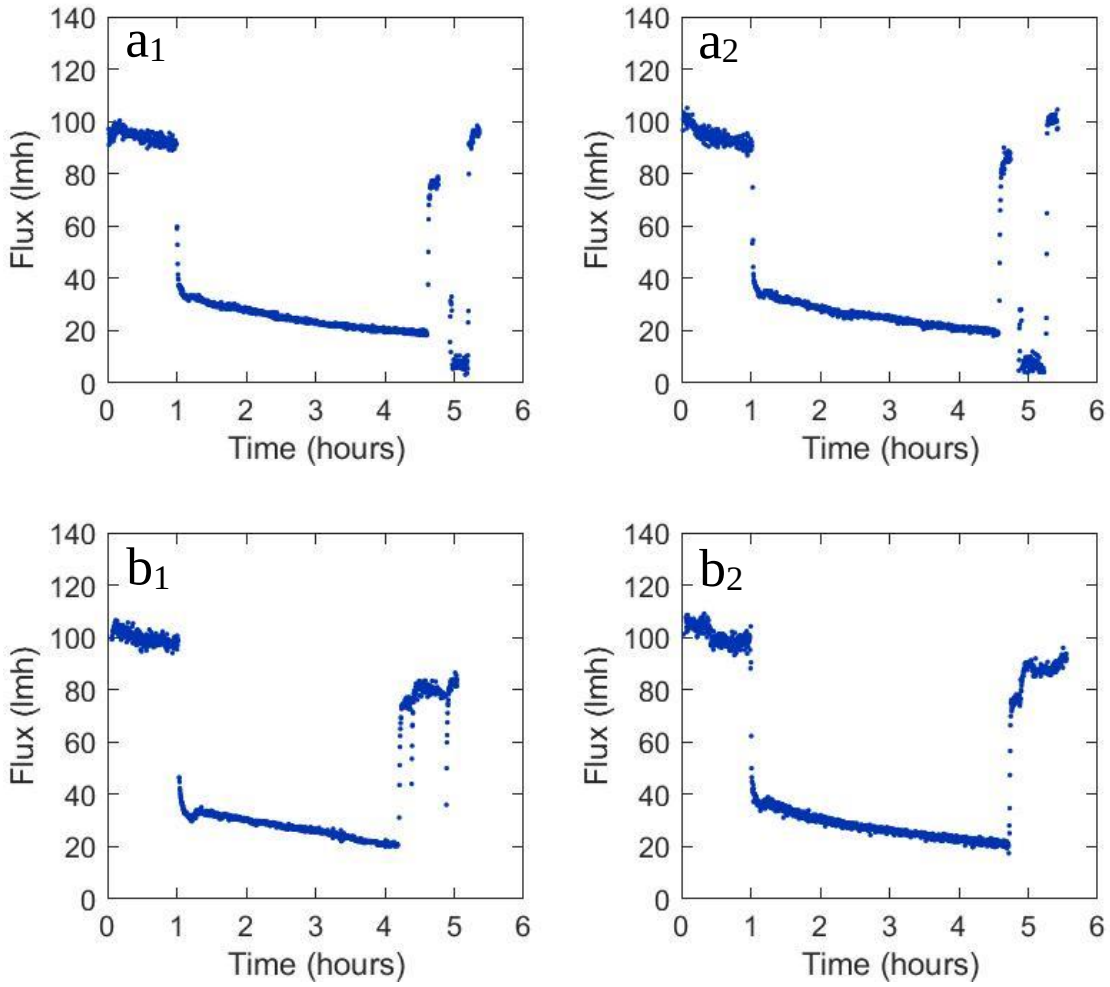

Figure F.7. *Permeate flux plots for combined fouling using: (a) dissolved CO_2, and (b) DI water.*

F.2 Carbon dioxide vs air

As previously mentioned, air has a much lower solubility in water than that of CO_2 which does not only limit the effectiveness of two-phase flow cleaning, but it increases the formation of undesired stagnant bubbles as well. Figure F.8 shows a comparison between the bubbles observed exiting the membrane cell when using dissolved CO_2 and air.

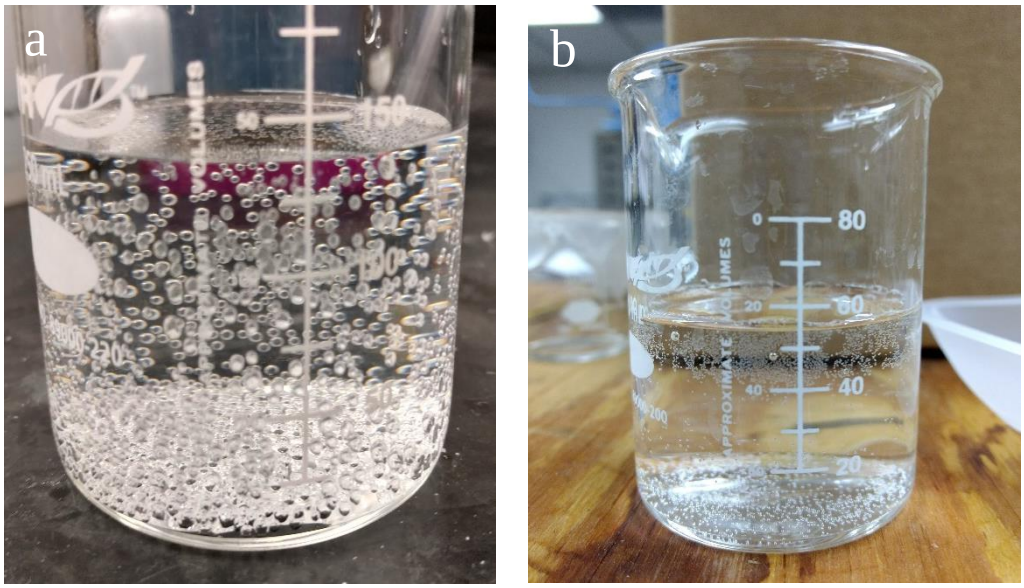

Figure F.8. *Glass containing (a) dissolved CO_2 and (b) air in water.*

CO_2 bubbles have a bigger size than air bubbles. This supports the theory that CO_2 exists as dissolved molecules which can easily pass through the membrane and then come out of the solution while air (which is mostly composed of nitrogen) exists as small bubbles which have difficulty permeating the membrane.

F.3 Combined fouling

The combined fouling solution was prepared by mixing first Na_2CO_3, Na_2SO_4, $CaCl_2$ and leaving the humid acid for last (see Figure F.9). Figure F.10 shows several pictures of the combined fouling membranes after the gas and DI water cleaning. It is noteworthy to mention that even though a lot of deposits can be observed on the surface of the membrane, the flux recovery went over 100% and 85% after CO_2 cleaning and DI water, respectively. This may also suggest that if we designed the module in a certain way, the bubbles could flow differently, and there might be more scouring.

Figure F.9. *Preparation of the combined fouling solution ($CaCO_3$, $CaSO_4$, and humic acid).*

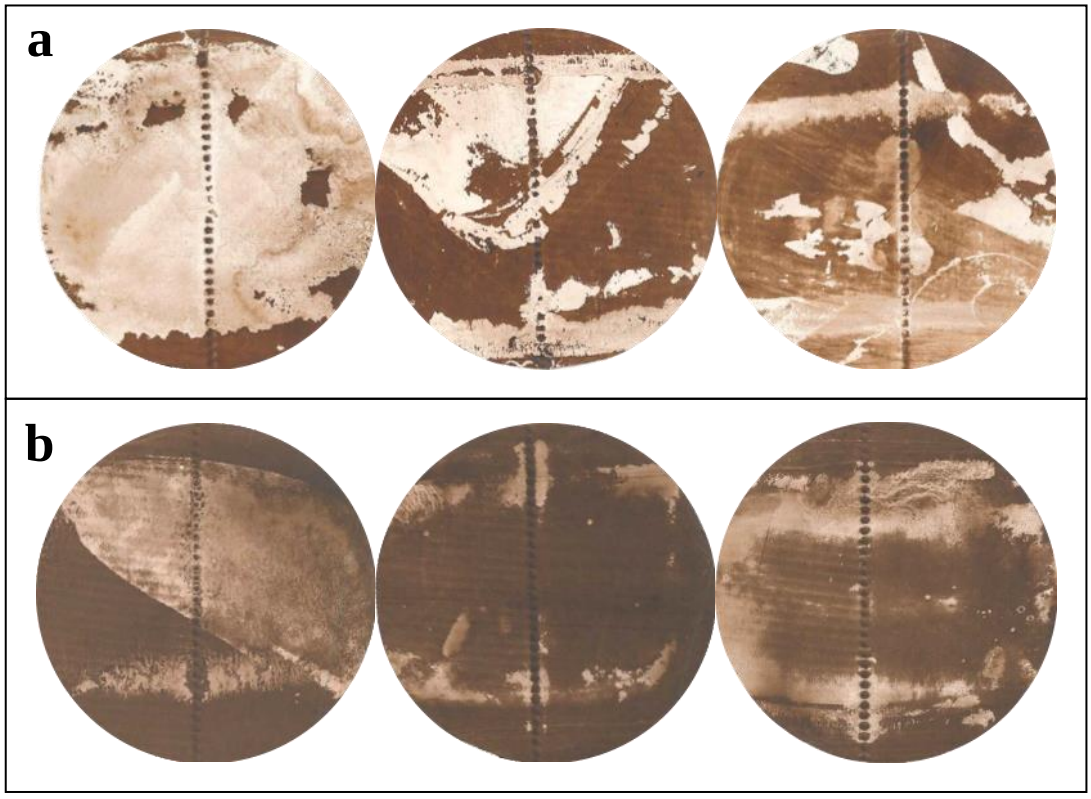

Figure F.10. *Combined fouling membranes after cleaning with (a) dissolved carbon dioxide, and (b) DI water.*

F.4 SEM Images

This section contains all the SEM images taken of RO membranes used in this study.

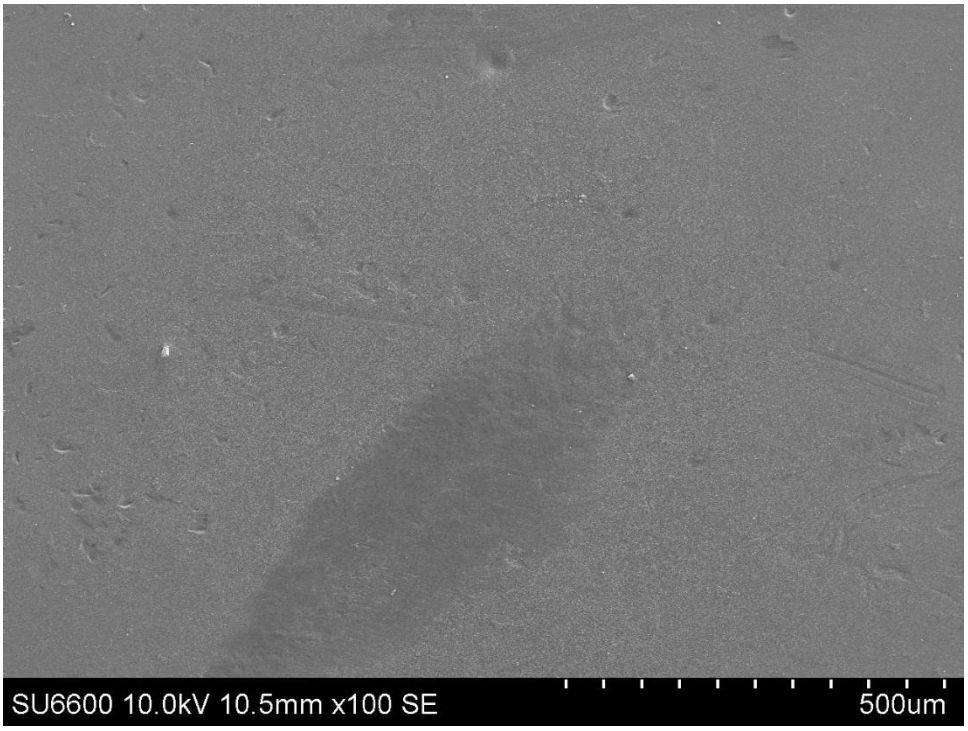

Scale: none
Cleaning: none
Zoom: 100X

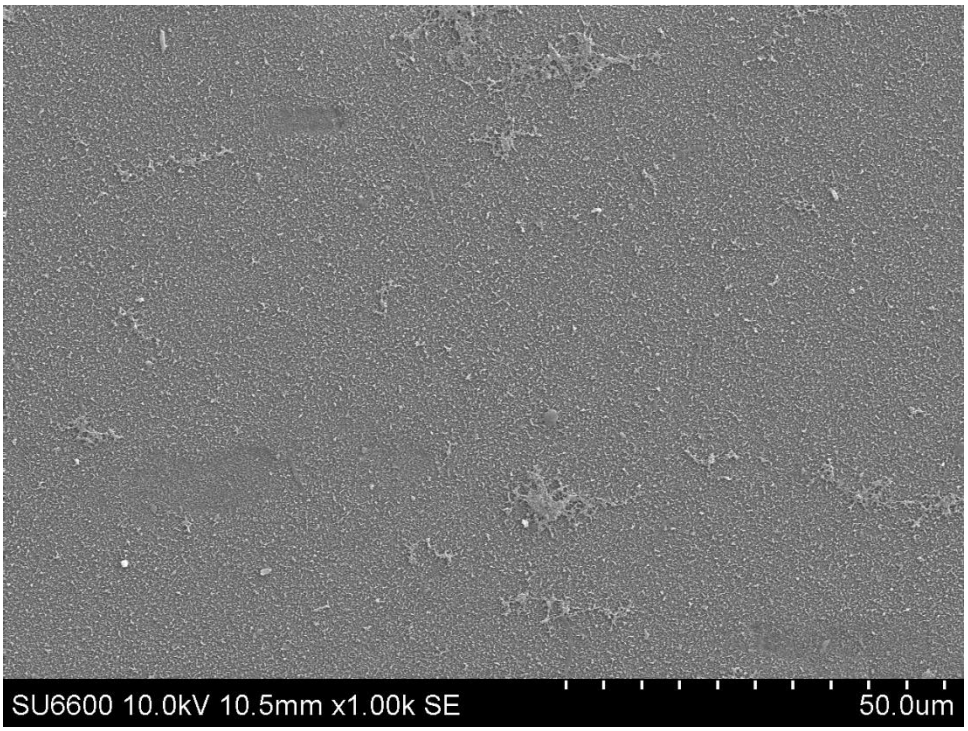

Scale: none
Cleaning: none
Zoom: 1kX

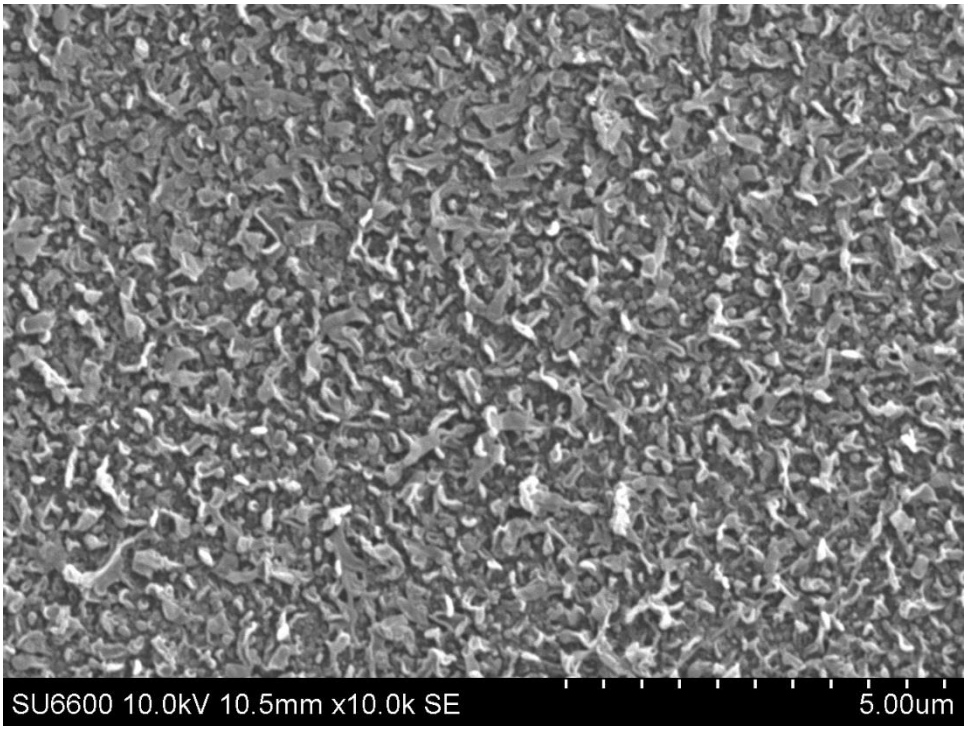

Scale: none
Cleaning: none
Zoom: 10kX

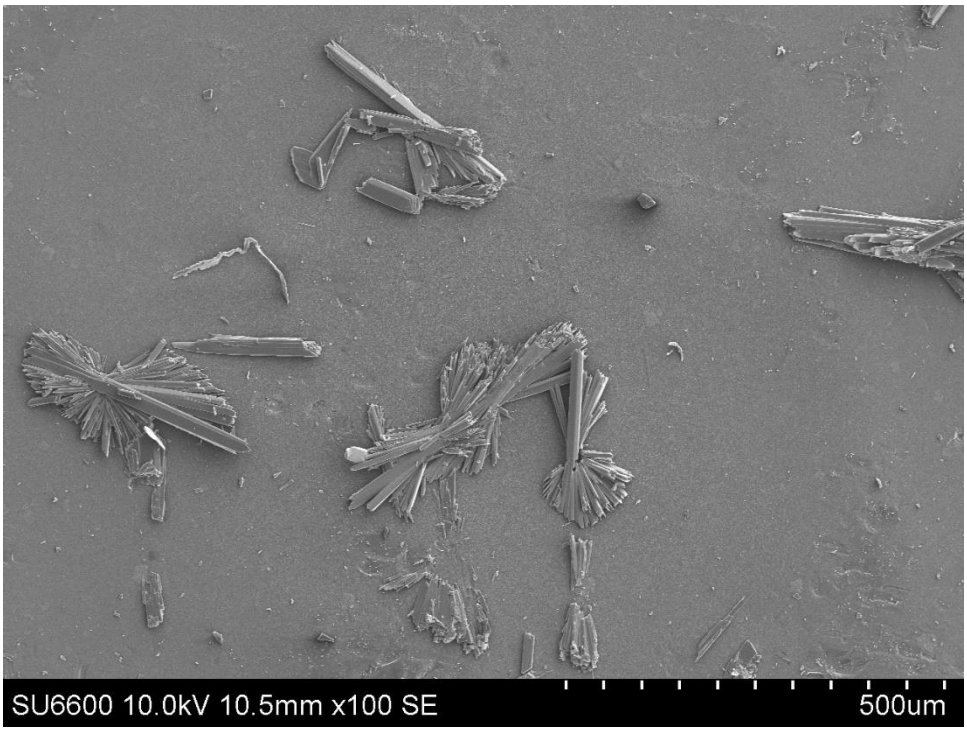

Scale: $CaSO_4$
Cleaning: none
Zoom: 100X

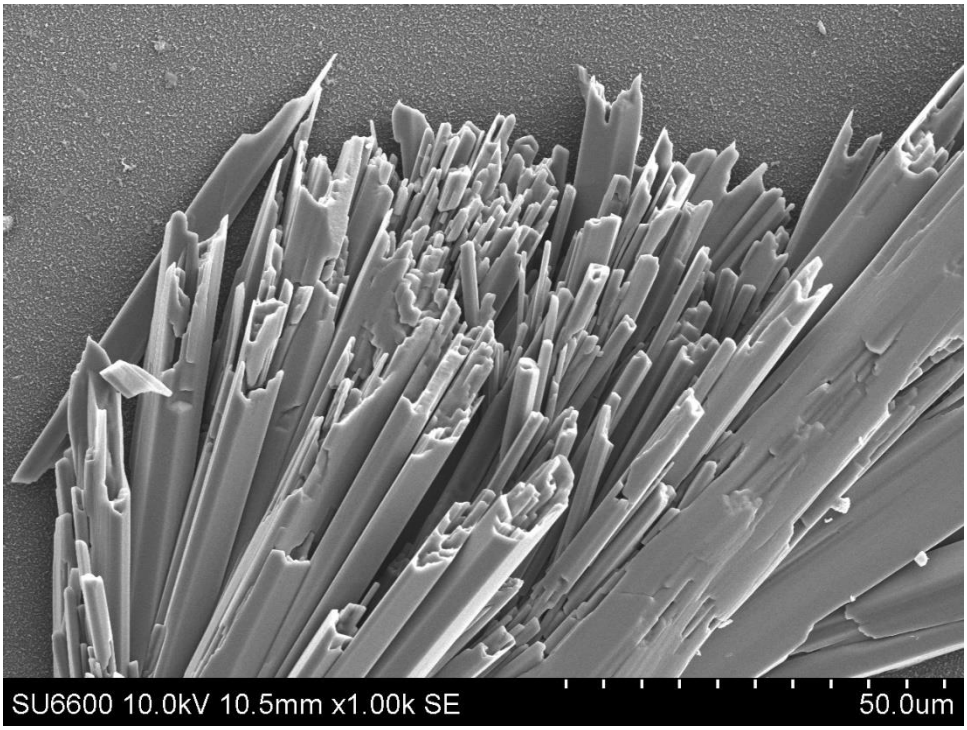

Scale: $CaSO_4$
Cleaning:
none
Zoom:
1kX

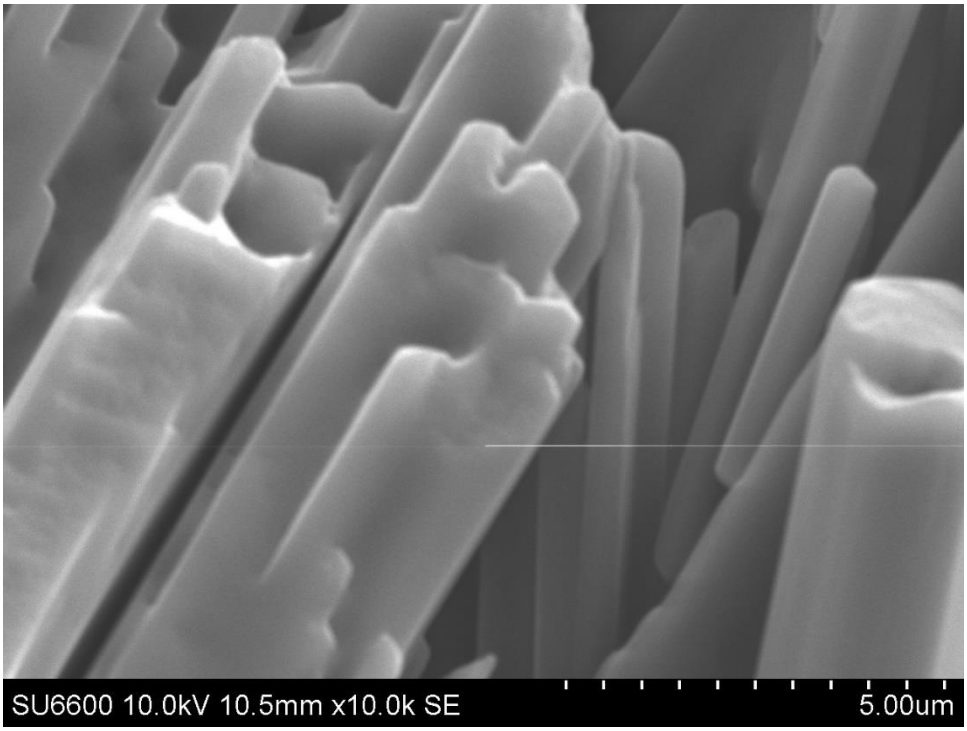

Scale: $CaSO_4$
Cleaning:
none
Zoom:
10kX

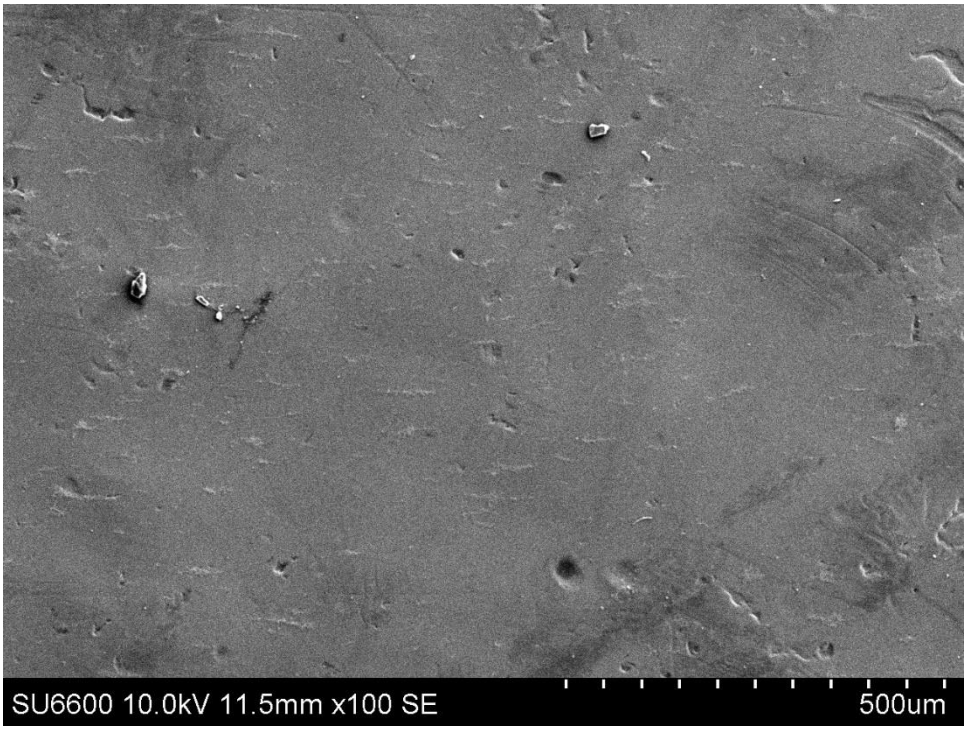

Scale: $CaSO_4$
Cleaning:
Dissolved CO_2
Zoom:
100X

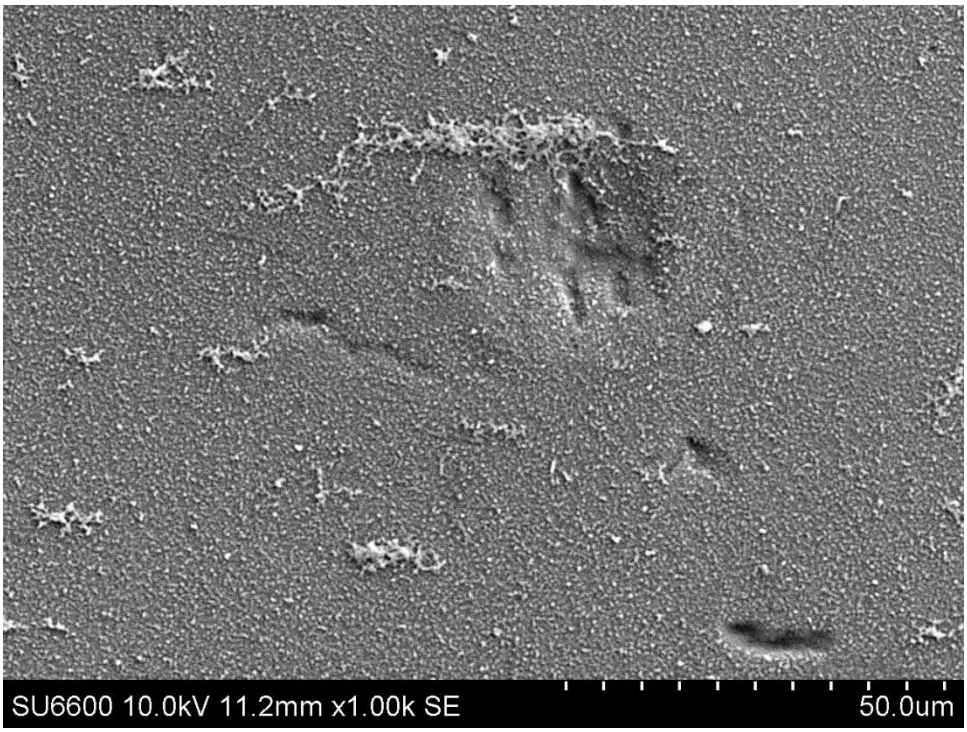

Scale: $CaSO_4$
Cleaning:
Dissolved CO_2
Zoom:
1kX

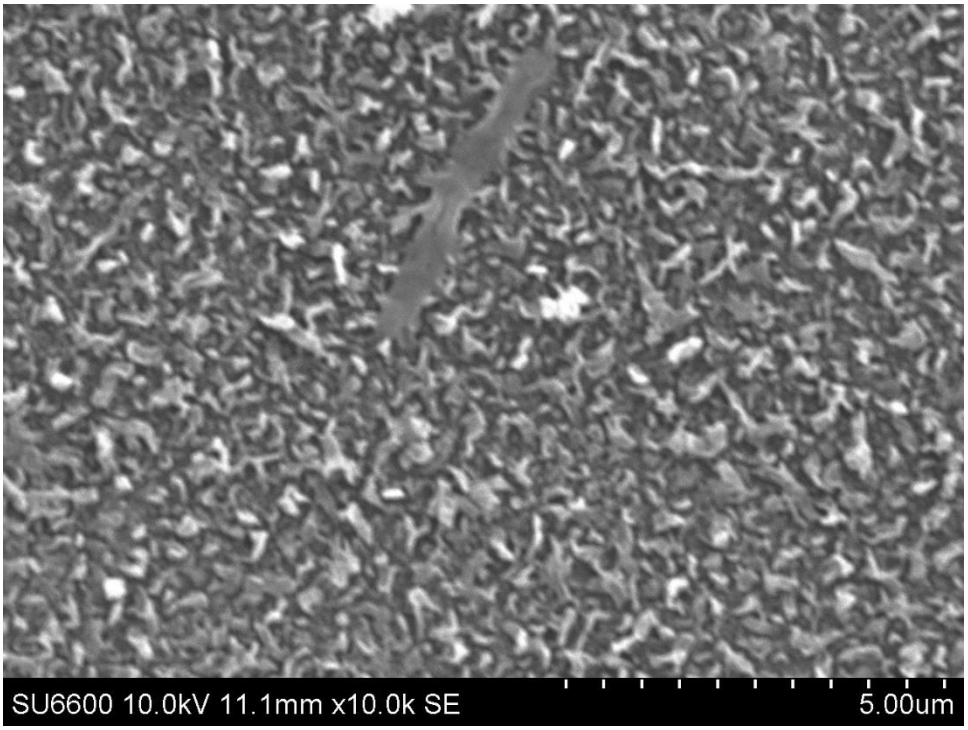

Scale: $CaSO_4$
Cleaning:
Dissolved CO_2
Zoom:
10kX

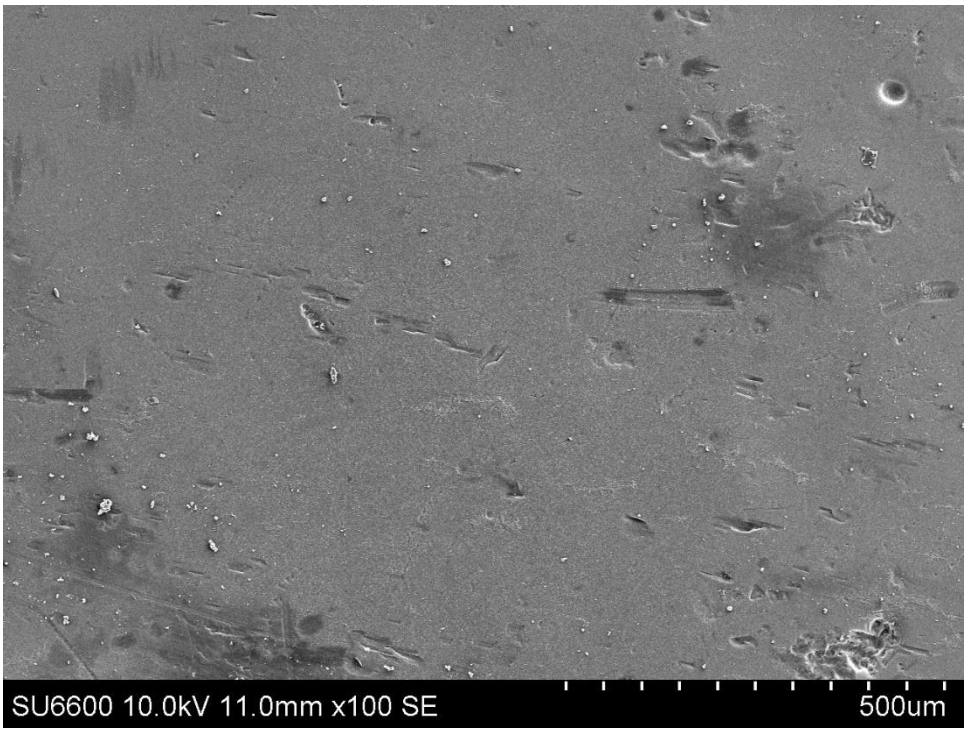

Scale: $CaSO_4$
Cleaning:
DI water
Zoom:
100X

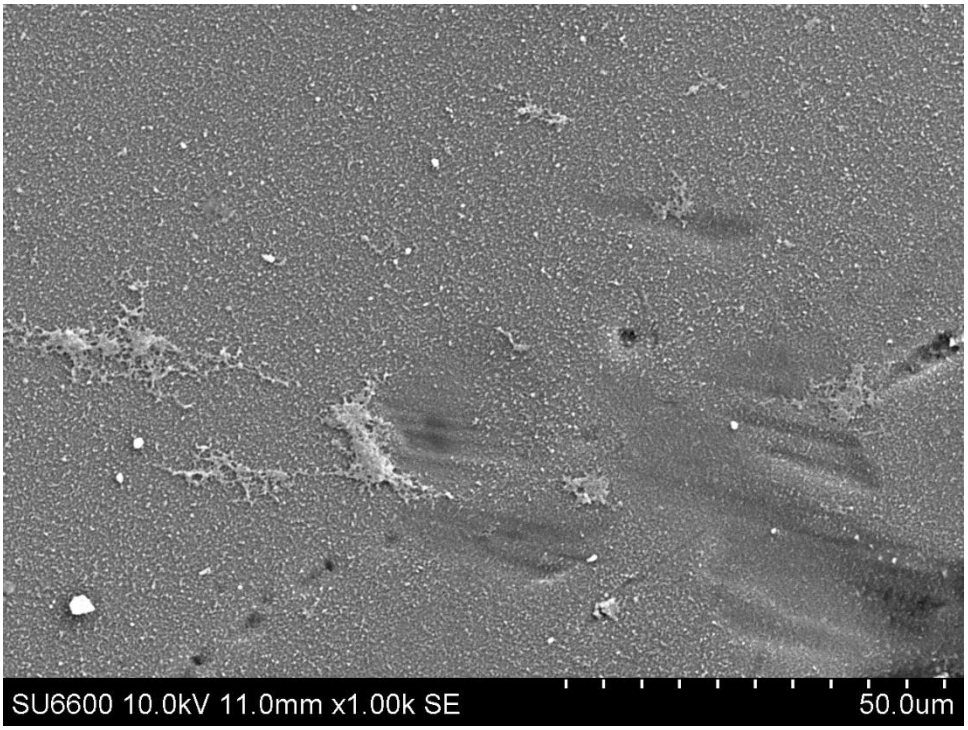

Scale: $CaSO_4$
Cleaning:
DI water
Zoom:
1kX

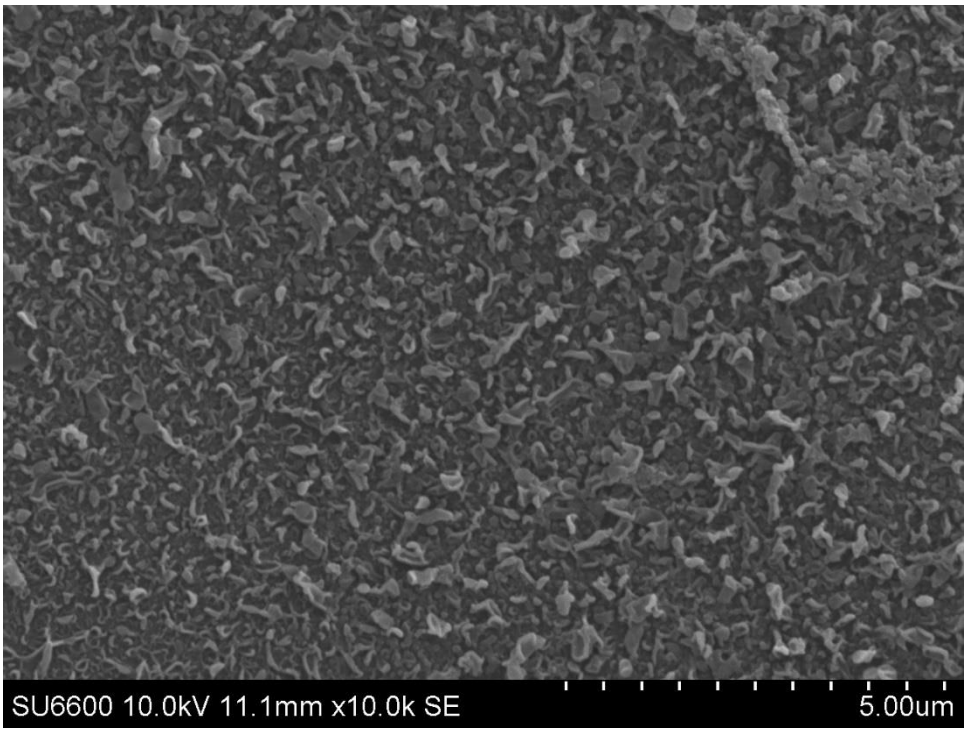

Scale: $CaSO_4$
Cleaning:
DI water
Zoom:
10kX

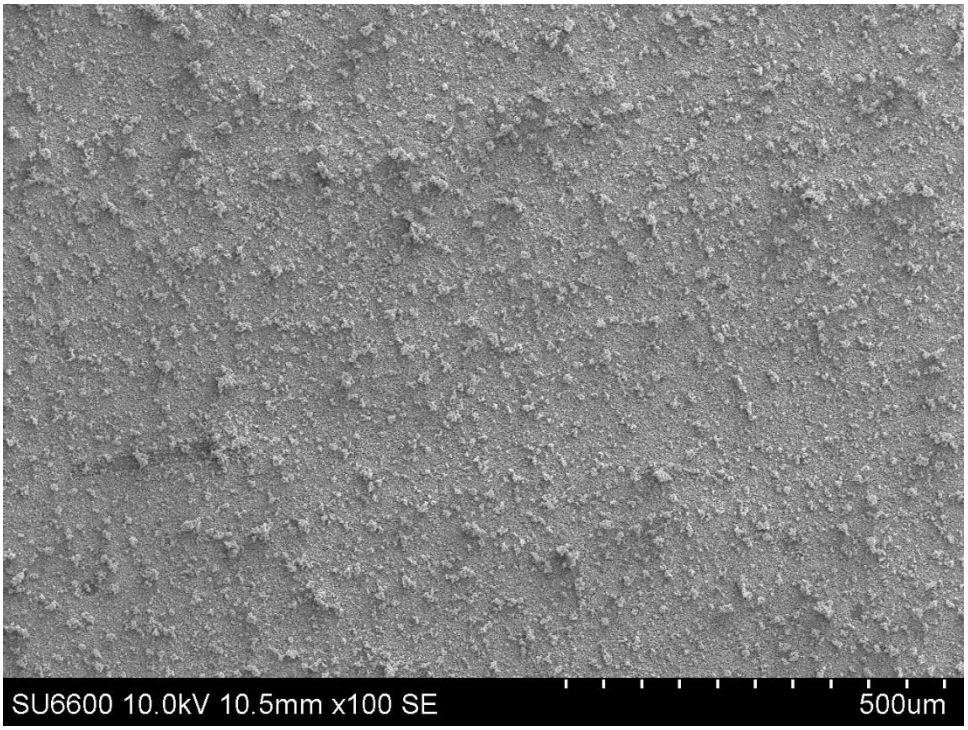

Scale: $CaCO_3$
Cleaning:
none
Zoom:
100X

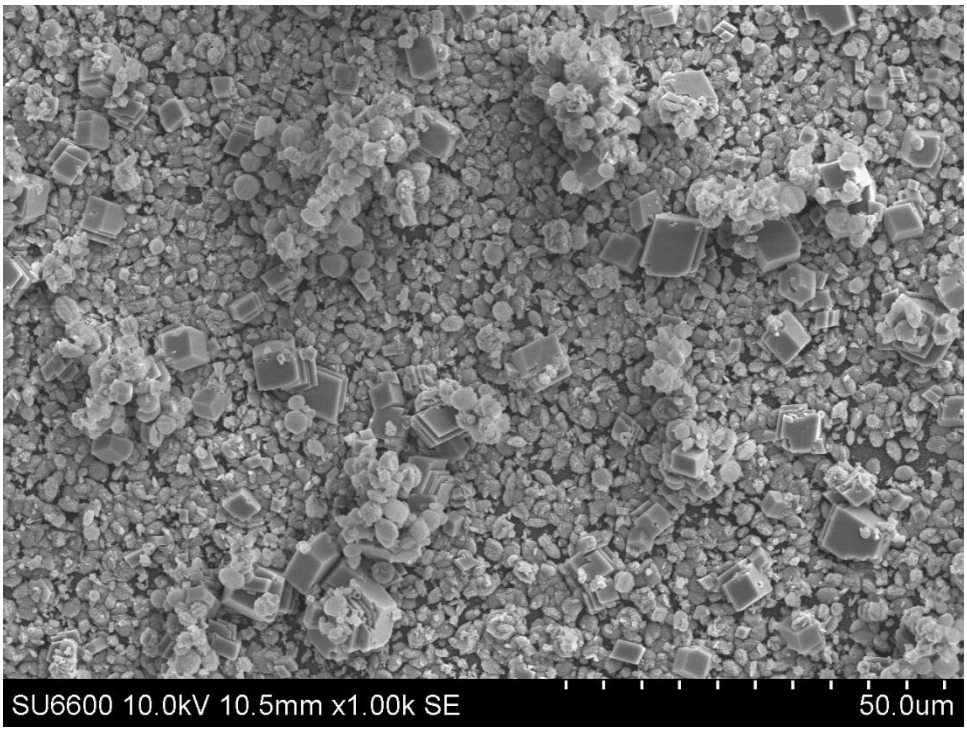

Scale: $CaCO_3$
Cleaning:
none
Zoom:
1kX

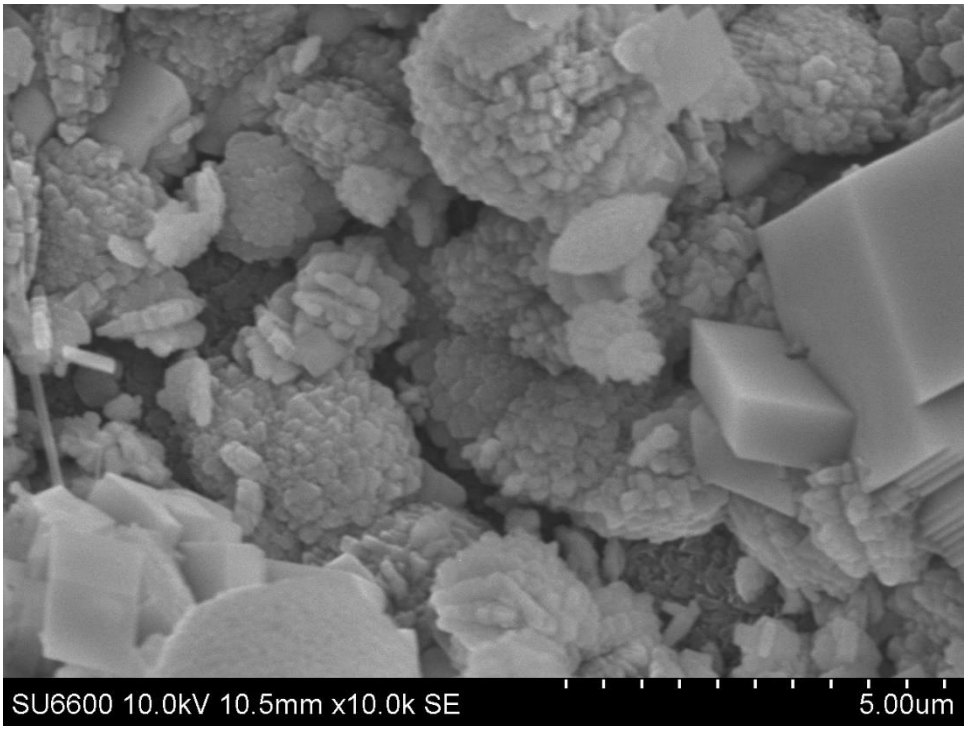

Scale: $CaCO_3$
Cleaning:
none
Zoom:
10kX

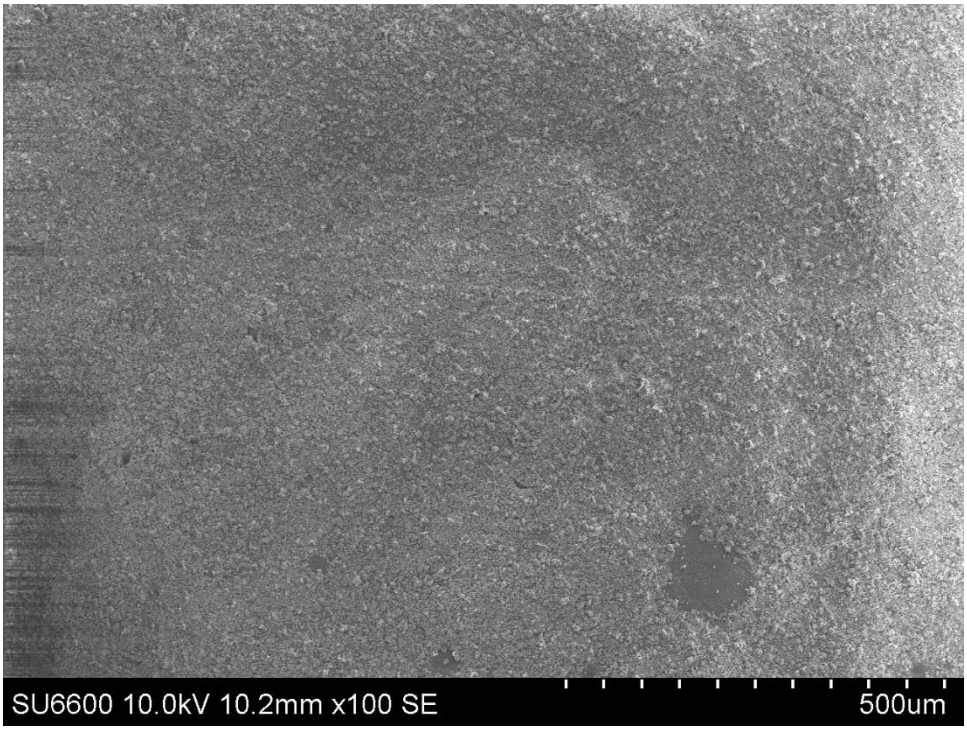

Scale: $CaCO_3$
Cleaning:
Dissolved CO_2
Zoom:
100X

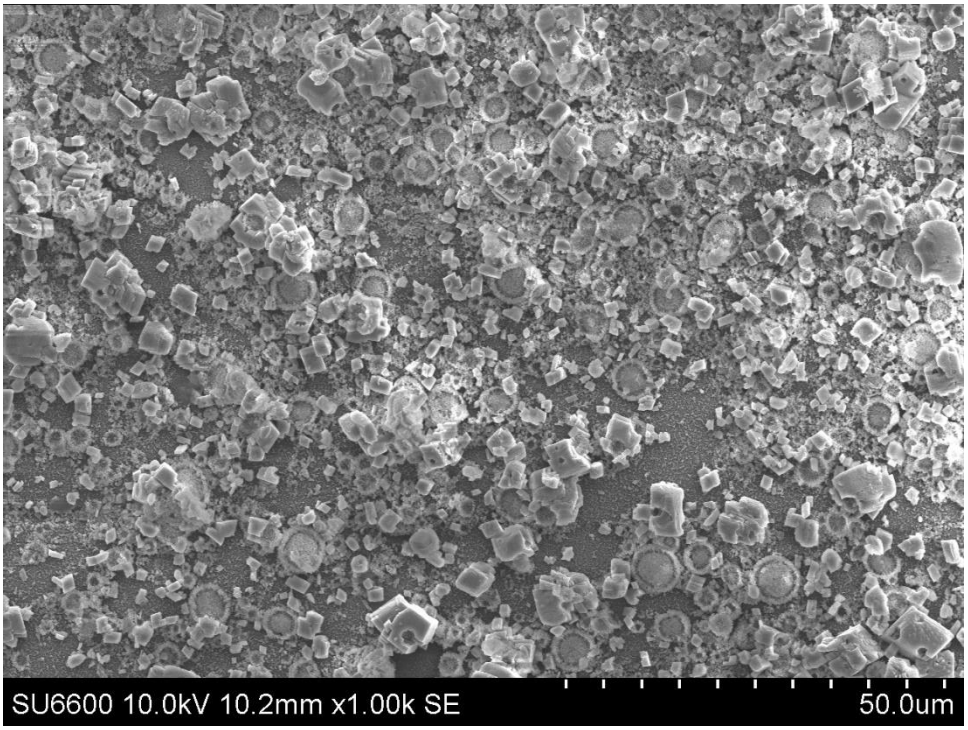

Scale: $CaCO_3$
Cleaning:
Dissolved CO_2
Zoom:
1kX

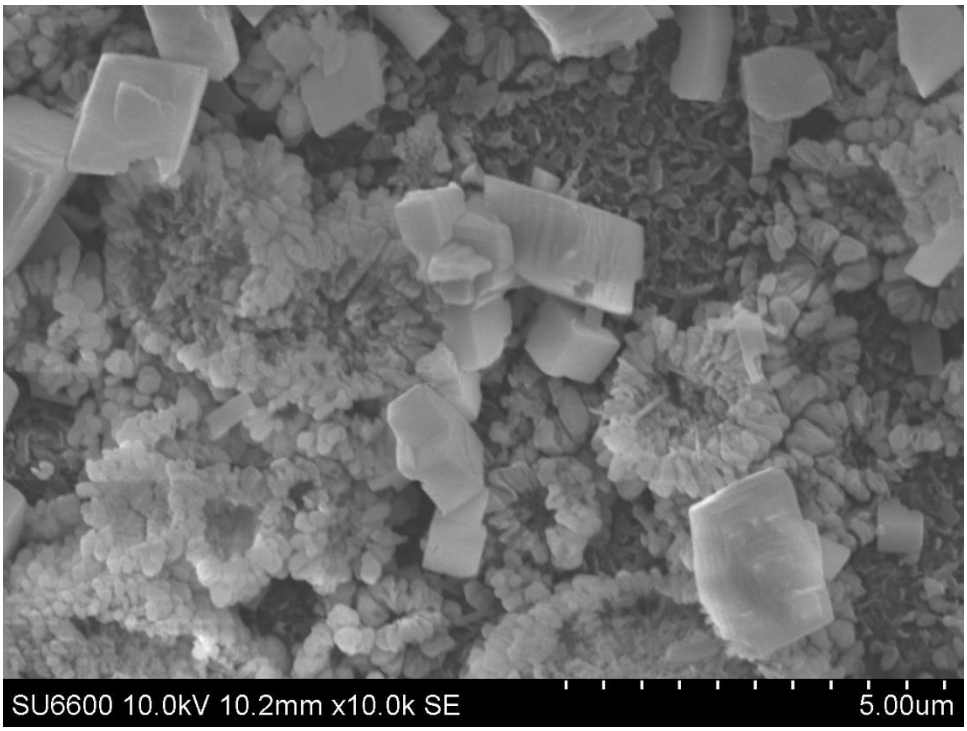

Scale: $CaCO_3$
Cleaning:
Dissolved CO_2
Zoom:
10kX

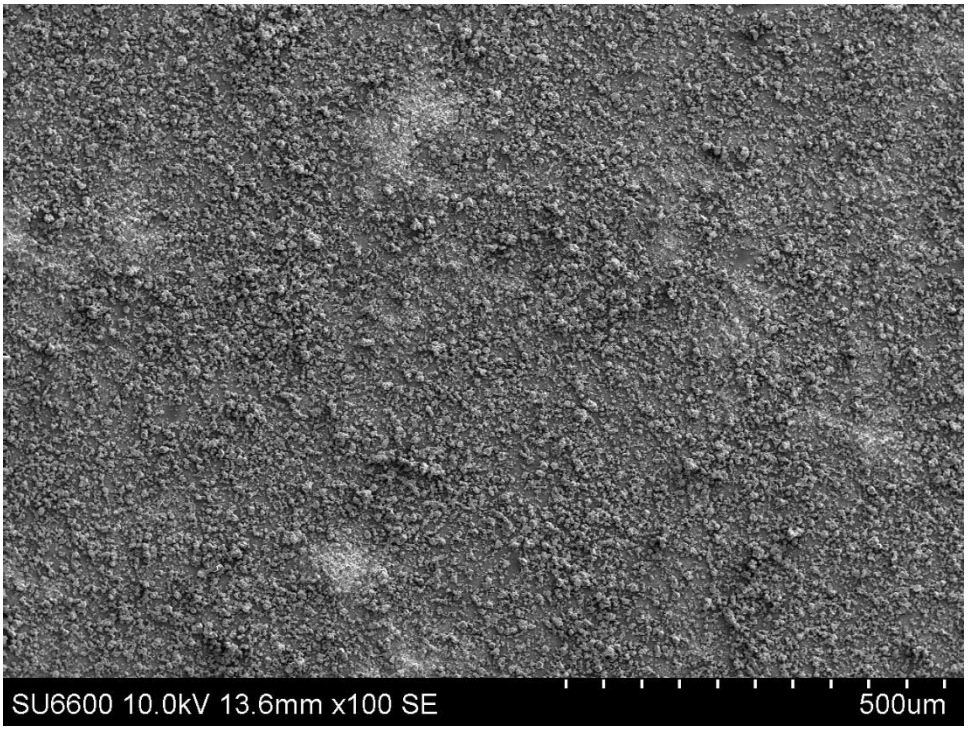

Scale: $CaCO_3$
Cleaning:
DI water
Zoom:
100X

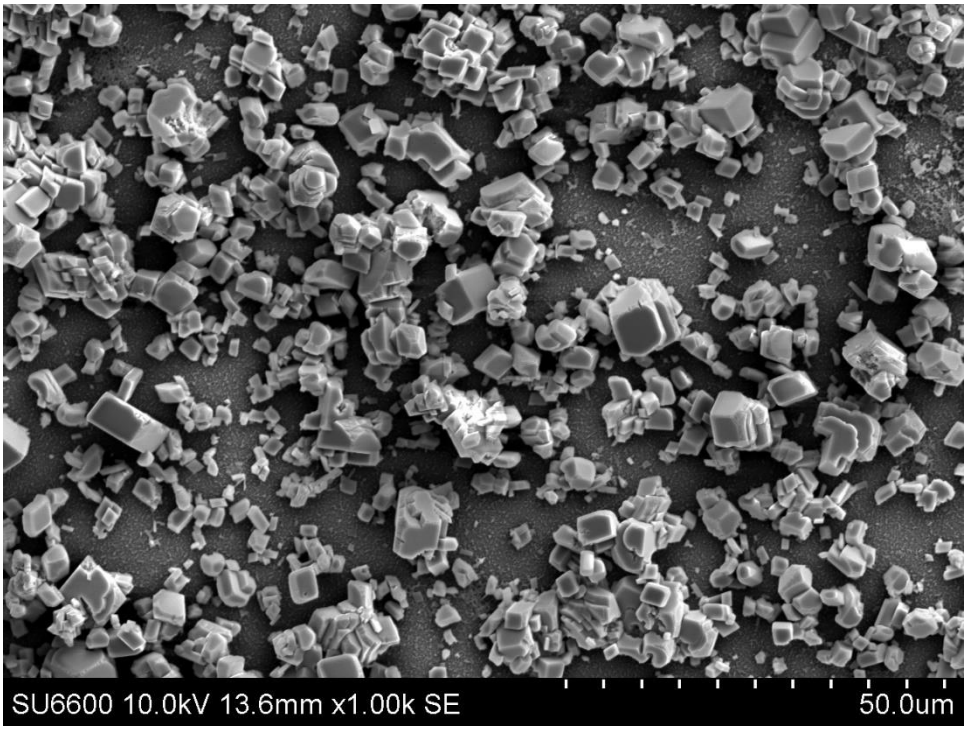

Scale: $CaCO_3$
Cleaning:
DI water
Zoom:
1kX

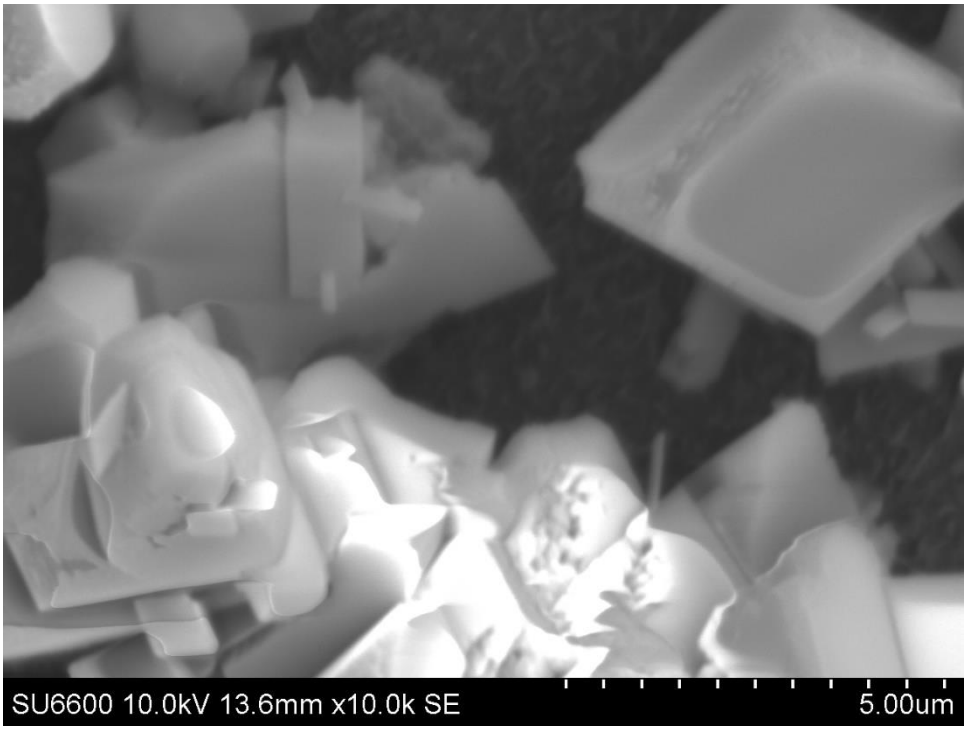

Scale: $CaCO_3$
Cleaning:
DI water
Zoom:
10kX

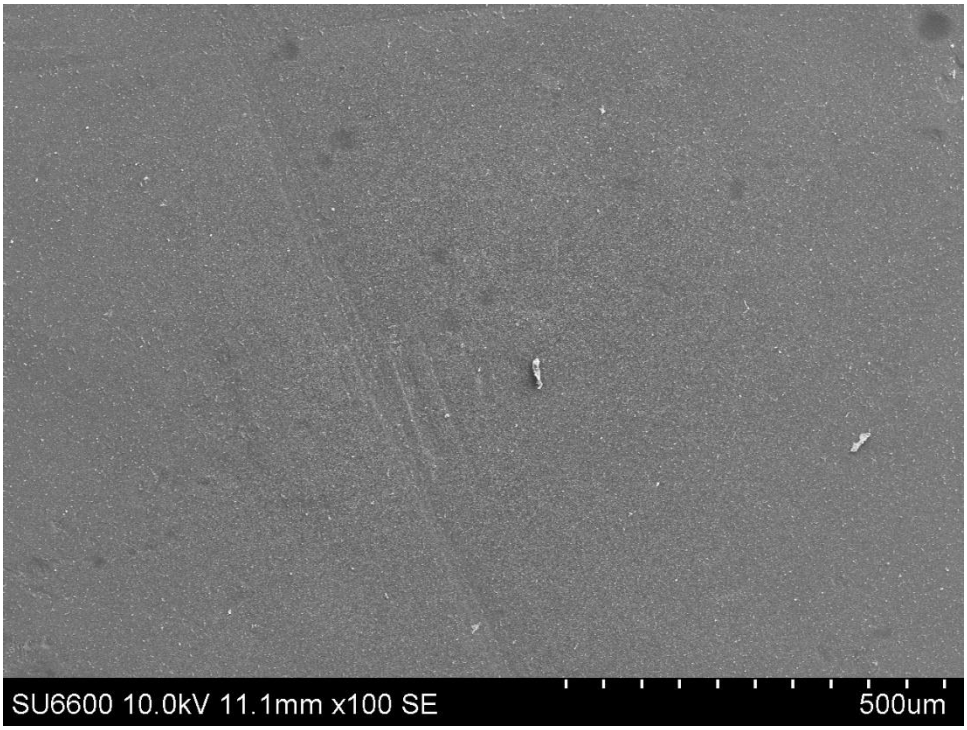

Scale: $CaSiO_3$
Cleaning:
none
Zoom:
100X

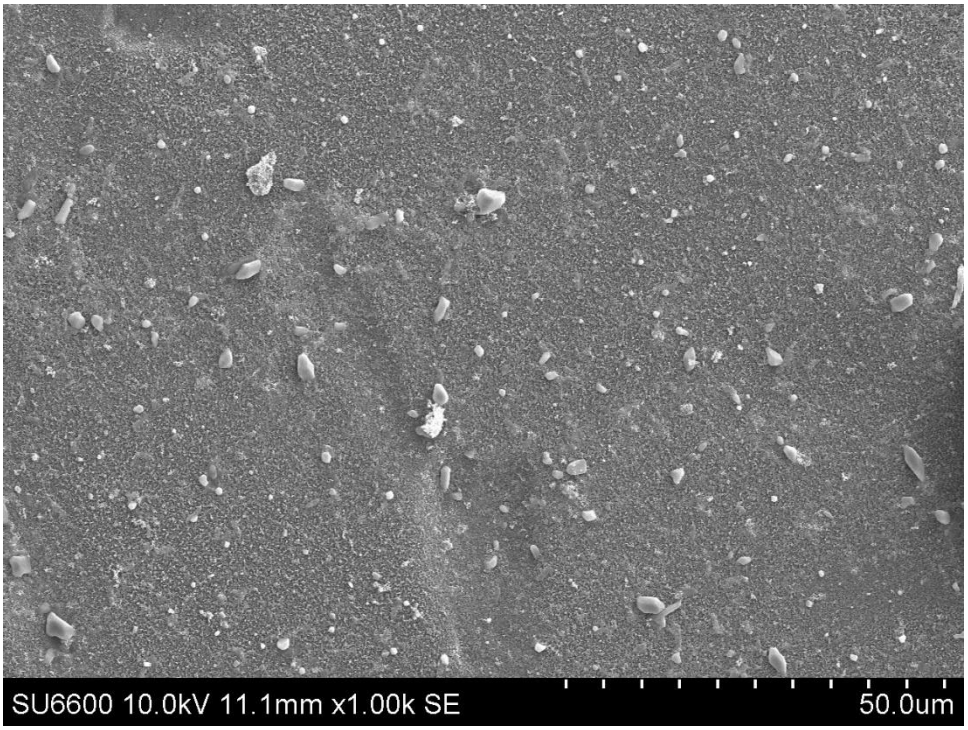

Scale: $CaSiO_3$
Cleaning:
none
Zoom:
1kX

Scale: $CaSiO_3$
Cleaning:
none
Zoom:
10kX

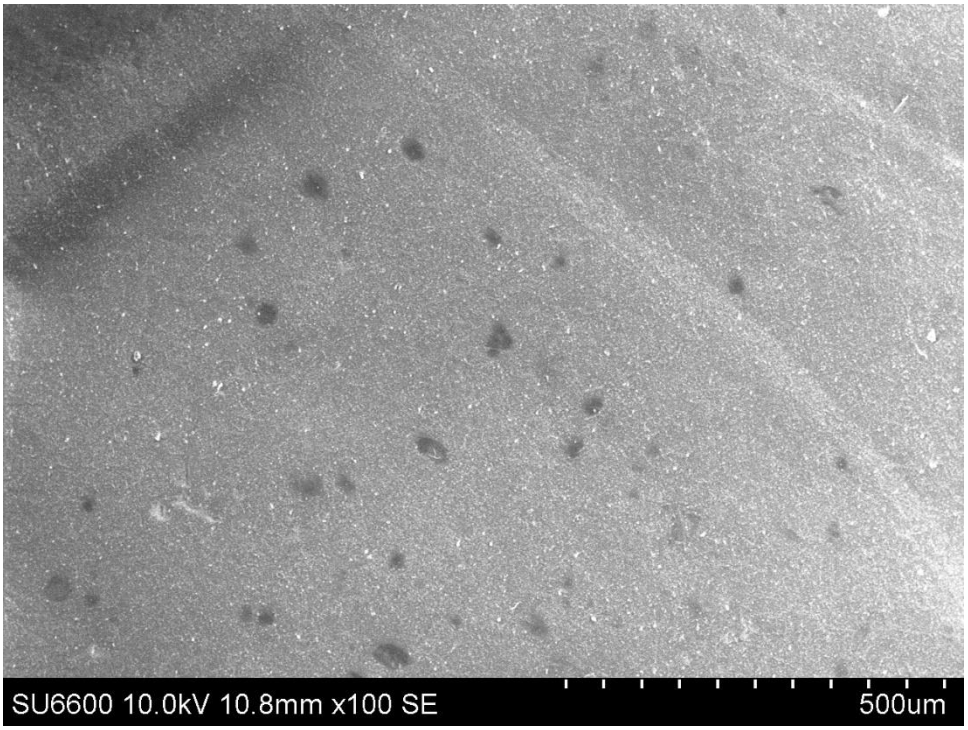

Scale: $CaSiO_3$
Cleaning:
Dissolved CO_2
Zoom:
100X

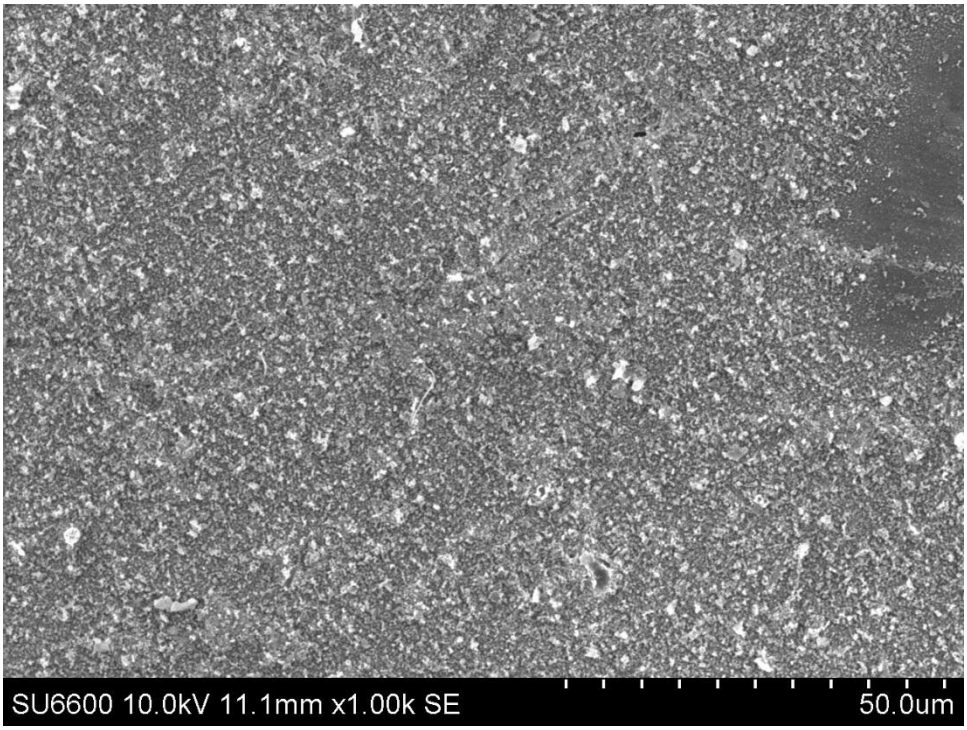

Scale: $CaSiO_3$
Cleaning:
Dissolved CO_2
Zoom:
1kX

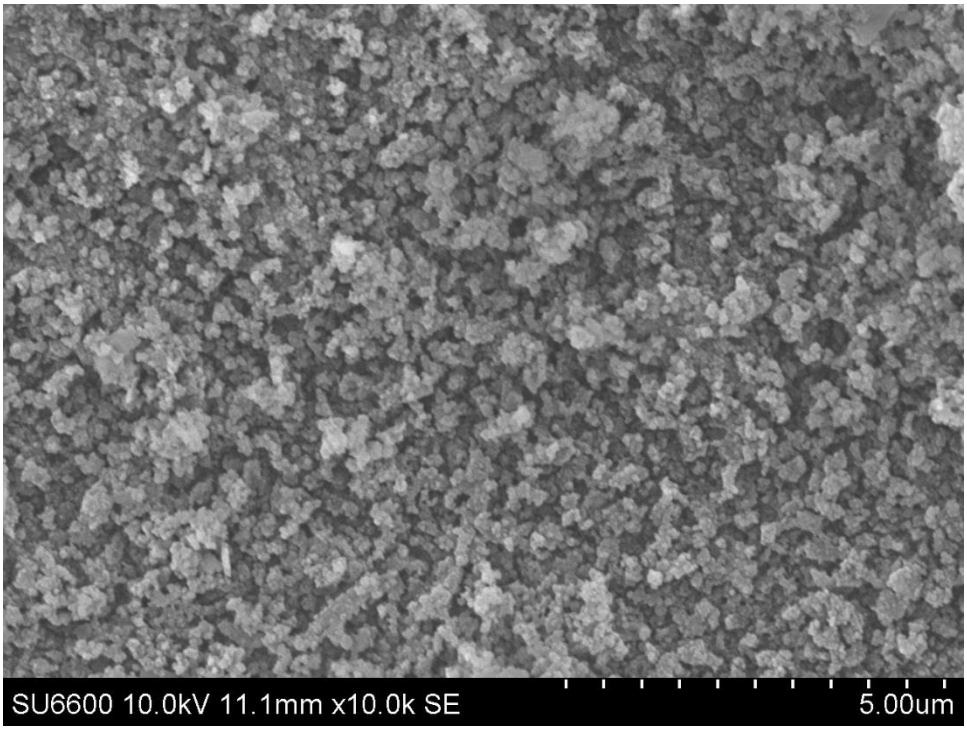

Scale: $CaSiO_3$
Cleaning:
Dissolved CO_2
Zoom:
10kX

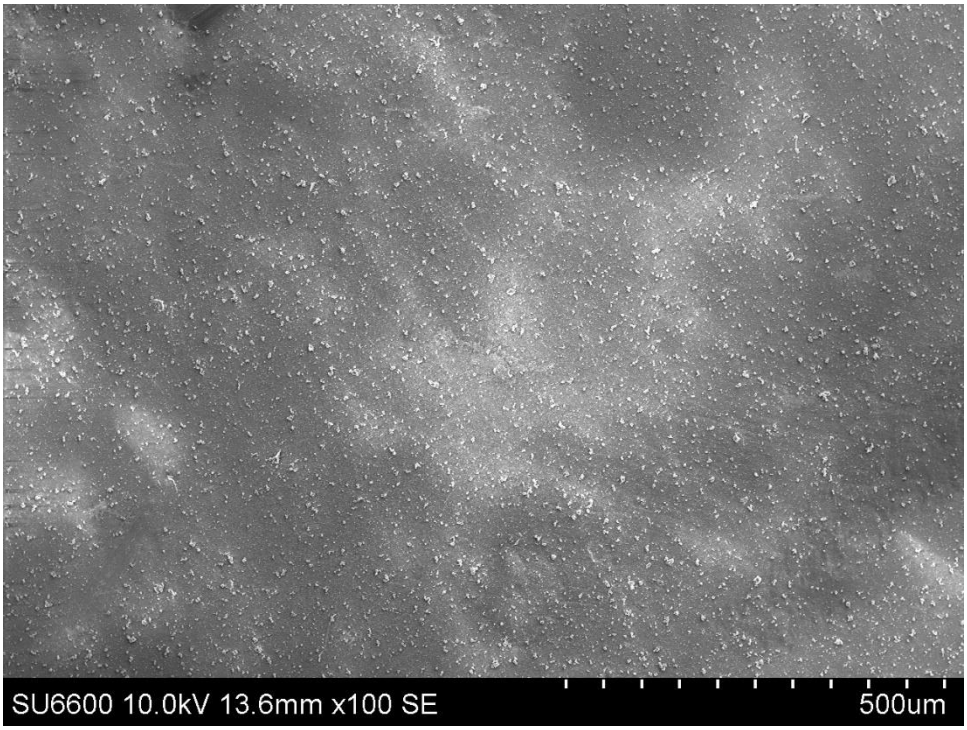

Scale: $CaSiO_3$
Cleaning:
DI water
Zoom:
100X

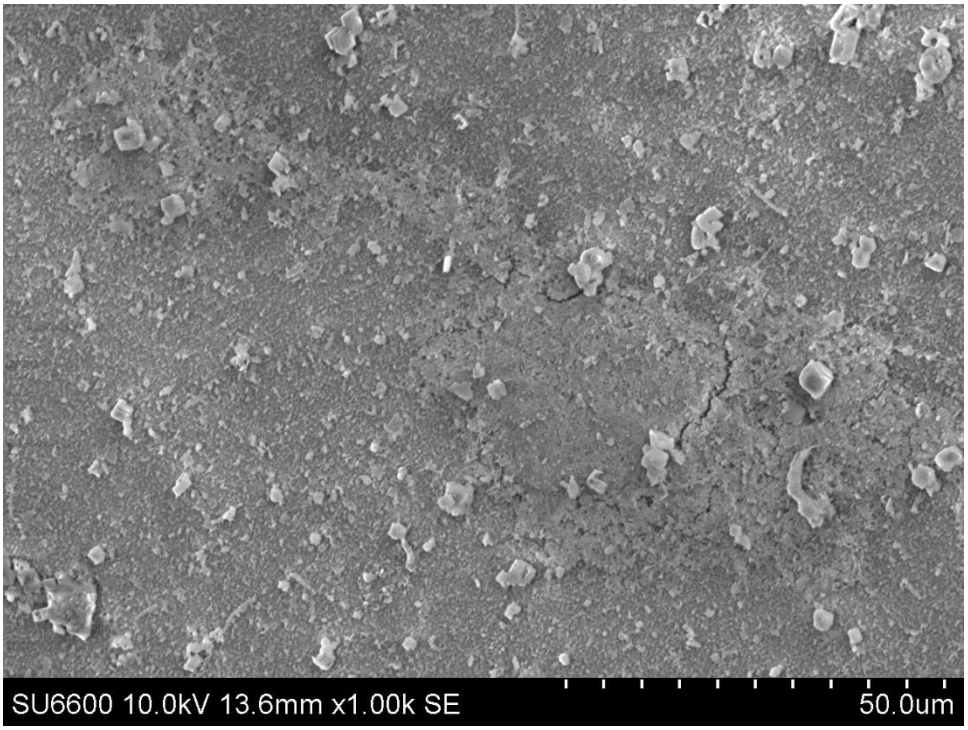

Scale: $CaSiO_3$
Cleaning:
DI water
Zoom:
1kX

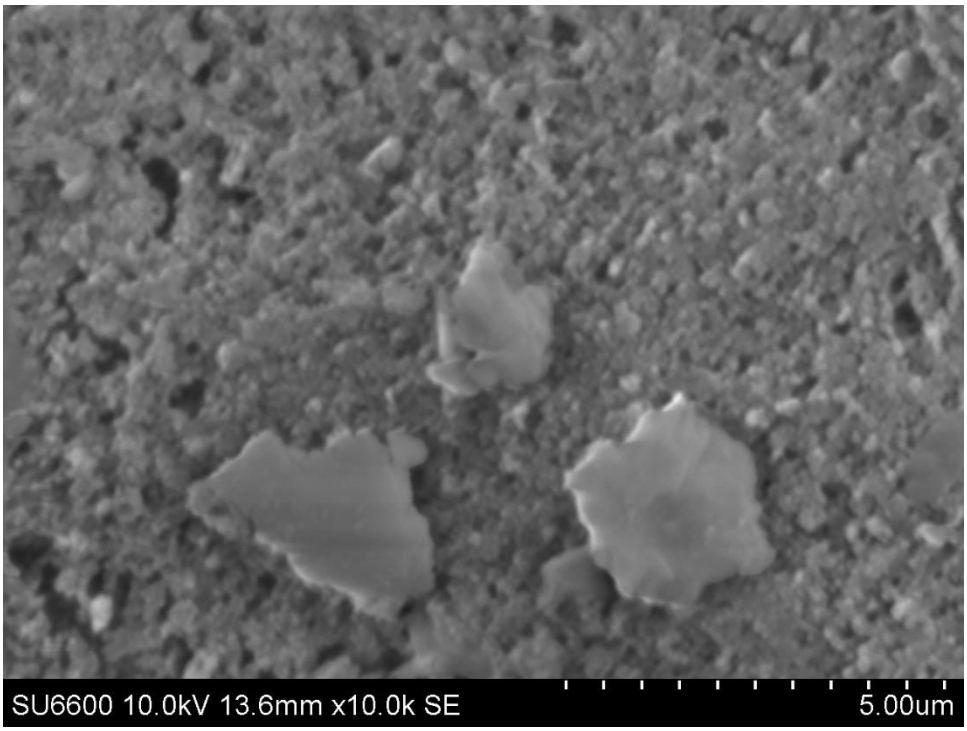

Scale: $CaSiO_3$
Cleaning:
DI water
Zoom:
10kX

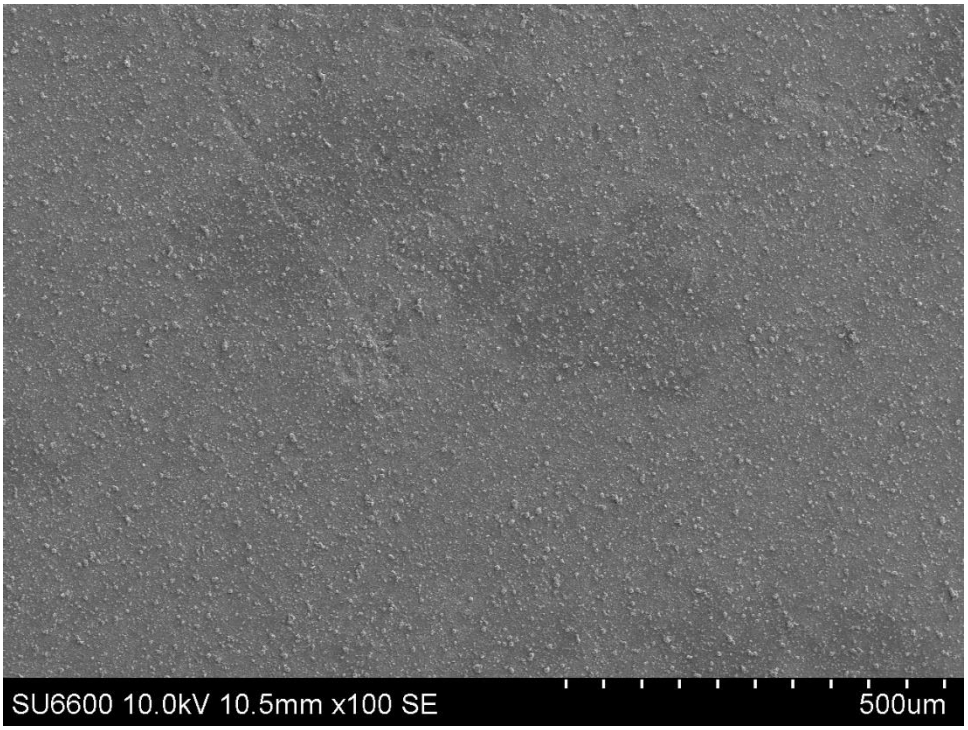

Scale: Combined fouling
Cleaning: none
Zoom: 100X

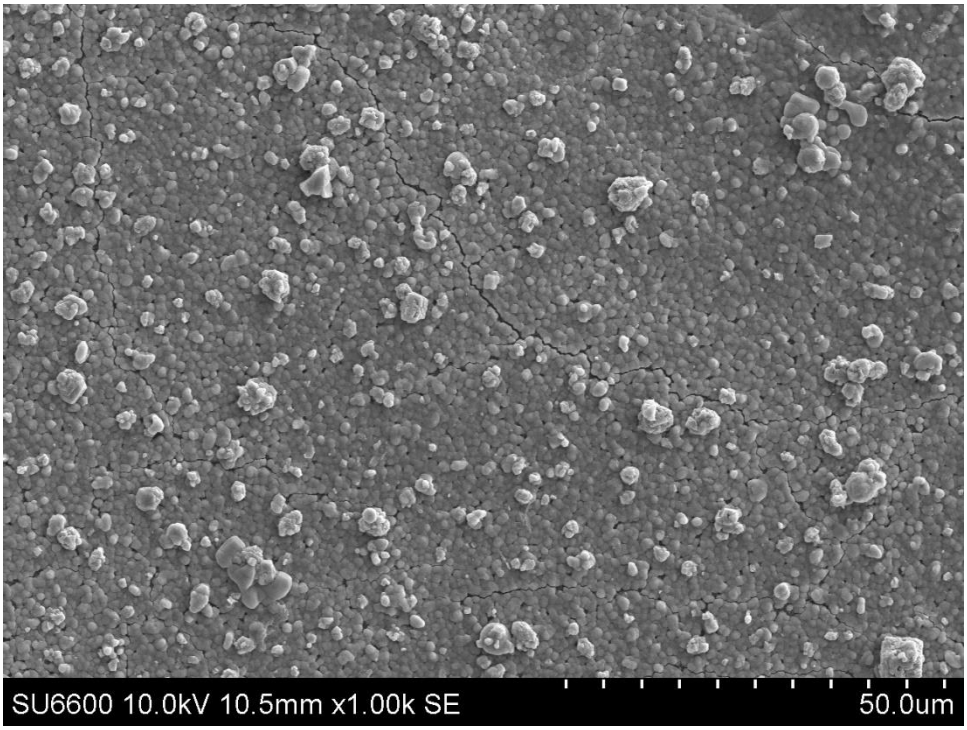

Scale: Combined fouling
Cleaning: none
Zoom: 1kX

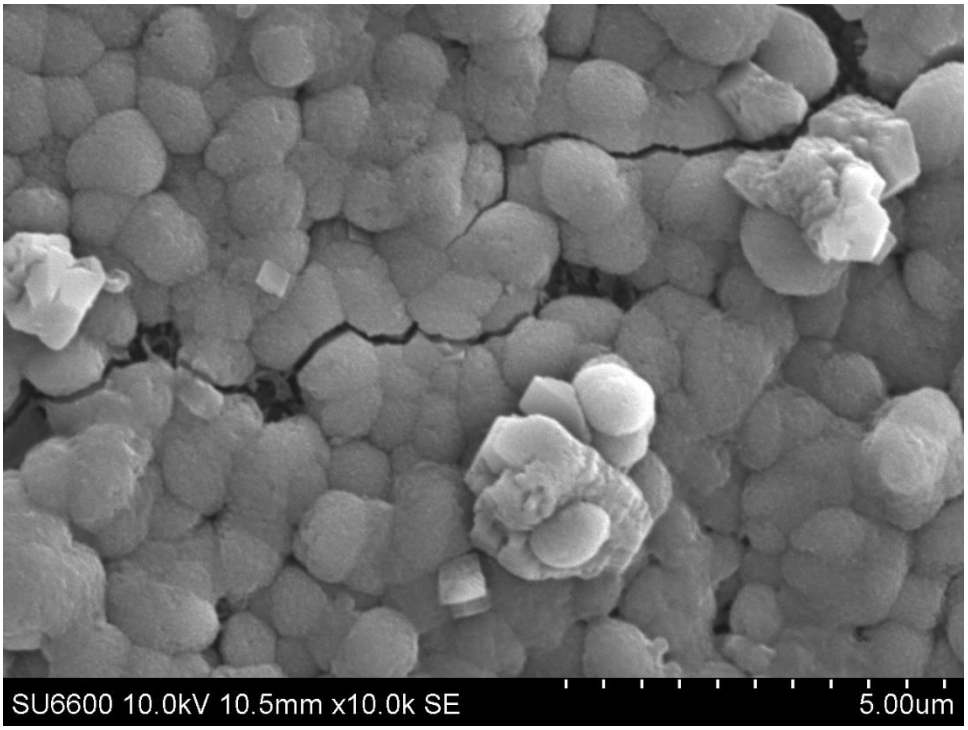

Scale: Combined fouling
Cleaning: none
Zoom: 10kX

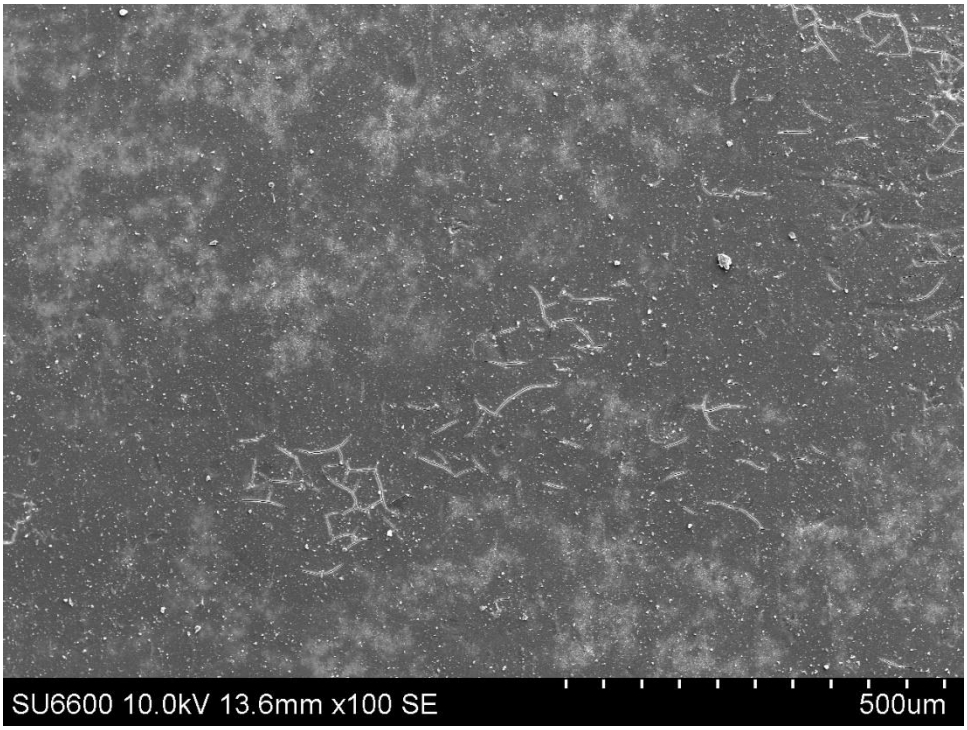

Scale: Combined fouling
Cleaning: Dissolved CO_2
Zoom: 100X

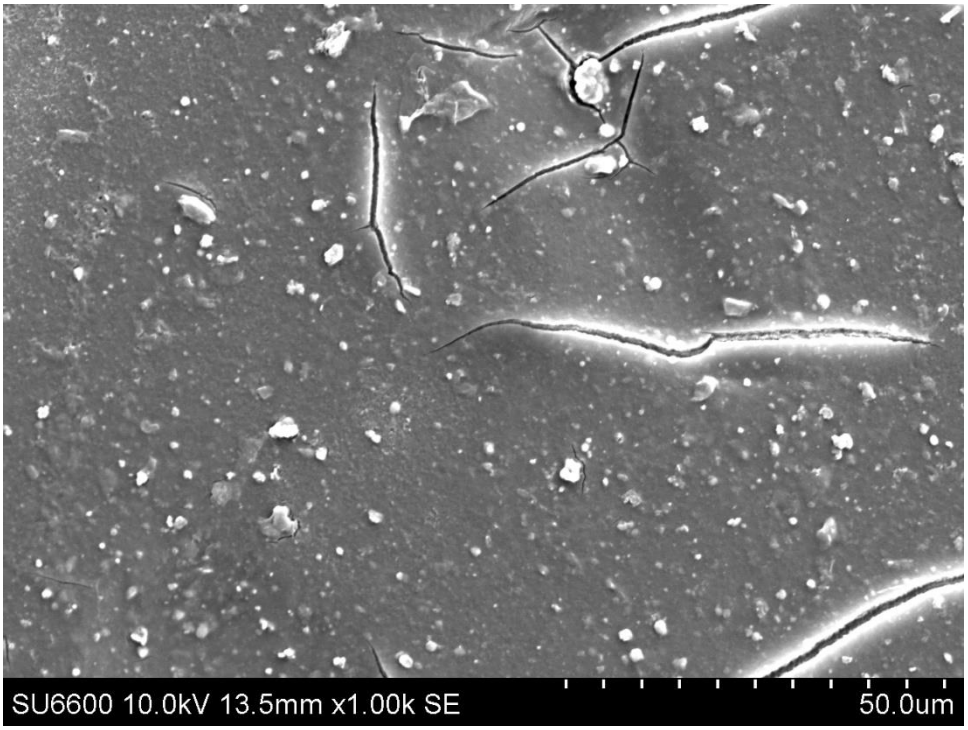

Scale: Combined fouling
Cleaning: Dissolved CO_2
Zoom: 1kX

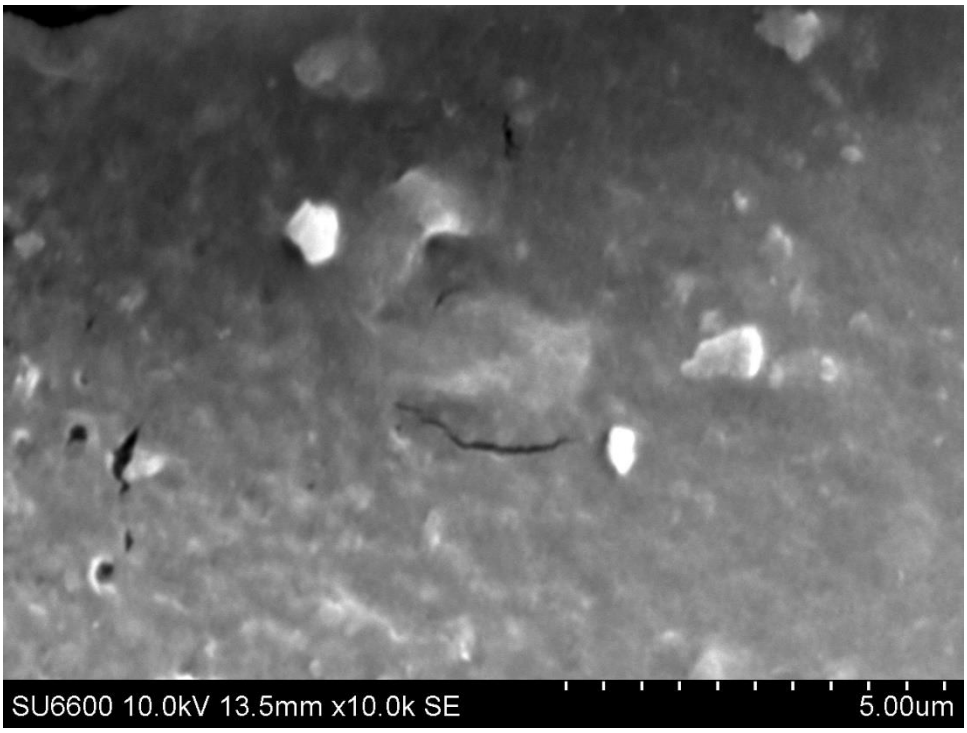

Scale: Combined fouling
Cleaning: Dissolved CO_2
Zoom: 10kX

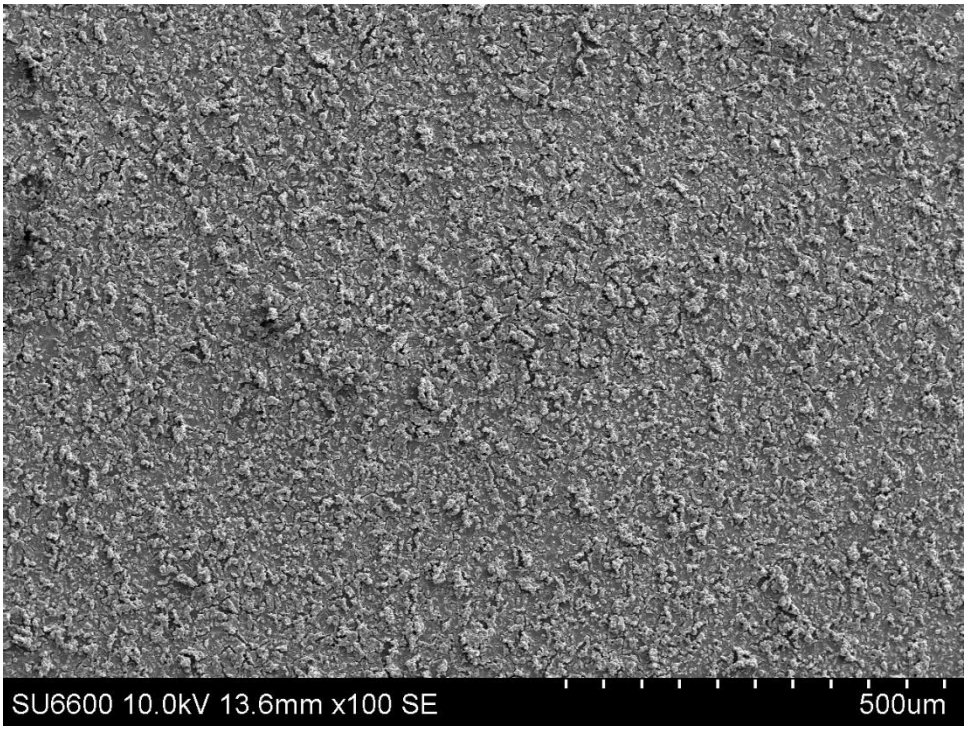

Scale: Combined fouling
Cleaning:
DI water
Zoom:
100X

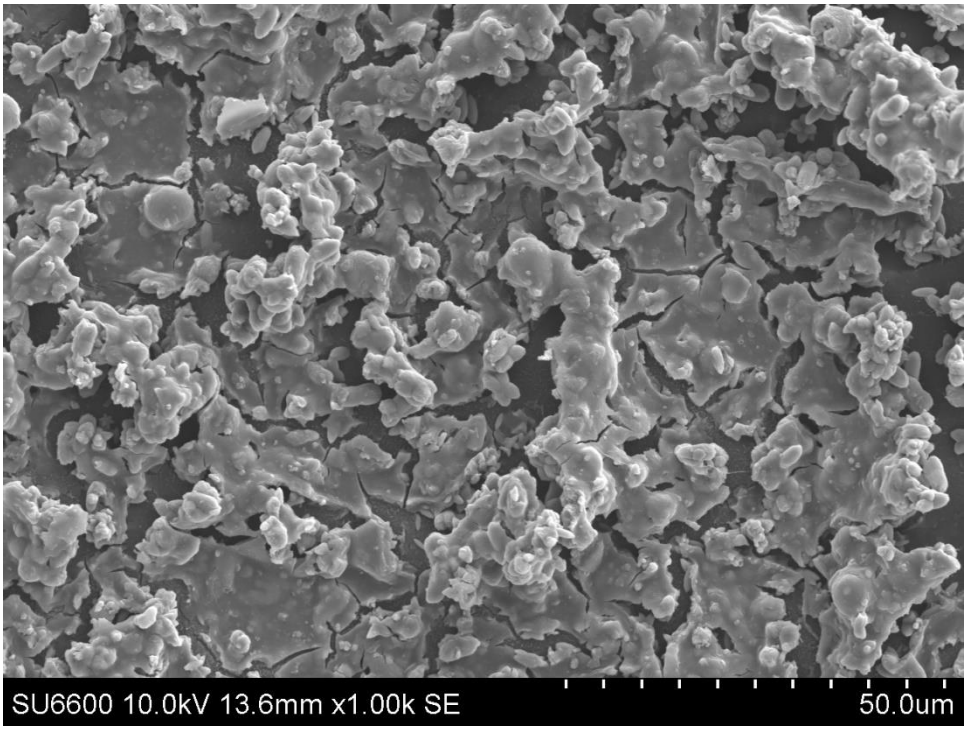

Scale: Combined fouling
Cleaning:
DI water
Zoom:
1kX

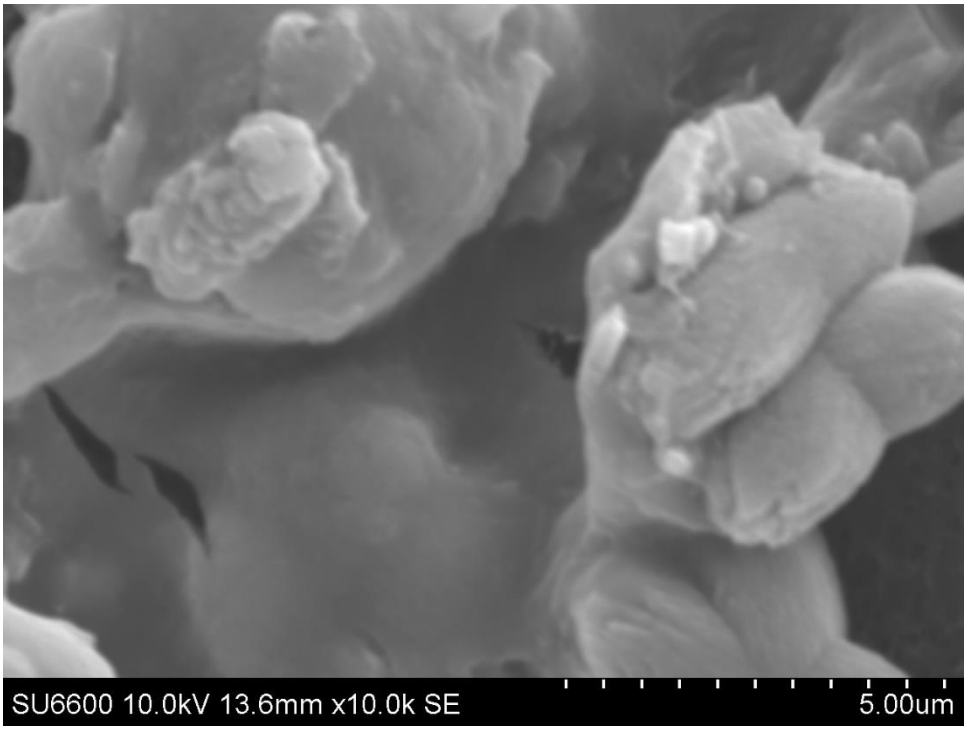

Scale: Combined fouling
Cleaning: DI water
Zoom: 10kX

F.5 Visual MINTEQ results

This section includes the results obtained with Visual MINTEQ software for the $CaSO_4$ and $CaCO_3$ fouling solutions (it was not possible to run this software for the rest of the fouling solutions because the ions present in the other solutions are not available). The pH values might differ from the current pH measurements because they were calculated based on mass and charge balances. An average temperature of 20°C was considered and mg/L was the unit input for the ion concentrations.

The equilibrated mass distribution shows that the current fouling recipes were completely dissolved. From the saturation index with negative values, we see the solutions are initially undersaturated; this is why the concentrate flow from the membrane cell was diverted to the feed tank for recycle, thus eventually obtaining saturated solutions.

F.5.1 $CaSO_4$ (30 mM)

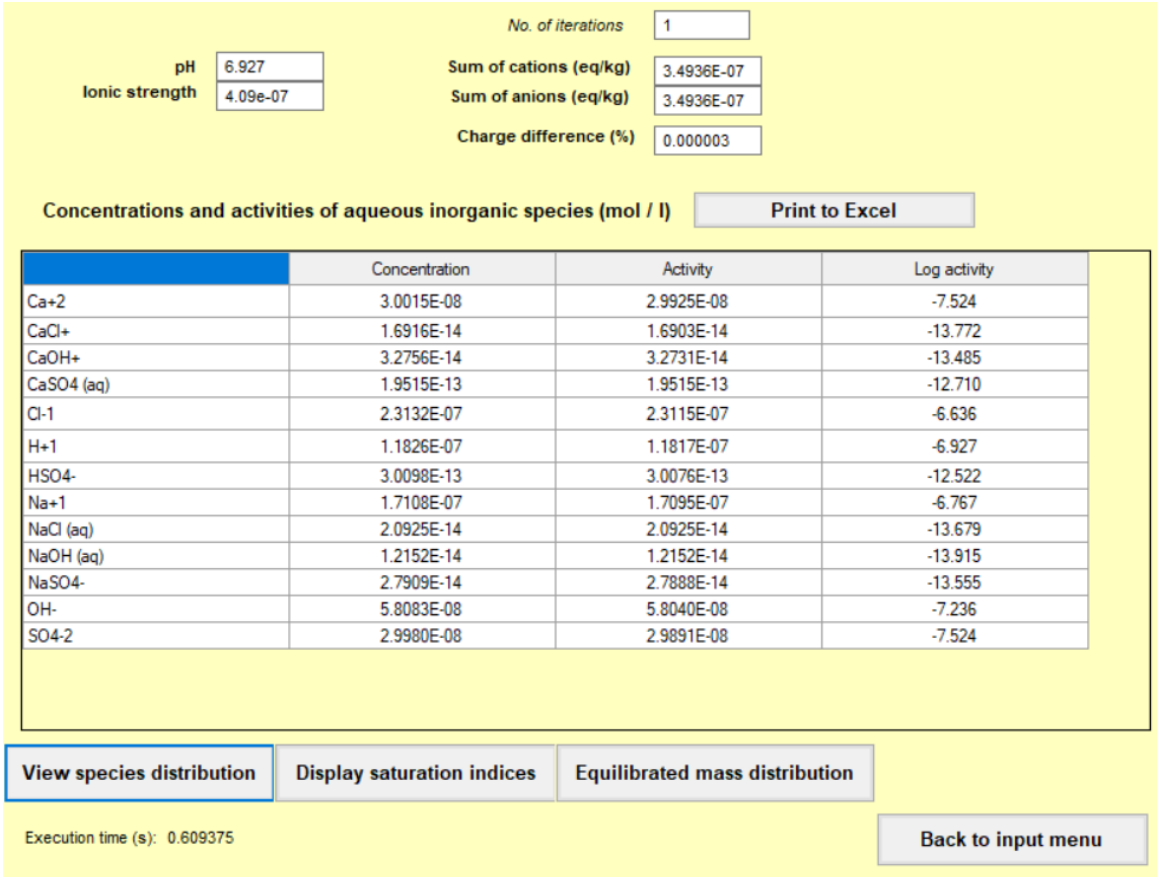

Mineral	log IAP	Sat. index	Ks									
Anhydrite	-15.05	-10.71	1	Ca^{+2}	1	SO_4^{-2}	7	H_2O	-6	H^{+1}	6	H_2O
Gypsum	-15.05	-10.44	1	Ca^{+2}	1	SO_4^{-2}	2	H_2O				
Halite	-13.40	-14.94	1	Na^{+1}	1	Cl^{-1}	-2	H^{+1}	1	H_2O	1	H_2O
Lime	6.33	-26.95	-2	H^{+1}	1	Ca^{+2}	1	H_2O	1	E^{-1}	6	H_2O
Mirabilite	-21.06	-19.71	2	Na^{+1}	1	SO_4^{-2}	10	H_2O	-12	H^{+1}	38	H_2O
Portlandite	6.33	-16.76	1	Ca^{+2}	2	H_2O	-2	H^{+1}				
Thenardite	-21.06	-21.41	2	Na^{+1}	1	SO_4^{-2}						

Equilibrated mass distribution (concentrations in molal)

Component	Total dissolved	% dissolved	Total sorbed	% sorbed	Total precipitated	% precipitated
Ca^{+2}	3.00E-08	100	0	0	0	0
Cl^{-1}	2.31E-07	100	0	0	0	0
H^{+1}	6.02E-08	100	0	0	0	0
Na^{+1}	1.71E-07	100	0	0	0	0
SO_4^{-2}	3.00E-08	100	0	0	0	0

F.5.2 $CaSO_4$ (48 mM)

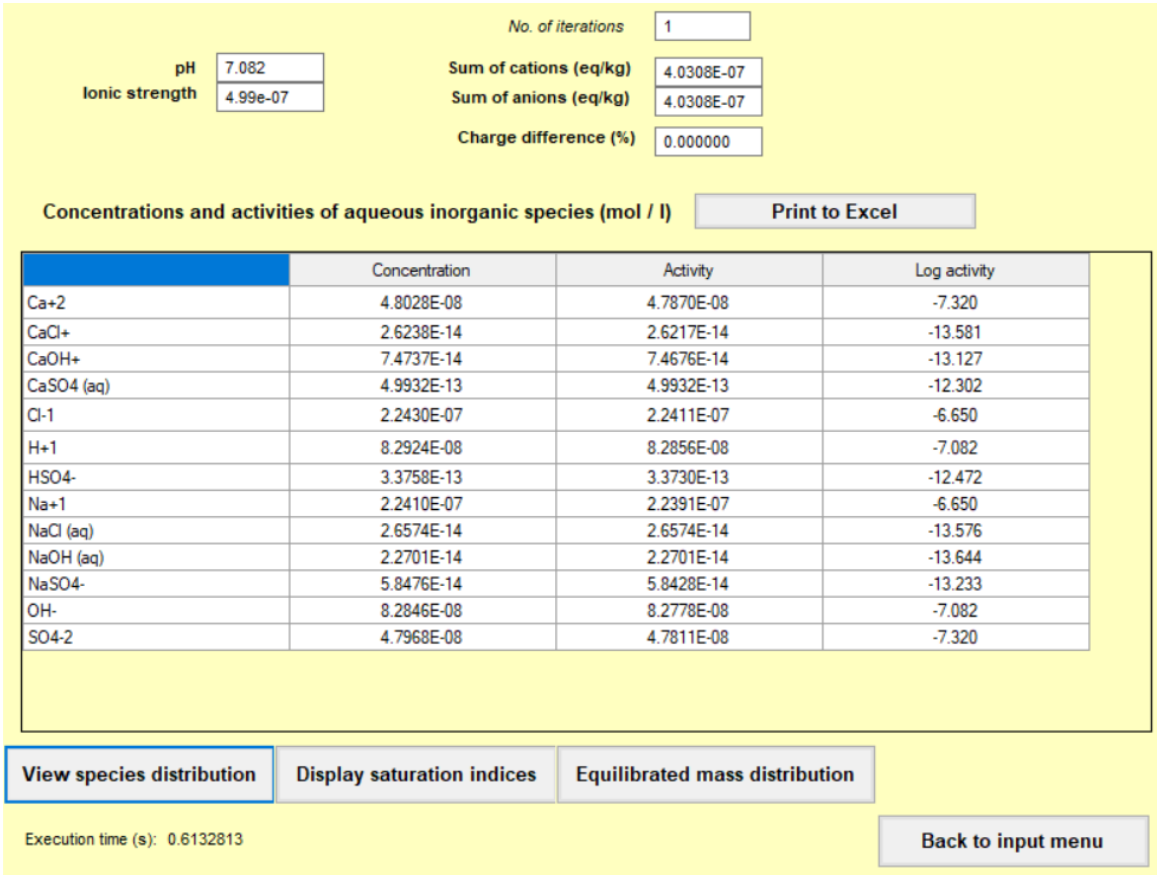

	Concentration	Activity	Log activity
Ca+2	4.8028E-08	4.7870E-08	-7.320
CaCl+	2.6238E-14	2.6217E-14	-13.581
CaOH+	7.4737E-14	7.4676E-14	-13.127
CaSO4 (aq)	4.9932E-13	4.9932E-13	-12.302
Cl-1	2.2430E-07	2.2411E-07	-6.650
H+1	8.2924E-08	8.2856E-08	-7.082
HSO4-	3.3758E-13	3.3730E-13	-12.472
Na+1	2.2410E-07	2.2391E-07	-6.650
NaCl (aq)	2.6574E-14	2.6574E-14	-13.576
NaOH (aq)	2.2701E-14	2.2701E-14	-13.644
NaSO4-	5.8476E-14	5.8428E-14	-13.233
OH-	8.2846E-08	8.2778E-08	-7.082
SO4-2	4.7968E-08	4.7811E-08	-7.320

Mineral	log IAP	Sat. index	Ks									
Anhydrite	-14.64	-10.30	1	Ca^{+2}	1	SO_4^{-2}	7	H_2O	-6	H^{+1}	6	H_2O
Gypsum	-14.64	-10.03	1	Ca^{+2}	1	SO_4^{-2}	2	H_2O				
Halite	-13.30	-14.84	1	Na^{+1}	1	Cl^{-1}	-2	H^{+1}	1	H_2O	1	H_2O
Lime	6.84	-26.44	-2	H^{+1}	1	Ca^{+2}	1	H_2O	1	E^{-1}	6	H_2O
Mirabilite	-20.62	-19.27	2	Na^{+1}	1	SO_4^{-2}	10	H_2O	-12	H^{+1}	38	H_2O
Portlandite	6.84	-16.25	1	Ca^{+2}	2	H_2O	-2	H^{+1}				
Thenardite	-20.62	-20.97	2	Na^{+1}	1	SO_4^{-2}						

Equilibrated mass distribution (concentrations in molal)

Component	Total dissolved	% dissolved	Total sorbed	% sorbed	Total precipitated	% precipitated
Ca^{+2}	4.80E-08	100	0	0	0	0
Cl^{-1}	2.24E-07	100	0	0	0	0
H^{+1}	7.81E-11	100	0	0	0	0
Na^{+1}	2.24E-07	100	0	0	0	0
SO_4^{-2}	4.80E-08	100	0	0	0	0

F.5.3 $CaCO_3$ (3 mM)

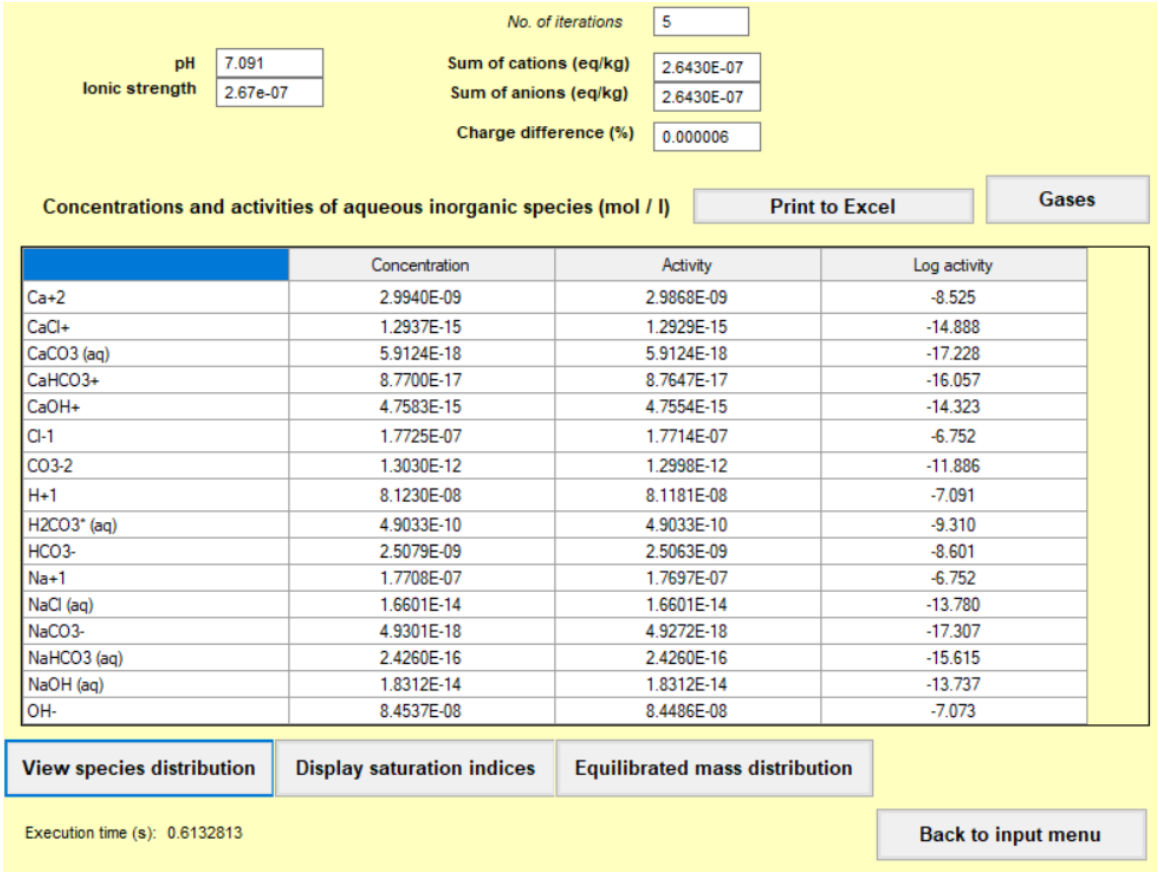

Mineral	log IAP	Sat. index	Ks									
Aragonite	-20.41	-12.11	1	Ca^{+2}	1	CO_3^{-2}	5	H_2O	6	H_2O	2	I^{-1}
$CaCO_3xH_2O(s)$	-20.41	-13.30	1	Ca^{+2}	1	CO_3^{-2}	1	H_2O				
Calcite	-20.41	-11.96	1	Ca^{+2}	1	CO_3^{-2}						
Halite	-13.50	-15.04	1	Na^{+1}	1	Cl^{-1}	-2	H^{+1}	1	H_2O	1	H_2O
Lime	5.66	-27.62	-2	H^{+1}	1	Ca^{+2}	1	H_2O	1	E^{-1}	6	H_2O
Natron	-25.39	-23.88	2	Na^{+1}	1	CO_3^{-2}	10	H_2O	4	H_2O		
Portlandite	5.66	-17.43	1	Ca^{+2}	2	H_2O	-2	H^{+1}				
Thermonatrite	-25.39	-26.06	2	Na^{+1}	1	CO_3^{-2}	1	H_2O				
Vaterite	-20.41	-12.54	1	Ca^{+2}	1	CO_3^{-2}						

Equilibrated mass distribution (concentrations in molal)

Component	Total dissolved	% dissolved	Total sorbed	% sorbed	Total precipitated	% precipitated
Ca^{+2}	2.99E-09	100	0	0	0	0
Cl^{-1}	1.77E-07	100	0	0	0	0
CO_3^{-2}	3.00E-09	100	0	0	0	0
H^{+1}	1.81E-10	100	0	0	0	0
Na^{+1}	1.77E-07	100	0	0	0	0

F.5.4 $CaCO_3$ (4.5 mM)

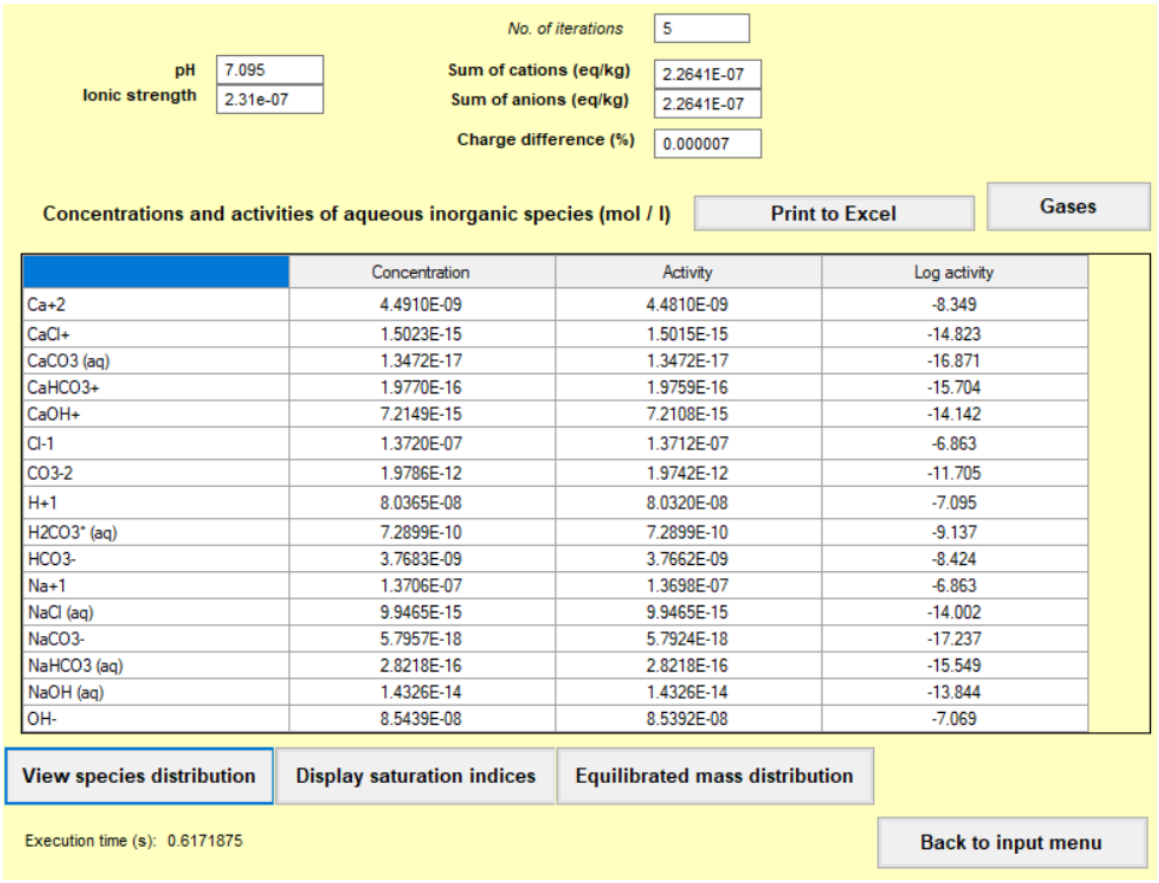

No. of iterations: 5

pH: 7.095
Ionic strength: 2.31e-07

Sum of cations (eq/kg): 2.2641E-07
Sum of anions (eq/kg): 2.2641E-07
Charge difference (%): 0.000007

Concentrations and activities of aqueous inorganic species (mol / l)

Print to Excel | Gases

	Concentration	Activity	Log activity
Ca+2	4.4910E-09	4.4810E-09	-8.349
CaCl+	1.5023E-15	1.5015E-15	-14.823
CaCO3 (aq)	1.3472E-17	1.3472E-17	-16.871
CaHCO3+	1.9770E-16	1.9759E-16	-15.704
CaOH+	7.2149E-15	7.2108E-15	-14.142
Cl-1	1.3720E-07	1.3712E-07	-6.863
CO3-2	1.9786E-12	1.9742E-12	-11.705
H+1	8.0365E-08	8.0320E-08	-7.095
H2CO3* (aq)	7.2899E-10	7.2899E-10	-9.137
HCO3-	3.7683E-09	3.7662E-09	-8.424
Na+1	1.3706E-07	1.3698E-07	-6.863
NaCl (aq)	9.9465E-15	9.9465E-15	-14.002
NaCO3-	5.7957E-18	5.7924E-18	-17.237
NaHCO3 (aq)	2.8218E-16	2.8218E-16	-15.549
NaOH (aq)	1.4326E-14	1.4326E-14	-13.844
OH-	8.5439E-08	8.5392E-08	-7.069

View species distribution | Display saturation indices | Equilibrated mass distribution

Execution time (s): 0.6171875

Back to input menu

Mineral	log IAP	Sat. index	Ks									
Aragonite	-20.05	-11.75	1	Ca^{+2}	1	CO_3^{-2}	5	H_2O	6	H_2O	2	I^{-1}
$CaCO_3xH_2O(s)$	-20.05	-12.94	1	Ca^{+2}	1	CO_3^{-2}	1	H_2O				
Calcite	-20.05	-11.60	1	Ca^{+2}	1	CO_3^{-2}						
Halite	-13.73	-15.27	1	Na^{+1}	1	Cl^{-1}	-2	H^{+1}	1	H_2O	1	H_2O
Lime	5.84	-27.44	-2	H^{+1}	1	Ca^{+2}	1	H_2O	1	E^{-1}	6	H_2O
Natron	-25.43	-23.92	2	Na^{+1}	1	CO_3^{-2}	10	H_2O	4	H_2O		
Portlandite	5.84	-17.25	1	Ca^{+2}	2	H_2O	-2	H^{+1}				
Thermonatrite	-25.43	-26.10	2	Na^{+1}	1	CO_3^{-2}	1	H_2O				
Vaterite	-20.05	-12.18	1	Ca^{+2}	1	CO_3^{-2}						

Equilibrated mass distribution (concentrations in molal)

Component	Total dissolved	% dissolved	Total sorbed	% sorbed	Total precipitated	% precipitated
Ca^{+2}	4.49E-09	100	0	0	0	0
Cl^{-1}	1.37E-07	100	0	0	0	0
CO_3^{-2}	4.50E-09	100	0	0	0	0
H^{+1}	1.51E-10	100	0	0	0	0
Na^{+1}	1.37E-07	100	0	0	0	0

REFERENCES

Alnajjar, H., 2017. Carbon Dioxide Nucleation as a Novel Cleaning Method for Sodium Alginate Fouling Removal from Reverse Osmosis Membranes desalination. *Dissertation,* King Abdullah University of Science and Technology, Thuwal, Saudi Arabia.

Alsalhy, Q.F., Albyati, T.M. & Zablouk, M.A., 2013. a Study of the Effect of Operating Conditions on Reverse Osmosis Membrane Performance With and Without Air Sparging Technique. *Chemical Engineering Communications*, 200(1), pp.1–19.

Ang, W.S., Yip, N.Y., Tiraferri, A. & Elimelech, M., 2011. Chemical cleaning of RO membranes fouled by wastewater effluent: Achieving higher efficiency with dual-step cleaning. *Journal of Membrane Science*, 382(1–2), pp.100–106.

Ang, W.S., Tiraferri, A., Chen, K.L. & Elimelech, M., 2011. Fouling and cleaning of RO membranes fouled by mixtures of organic foulants simulating wastewater effluent. *Journal of Membrane Science*, 376(1–2), pp.196–206.

Antony, A., Low, J.H., Gray, S., Childress, A.E., Le-Clech, P. & Leslie, G., 2011. Scale formation and control in high pressure membrane water treatment systems: A review. *Journal of Membrane Science*, 383(1–2), pp.1–16.

Burton, F., Tchobanoglous, G., Tsuchihashi, R. & Stensel, H.D., Metcalf Eddy, I., 2013. *Wastewater Engineering: Treatment and Resource Recovery* McGraw-Hill Education.

Cadotte, J.E., Petersen, R.J., Larson, R.E. & Erickson, E.E., 1980. A new thin-film composite seawater reverse osmosis membrane. *Desalination*, 32, pp.25–31.

Childress, A.E. & Elimelech, M., 1996. Effect of solution chemistry on the surface charge of polymeric reverse osmosis and nanofiltration membranes. *Journal of Membrane Science*, 119(2), pp.253–268.

Chong, T.H. & Sheikholeslami, R., 2001. Thermodynamics and kinetics for mixed calcium carbonate and calcium sulfate precipitation. *Chemical Engineering Science*, 56(18), pp.5391–5400.

Coffey, T.S., 2008. Diet Coke and Mentos: What is really behind this physical reaction? *American Journal of Physics*, 76(6), pp.551–557.

Coutinho de Paula, E. & Amaral, M.C.S., 2017. Extending the life-cycle of reverse osmosis membranes: A review. *Waste Management & Research*, p.0734242X1668438.

Crittenden, JC; Trussell, RR; Hand, DW; Howe, KJ; & Tchobanoglous, G., 2005. *Reverse osmosis. Water treatment principles and design,* 2nd ed., John Wiley & Sons, Inc.

Cui, Z.F., Chang, S. & Fane, A.G., 2003. The use of gas bubbling to enhance membrane processes. *Journal of Membrane Science*, 221(1–2), pp.1–35.

D'Souza, N.M. & Mawson, A.J., 2005. Membrane Cleaning in the Dairy Industry: A Review. *Critical Reviews in Food Science and Nutrition*, 45(2), pp.125–134.

Descoins, C., Mathlouthi, M., Le Moual, M., and Hennequin, J., 2006. Carbonation monitoring of beverage in a laboratory scale unit with on-line measurement of dissolved CO2. *Food Chemistry*, 95(4), pp.541–553.

Douglas, A. & Costas, T., 2005. Separation of CO2 from Flue Gas: A Review. *Separation Science and Technology*, 40(1–3), pp.321–348.

Fritzmann, C., Löwenberg, J., Wintgens, T. & Melin, T., 2007. State-of-the-art of reverse osmosis desalination. *Desalination*, 216(1–3), pp.1–76.

Gilron, J. & Hasson, D., 1987. Calcium sulphate fouling of reverse osmosis membranes: Flux decline mechanism. *Chemical Engineering Science*, 42(10), pp.2351–2360.

Greenlee, L.F., Lawler, D.F., Freeman, B.D., Marrot, B. & Moulin, P., 2009. Reverse osmosis desalination: Water sources, technology, and today's challenges. *Water Research*, 43(9), pp.2317–2348.

Greenlee, L.F., Testa, F., Lawler, D.F., Freeman, B.D. & Moulin, P., 2010. The effect of antiscalant addition on calcium carbonate precipitation for a simplified synthetic brackish water reverse osmosis concentrate. *Water Research*, 44(9), pp.2957–2969.

Hart, P.W., Colson, G.W. & Burris, J., 2011. Application of carbon dioxide to reduce water-side lime scale in heat exchangers. *Pulp and Paper Canada*, 114(1), pp.21–24.

Jiang, S., Li, Y. & Ladewig, B.P., 2017. A review of reverse osmosis membrane fouling and control strategies. *Science of the Total Environment*, 595, pp.567–583.

Joss, A., Baenninger, C., Foa, P., Koepke, S., Krauss, M., McArdell, C.S., Rottermann, K., Wei, Y., Zapata, A. & Siegrist, H., 2011. Water reuse: >90% water yield in MBR/RO through concentrate recycling and CO2 addition as scaling control. *Water Research*, 45(18), pp.6141–6151.

Kucera, J., 2015. *Reverse Osmosis: Design, Processes, and Applications for Engineers* 2nd Edition, NY.

Ladner, D.A., Subramani, A., Kumar, M., Adham, S.S. & Clark, M.M., 2010. Bench-scale evaluation of seawater desalination by reverse osmosis. *Desalination*, 250(2), pp.490–499.

Lee, S. & Lee, C.H., 2000. Effect of operating conditions on $CaSO_4$ scale formation mechanism in nanofiltration for water softening. *Water Research*, 34(15), pp.3854–

3866.

Lee, S. & Elimelech, M., 2007. Salt cleaning of organic-fouled reverse osmosis membranes. *Water Research*, 41(5), pp.1134–1142.

Matin, A., Khan, Z., Zaidi, S.M.J. & Boyce, M. C., 2011. Biofouling in reverse osmosis membranes for seawater desalination: Phenomena and prevention. *Desalination*, 281(1), pp.1–16.

Michałek, K., Krzysztoforski, J., Henczka, M., Da Ponte, M.N. & Bogel-Łukasik, E., 2015. Cleaning of microfiltration membranes from industrial contaminants using "greener" alternatives in a continuous mode. *Journal of Supercritical Fluids*, 102, pp.115–122.

Moreno, J., de Hart, N., Saakes, M. & Nijmeijer, K., 2017. CO_2 saturated water as two-phase flow for fouling control in reverse electrodialysis. *Water Research*, 125(August), pp.23–31.

Mun, S., Baek, Y., Kim, C., Lee, Y.W., & Yoon, J., 2012. Feasibility of supercritical CO_2 treatment for controlling biofouling in the reverse osmosis process. *Biofouling*, 28(6), pp.627–633.

Ngene, I.S., Lammertink, R.G.H., Kemperman, A.J.B., Van De Ven, W.J.C., Wessels, L.P., Wessling, M., Van Der Meer, W.G.J., 2010. CO_2 nucleation in membrane spacer channels remove biofilms and fouling deposits. *Industrial and Engineering Chemistry Research*, 49(20), pp.10034–10039.

Oh, H., Choung, Y., Lee, S., Choi, J., Hwang, T. & Kim, J., 2009. Scale formation in reverse osmosis desalination: model development. *Desalination*, 238(1–3), pp.333–346.

Partlan, E., 2013. Dissolved Carbon Dioxide for Scale Removal in Reverse Osmosis. *Thesis*, Clemson University, Clemson, SC, United States.

Ray, J.R., Wong, W. & Jun, Y.S., 2017. Antiscaling efficacy of $CaCO_3$ and $CaSO_4$ on polyethylene glycol (PEG)-modified reverse osmosis membranes in the presence of humic acid: interplay of membrane surface properties and water chemistry. *Physical Chemistry Chemical Physics*, 19(7), pp.5647–5657.

Shaffer, D.L., Tousley, M.E. & Elimelech, M., 2017. Influence of polyamide membrane surface chemistry on gypsum scaling behavior. *Journal of Membrane Science*, 525(November 2016), pp.249–256.

Shahid, M.K. & Choi, Y.G., 2018. The comparative study for scale inhibition on surface of RO membranes in wastewater reclamation: CO_2 purging versus three different antiscalants. *Journal of Membrane Science*, 546(June 2017), pp.61–69.

Shahid, M.K., Pyo, M. & Choi, Y.G., 2017. Carbonate scale reduction in reverse osmosis

membrane by CO_2 in wastewater reclamation. *Membrane Water Treatment*, 8(2), pp.125–136.

Shahid, M.K., Pyo, M. & Choi, Y.G., 2017. Inorganic fouling control in reverse osmosis wastewater reclamation by purging carbon dioxide. *Environmental Science and Pollution Research*, pp.1–9.

She, Q., Wang, R., Fane, A.G., & Tang, C.Y., 2016. Membrane fouling in osmotically driven membrane processes: A review. *Journal of Membrane Science*, 499, pp.201–233.

Tzotzi, C., Pahiadaki, T., Yiantsios, S. G., Karabelas, A. J. & Andritsos, N., 2007. A study of $CaCO_3$ scale formation and inhibition in RO and NF membrane processes. *Journal of Membrane Science*, 296(1–2), pp.171–184.

Uchymiak, M., Lyster, E., Glater, J. & Cohen, Y., 2008. Kinetics of gypsum crystal growth on a reverse osmosis membrane. *Journal of Membrane Science*, 314(1–2), pp.163–172.

Van Der Bruggen, B., Vandecasteele, C., Van Gestel, T., Doyen, W. & Leysen, R., 2003. A review of pressure-driven membrane processes in wastewater treatment and drinking water production. *Environmental Progress*, 22(1), pp.46–56.

Wibisono, Y., Cornelissen, E. R., Kemperman, A.J.B., Van Der Meer, W.G.J. & Nijmeijer, K., 2014. Two-phase flow in membrane processes: A technology with a future. *Journal of Membrane Science*, 453, pp.566–602.

Willems, P., Kemperman, A.J.B, Lammertink, R.G.H., Wessling, M., van Sint Annaland, M., Deen, N.G., Kuipers, J.A.M & van der Meer, W.G.J., 2009. Bubbles in spacers: Direct observation of bubble behavior in spacer filled membrane channels. *Journal of Membrane Science*, 333(1–2), pp.38–44.

Xie, P., Murdoch, L. & Husson, S., 2016. Simulation of Reverse Osmosis and Osmotically Driven Membrane Processes. *Dissertation*, Clemson University, Clemson, SC, United States.

Zondervan, E. & Roffel, B., 2007. Evaluation of different cleaning agents used for cleaning ultra filtration membranes fouled by surface water. *Journal of Membrane Science*, 304(1–2), pp.40–49.